*Scuola Dottorale di Ingegneria*
*Sezione di Ingegneria dell'Elettronica Biomedica,*
*dell'Elettromagnetismo e delle Telecomunicazioni*

# NEXT GENERATION OPTICAL ACCESS NETWORKS

*Valentina Sacchieri*

*Advisor:* *Prof. Gabriella Cincotti*
*Applied Electronic Department*
*Roma Tre University*

A dissertation submitted to

Roma Tre University
Department of Applied Electronics

in partial fulfillment of the requirements for the degree of

DOCTOR OF PHILOSOPHY

Rome, March 8th, 2010

*Scuola Dottorale di Ingegneria*
*Sezione di Ingegneria dell'Elettronica Biomedica,*
*dell'Elettromagnetismo e delle Telecomunicazioni*

# RETI DI ACCESSO OTTICHE DI NUOVA GENERAZIONE

*Valentina Sacchieri*

*Docente-guida:* *Prof. Gabriella Cincotti*
*Dipartimento di Elettronica Applicata*
*Università degli Studi Roma Tre*

Tesi sottomessa

all'Università degli Studi Roma Tre
Dipartimento di Elettronica Applicata

per il conseguimento del titolo di

DOTTORE DI RICERCA

Roma, 8 Marzo 2010

To all those who made this possible,

each in their own special way...

# ACKNOWLEDGMENTS

Ph.D. is like a long journey, during which you have the chance to learn a lot, to have very nice experiences, and, as in any journey, there can be difficult moments when you think you do not have the strength to continue. But above all, during this journey you have the opportunity to meet extraordinary people that make the trip special with their help and allow you to find the strength you need.

I gladly acknowledge the Coordinator Prof. Lucio Vegni, Prof. Giorgio Guattari and my supervisor Prof. Gabriella Cincotti for giving me the opportunity to live this experience. I also wish to warmly thank my supervisor for her advices and for giving me the chance to discover what the research is.

I would like to acknowledge Prof. António Teixeira for being a very good advisor and a thoughtful host when I was in IT, and for teaching me that "Life is simpler, Valentina, don't be stressed, smile!". Together with him, Prof. Rogério Nogueira, for his kindness and his explanation on the theory of FBGs, and Pedro, for his essential help with Matlab.

I thank a lot Nataša, with Sveta and Alexander, Joao, Leandro, Ana, Berta, and Ash for making Aveiro my home and all the other friends in IT for their friendly welcome.

I wish to thank Dr. Michela Svaluto Moreolo, for being a loving "colleghina" and for her help, when she was in our lab. I also thank Federico for his kindness and his help in these last months.

I would like to acknowledge my family for being my guide every day and for having supported me in every choice I made. Together with them, I wish to thank my sister Camilla, because she is more than a sister, a friend always ready when I need her.

I wish to thank Andrea for being the wonderful person he is, for teaching me to be positive towards life and because he made me feel his support and his closeness even when we were apart.

Finally, I would like to acknowledge my dear friends Ilaria, Nadia, Valentina and Valeria, who always stand by me and always support me, and Alessandra, Michele, Raffaella, Sabina

and Valentina for their loving friendship. I also wish to thank a lot my friends Fabio, Adriano and Francesco for their fundamental help in my “fight” with LaTex.

I wish to thank you all for walking with me during this journey, and all those not explicitly mentioned for space reasons, but who have made this experience even more memorable, with a smile or a kind word.

# ABSTRACT

## NEXT GENERATION OPTICAL ACCESS NETWORKS

Valentina Sacchieri

This thesis reports some investigations on different aspects that characterize the next generation optical access networks (NGAN) and that contribute in improving the performance of such networks.

Due to the increasing demand for high speed transmission services from private and business users, the development of access network is evolving to the use of optical technologies. Passive optical networks (PON) seems to be the most promising solution for NGAN. This kind of networks has a simple topology, where the optical line terminator (OLT) sends the downstream information broadcast to the end users (optical network units – ONU). Therefore, data confidentiality is one of the major issues and it is critically important that data transmitted cannot be theft at any point along the communication link by a potential eavesdropper.

Optical code division multiple access (OCDMA) seems to have all the advantages to be a valid solution, since many users share the same optical resources by assigning a specific code to each user and the encoded signal shows a noise-like waveform. On the other side, an authorized user can decipher the transmission by the use of the correct code. Various OCDMA schemes had been proposed and demonstrated. When multiple users send simultaneously information with different codes, it is very difficult for an eavesdropper to intercept the correct data, without knowing the code. However, when a single user is active in the network, the security is not guaranteed, because an unauthorized user can easily detect the signal with a standard power detector. To cope with this vulnerability, code switching scheme have been proposed, where both marks and spaces are encoded with two different codes. In this case the information is hidden for an eavesdropper using a simple

energy detector, but the system is still vulnerable against a differential detection.

In this work, two different solutions have been proposed in order to increase the confidentiality level of an OCDMA network. The first exploits the properties of a multiport encoder/decoder (E/D) with an arrayed waveguide grating (AWG) configuration. This device has $N$ input and $N$ output ports and by a single input laser pulse a set of phase shifted keyed (PSK) codes is generated. The code cardinality equals the number of the device output ports. It is possible to enlarge the code cardinality and generate $n$-dimensional codes by sending $n$ laser pulses into $n$ different encoder input ports at the same time. Considering different configurations, the multiport E/D is able to perform bit and block coding using 1-dimensional and $n$-dimensional codes. Moreover, to enlarge the cardinality in the case of bit-ciphering, spectral phase codes have been introduced. The security performance of a point-to-point (P2P) transmission have been analyzed in terms of robustness against *brute-force code searching*, *known-plaintext* and *chosen plaintext* attacks.

Another possible solution to increase the confidentiality level of an OCDMA transmission and to avoid simple differential detection is to make the transmitted signal fully distorted, by the introduction of scrambling in optical signal processing. The concept of scrambling is borrowed from electronic encoding and wireless communications, where it has been introduced for data protection. It could be performed by adding or modifying components of the original signal, to make the extraction of the original signal difficult from an unauthorized user. Optically, a signal can be scrambled by adding one or more encoders in cascade with the primary OCDMA encoder. A scrambled signal is fully distorted and has a multilevel eye diagram. Therefore, a potential attacker has to try all the possible combinations between the code words to break the transmission. The security performance have been analyzed in terms of robustness against *brute-force* attack. A P2P transmission and two multi-user configurations have been proposed and numerically simulated by *VPItransmissionMaker* software. The encoder/decoder devices have been simulated as *Super Structured Fibre Bragg Gratings (SSFBGs)* that generates 15 chip codes, realizing a simple, feasible and compatible with current optical technologies system.

A critical parameter in the next generation optical networks is the spectral efficiency,

because all the new applications, such ad video conferences or real time games, require high information density. Advanced modulation schemes, such as differential phase shift keying (DPSK) and differential quadrature shift keying (DQPSK), have been applied to increase the spectral efficiency in optical transmissions. On the other hand, OCDMA technique offers extraordinary network capabilities, allowing a large number of users to share the same bandwidth. In this case, the spectral efficiency is $\eta = KB/\Delta f$, where $K$ is the number of simultaneous users transmitting at a bit rate $B$ and $\Delta f$ is the optical bandwidth. Therefore, the influence of different advanced modulation formats on OCDMA transmission have been investigated in terms of spectral efficiency and bit error rate (BER). In particular, the following modulation formats have been compared: on-off keying (OOK), DUOBINARY, DPSK and DQPSK. Both incoherent and coherent encoding techniques have been analyzed, considering optical orthogonal codes (OOC) and *Gold* codes respectively. Multiple access interference (MAI) and beat noises have been also taken into account.

In the future optical networks, besides high-speed Internet, voice over IP and broadcast video, the service demand will evolve to high bit rate and customization, namely a wide variety demand of quality of service (QoS). Optical Orthogonal Frequency Division Multiplexing (Optical OFDM) is a promising candidate in such networks, thanks to the fact that it meets the twofold requirement of mitigating transmission impairments and providing high bit rates. Moreover, due to the small bandwidth occupied by a single OFDM channel, it is characterized by high spectral efficiency and high tolerance to the fibre dispersions. Applied to PON networks, this technique allows to dinamically allocate different subbands for different services. Traditional OFDM system uses the Fast Fourier Transform (FFT) algorithm to process the signal. Exploiting the properties of the Hartley transform, a real-valued trigonometric transform, a different optical OFDM system has been proposed and numerically simulated, achieving good transmission distances suitable for optical access networks. Instead of the FFT algorithm, the signal processing has been performed by the Fast Hartley Transform (FHT) algorithm that gives a real valued signal. This simplifies the conversion of the OFDM signal into an optical signal and allows to halve the number of the necessary digital-to-analog (DAC) and analog-to-digital (ADC) converters, because

only the in-phase component has to be processed. Moreover, the frequency separation and orthogonality between the subchannels are kept and, thanks to the kernel of the Hartley transform, each symbol of the data sequence is carried by two symmetrical subbands, increasing the frequency diversity.

In order to extend optical transparency to the access networks, providing the same bandwidth of the fibre, optical wireless systems can be a suitable alternative when wired connections cannot be established. In free space optics transmissions light is used as a carrier, but, unlike optical fibres, the light beam is transmitted through the air. A transparent wireless optical system have been experimentally tested, in order to overcome the electrical-to-optical-to-electrical (E-O-E) conversion impairments. The optical beam is transmitted directly into the free space channel by a trunked fibre and a system of lens capable to collimate the beam over long distances. At the receiver, the beam is focused into the core of a standard single mode fibre (SMF), by means of a focusing lens and a GRIN lens. Such a system allows an all-optical processing of the transmitted data, the use of Dense Wavelength Division Multiplexing (DWDM) technique, to increase the bit rate, and provides a fast and cost-effective connection for the access segment.

# ABSTRACT

## RETI DI ACCESSO OTTICHE DI NUOVA GENERAZIONE

Valentina Sacchieri

Il frenetico sviluppo delle reti ottiche durante l'ultimo decennio ha creato una situazione caratterizzata da pesanti disparità tra le diverse sezioni. L'utilizzo della fibra ha permesso la realizzazione di collegamenti a lunga distanza (Wide Area Network, backbone) con larga banda ed elevato bit rate. Dall'altra parte, le Local Area Network (LAN) si sono sviluppate assicurando un livello molto alto di affidabilità e velocità. Allo stesso tempo è aumentata la richiesta di servizi che richiedono sempre maggiore disponibilità di banda, quali ad esempio video on demand, voice over IP, accessi internet veloci, pagine web ad elevato contenuto multimediale. Pertanto, ad oggi il collo di bottiglia risiede nel segmento finale della rete, che rappresenta proprio il ponte tra gli utenti finali e le reti di maggiore estensione: la cosiddetta rete di accesso. Attualmente, c'è un grande interesse nell'utilizzo delle tecnologie ottiche nella rete di accesso per estendere la trasparenza all'*Ultimo Miglio* e far fronte alla necessità di accesso ad alta velocità ed alla sempre crescente richiesta di banda da parte dell'utente finale, dovuta alla necessità di integrare servizi voce, video broadcast e dati (*triple play*).

I miglioramenti nella tecnologia dei componenti ottici hanno permesso di realizzare reti *backbone* in fibra ottica con capacità che superano i 40Gb/s. L'evoluzione delle reti completamente ottiche è andata di pari passo con l'evoluzione dei sistemi di comunicazione in fibra ottica. Così come le fibre ottiche hanno visto diverse generazioni grazie al progressivo avanzamento della tecnologia, anche per le reti ottiche si possono distinguere due generazioni. Nella prima generazione sono stati sfruttati tutti i vantaggi dovuti all'utilizzo della fibra ottica come mezzo di comunicazione, lasciando però le funzionalità di *switching* e processamento dei segnali ai dispositivi elettronici. Inoltre, per aumentare la

capacità della rete senza dover aumentare il numero di fibre usate, sono state introdotte tecniche di modulazione nel domino ottico come la multiplazione a divisione di tempo (*Optical Time Division Multiplexing*, OTDM) e la multiplazione a divisione di lunghezze d'onda (*Wavelength Division Multiplexing*, WDM). La seconda generazione di reti ottiche è, invece, caratterizzata da un più elevato grado di trasparenza, grazie ad una riduzione nell'impiego dell'elettronica. Di conseguenza, queste reti sono in grado di offrire maggiori funzionalità, tra le quali *switching* ed instradamento dei pacchetti. Nel 2001, l'organismo di standardizzazione ITU-T ha definito l'architettura per le reti Automatically Switched Optical Network (ASON), reti di trasporto ottiche che includono anche funzionalità di *switching* dinamico e controllo.

Al contrario, nelle reti di accesso i principali mezzi di trasporto sono ancora il doppino in rame ed il cavo coassiale che non sono in grado di far fronte alla richiesta di nuovi servizi ed applicazioni. Di conseguenza, si è generato un forte squilibrio tra i diversi segmenti della rete, il cosiddetto *collo di bottiglia dell'ultimo miglio*.

Le attuali tecnologie di accesso a larga banda, quali l'*Asynchronous Digital Subscriber Line* (ADSL) ed il *cable modem*, sono in grado di fornire servizi base, come la navigazione *Web* e la posta elettronica, ma non sono in grado di far fronte all'elevata banda necessaria ai sempre più richiesti servizi multimediali. Pertanto, le tecnologie ottiche rappresentano il trend di sviluppo della futura generazione di reti di accesso.

L'architettura più semplice è la Passive Optical Network (PON), una rete ottica priva di elementi attivi nel percorso da sorgente a destinazione. Permette di minimizzare l'uso della fibra ed il numero di *transceiver*, utilizzando solo splitter/accoppiatori passivi in grado di dividere la potenza di un segnale ottico proveniente da una fibra su più fibre e viceversa. In questo modo sia i costi che le necessità di alimentazione dei dispositivi vengono ridotti. Inoltre è in grado di gestire segnali di qualunque formato e velocità di trasmissione. Una rete PON è costituita da un *Optical Line Terminal* (OLT), che fornisce i servizi ed invia i segnali broadcast ai vari utenti, da uno splitter passivo, che divide la potenza del segnale inviato, e dalle interfacce degli utenti (*Optical Network Unit* – ONU o *Network Interface Unit* – NIU), che sono le interfacce tra gli utenti ed i servizi offerti dalla rete. Si possono

distinguere diverse architetture, indicate con il termine generale Fiber To The x (FTTx), a seconda che il link ottico arrivi fino alla centrale locale (FTTC: Fiber To The Curb, FTTCab: Fiber To The Cabinet), dalla quale poi il segnale viene inviato agli utenti finali mediante collegamenti in rame, oppure che il link arrivi fino ad un singolo edificio (FTTB: Fiber To The Building) o fino al singolo utente finale (FTTH: Fiber To The Home).

Le reti TDM-PON e WDM-PON costituiscono le due princiapli categorie di reti ottiche passive. Le prime utilizzano la tecnica di multiplazione a divisione di tempo per la gestione del traffico uplink, restringendo però la banda disponibile per il singolo utente; le seconde, invece, utilizzano la tecnica di multiplazione a divisione di lunghezza d'onda e presentino molti vantaggi rispetto alle TDM-PON, tuttavia non godono di sufficienti caratteristiche di flessibilità per allocare dinamicamente la banda tra i vari servizi ed inoltre i costi del sistema risultano maggiori a causa dell'elevato numero di trasmettitori e ricevitori diversi necessari.

Pertanto, si è alla ricerca di soluzioni per migliorare le prestazioni delle reti ottiche passive, garantendo la trasparenza e, di conseguenza, un'elevata banda.

In questo lavoro di tesi sono stati analizzati diversi aspetti relativi all'uso di tecnologie ottiche avanzate nella rete di accesso. E' stata studiata la tecnica di accesso multiplo a divisione di codice (*Optical Code Division Multiple Access*, OCDMA), proponendo due diversi sistemi che concorrano ad incrementarne il grado di sicurezza; inoltre sono state analizzate tecniche di modulazione avanzate per aumentare l'efficienza spettrale della trasmissione; infine, è stata valutata la possibilità di estendere la trasparenza al segmento di accesso, proponendo una soluzione ottica *wireless* come alternativa alle connessioni fibra ottica.

La tecnica OCDMA risulta essere una valida alternativa nelle reti ottiche ad accesso multiplo, rispetto alle tecniche di multiplazione standard quali *Wavelength Division Multiple Access* (WDMA), *Time Division Multiple Access* (TDMA) e *Space Division Multiple Access* (SDMA), in quanto permette un'efficace suddivisione delle risorse disponibili nella rete tra i diversi utenti, assegnando un codice a ciascuno di essi. In questo modo, tutti gli utenti possono trasmettere su tutta la banda disponibile nello stesso intervallo di tempo. Il segnale trasmesso viene codificato mediante un codice specifico per ogni utente e può

essere ricevuto solo usando lo stesso codice. Inoltre, sovrapponendo i segnali codificati, provenienti da differenti utenti, si ottiene un segnale molto simile al rumore. Queste due caratteristiche fanno si che la tecnica OCDMA goda dell'intrinseco vantaggio di aumentare la sicurezza della comunicazione.

La sicurezza nello strato fisico è di grande interesse nelle reti ottiche di nuova generazione per evitare che un potenziale malintenzionato possa accedere ai dati trasmessi lungo il cammino ottico. In particolare nelle reti PON attuali, a causa della loro semplice topologia, la confidenzialità del dato trasmesso non è garantita, in quanto le informazioni vengono inviate broadcast dall'OLT a tutti gli utenti ed un potenziale malintenzionato potrebbe intercettare i dati diretti ad un altro utente.

Diversi studi hanno dimostrato che, dal punto di vista della protezione del dato, la semplice tecnica OCDMA applicata ad un segnale modulato mediante *On-Off Keying* (OOK) risulta vulnerabile e può essere intercettata con un rivelatore di potenza. D'altra parte, anche l'utilizzo di due codici differenti per il bit "1" e per il bit "0" è vulnerabile con una rivelazione differenziale. Inoltre la confidenzialità offerta dalla tecnica OCDMA è principalmente legata al numero di codici che possono essere generati e processati. Tuttavia, questo comporta un aumento del numero di codificatori e decodificatori necessari, aumentando così la complessità del sistema.

Utilizzando un dispositivo encoder/decoder (E/D) multiporte è possibile realizzare diversi schemi di codifica che risultano robusti ai tre tipi di attacchi *Cyphertext Only Attack* (COA), *Known Plaintext Attack* (KPA) e *Chosen Plaintext Attack* (CPA). L'encoder/decoder multiporte è costituito da un array di guide d'onda (*Array Waveguide Grating*, AWG) con $N$ porte di ingresso ed altrettante di uscita, pertanto è in grado di generare e processare $N$ codici *Phase Shift Keying* (PSK) di lunghezza $N$, simultaneamente. Quando un singolo impulso viene inviato in una delle porte di ingresso, dopo la prima regione di slab si ottengono $N$ repliche dell'impulso, che percorrono un differente cammino ottico. Queste repliche si ricombinano poi alla fine della seconda regione di slab, generando un codice di fase diverso ad ogni porta di uscita. Il dispositivo genera perciò $N$ codici ottici PSK, realizzando una codifica unidimensionale. Per aumentare la cardinalità dei codici e,

di conseguenza, la sicurezza della codifica, può essere anche realizzata una configurazione $n$-dimensionale, nella quale $n$ impulsi vengono inviati ad altrettante porte di ingresso; i codici $n$-dimensionali generati sono la somma coerente di $n$ codici PSK. In tale configurazione, il set completo di codici che possono essere generati è $2^N$, dove $N$ rappresenta il numero di porte dell'E/D. La rivelazione viene effettuata mediante il medesimo dispositivo rilevando i picchi di autocorrelazione.

Il dispositivo E/D multiporte permette di realizzare una codifica del singolo bit oppure una codifica a blocchi del messaggio, che è una implementazione ottica delle tecniche crittografiche standard. Nel primo caso c'è una corrispondenza diretta tra bit di informazione e codice ottico, in quanto ciascun bit viene codificato con un codice diverso. Due diverse configurazioni del sistema permettono la generazione di codici $n$-dimensionali e codici spettrali di fase, come mostrato in Fig.1.

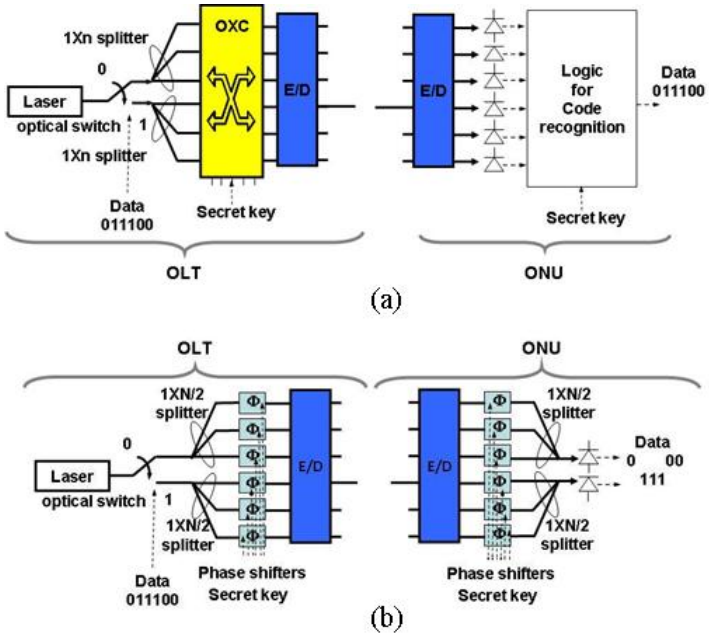


Figura 1: Sistemi per la codifica bit a bit con E/D multiporte. (a) codici $n$-dimensionali; (b) codici spettrali di fase.

Nel secondo caso, invece, l'informazione da trasmettere viene suddivisa in una sequenza di $m$ bits e codificata con un alfabeto costituito da $M = 2^m$ simboli, che corrispondono

ai codici ottici. In questo tipo di codifica la chiave risiede nella logica di assegnazione del codice ottico ad una data sequenza di bit. Due esempi di sistemi per la codifica a blocchi realizzati mediante il dispositivo multiporte sono mostrati in Fig.2 (a) e (b), utilizzando ripsettivamente codici unidimensionali ed $n$-dimensionali.

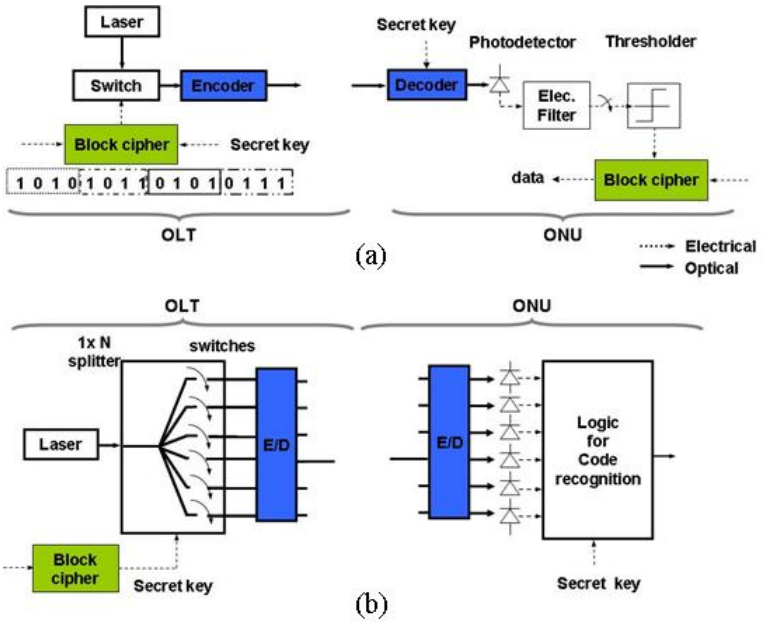


Figura 2: Sistemi per la codifica a blocchi con E/D multiporte. (a) codici 1-dimensionali; (b) codici $n$-dimensionali.

La codifica bit a bit risulta robusta solo contro il più semplice tipo di attacco alla sicurezza, il COA, mentre risulta vulnerabile agli altri due più complessi attacchi, il KPA ed il CPA, per i quali risulta più robusta la codifica a blocchi. Quest'ultima, però, comporta una riduzione del bit rate massimo. L'attacco a *forza bruta* calcola il numero di tentativi che un potenziale malintenzionato deve effettuare per poter decifrare il messaggio, in funzione del numero delle porte dell'E/D. Il numero di tentativi è funzione del numero $K$ di codici che ciascuna tecnica di codifica è in grado di generare: nel caso della codifica a singolo bit con codici spettrali di fase risulta $K = 2^N$, mentre nel caso di codifica a blocchi si ha $K = N!$, per codici PSK unidimensionali, e $K = 2^N!$ per codici PSK $n$-dimensionali. Per valutare il CPA è stato considerato il numero di bit del messaggio in chiaro che è necessario

conoscere per violare il codice. Un solo bit è sufficiente nel caso di codifica a singolo bit, mentre per la codifica a blocchi è necessario un numero di bit pari a $(N-1)log_2N$, nel caso di codifica unidimensionale, oppure $N(2^N-1)$, nel caso di codifica $n$-dimensionale.

Un'altra possibile soluzione per incrementare il livello di sicurezza del segnale codificato è quella di renderlo completamente distorto così da avere un diagramma ad occhio multilivello e proteggere la trasmissione da rivelazione di potenza o differenziale. Questo può essere ottenuto introducendo lo scrambling nel dominio ottico.

Lo scrambling è una tecnica mutuata dalla codifica elettronica,dove viene utilizzata proprio per la protezione dei dati. Può essere applicata sia nel dominio digitale che analogico. Nel primo caso è una tecnica crittografica usata nel pre- o nel post-processing di un'immagine digitale o anche nel watermarking digitale. Essa genera un'immagine "caotica" che maschera l'informazione. L'immagine può essere ricostruita solo se il metodo con cui è stato effettuato lo scrambling e le variabili usate sono note. Nel caso analogico, lo scrambling consiste nella sovrapposizione di rumore al messaggio; dal lato del ricevitore, il rumore viene sottratto utilizzando un appropriato dispositivo. In entrambi i casi, la tecnica dello scrambling aggiunge o modifica alcune importanti componenti del segnale originale, al fine di rendere più difficile l'estrazione dello stesso. Pertanto nelle telecomunicazioni, lo scrambler può essere visto come un dispositivo che modifica un segnale o anche che codifica un messaggio dal lato del trasmettitore, rendendolo così inintelligibile per un ricevitore non equipaggiato con un opportuno dispositivo per la decodifica.

Nelle comunicazioni ottiche, sono state proposte diverse soluzioni per realizzare lo scrambling. Per esempio, un metodo consta dell'introduzione di segnali di rumore random codificati nella trasmissione e, allo stesso tempo, della variazione della fase di ogni chip del codice, sia che si tratti di dati codificati che di rumore. Un'altra è stata realizzata sfruttando i differenti ritardi tra i modi che si propagano all'interno di una fibra ottica multimodo, in questo modo la dispersione modale modifica il segnale trasmesso e viene poi compensata al ricevitore dell'utente autorizzato mediante una fibra multimodo analoga a quella usata nel trasmettitore. Dopo lo scrambling, il diagramma ad occhio del segnale trasmesso risulta chiuso e ciò indica che il segnale è completamente distorto, pertanto un eventuale intruso

non può rivelare il segnale attraverso una semplice rivelazione differenziale, ma ha bisogno di scoprire la chiave con la quale è stata codificata la trasmissione.

Al fine di utilizzare dispositivi già noti e disponibili in commercio, è stato proposto un sistema che realizzasse lo scrambling del segnale mediante due o più codificatori OCDMA in cascata, indicati come encoder e scrambler in Fig.2.22. Il segnale di informazione viene convoluto con due o più codici, cosicché la risposta impulsiva della catena di codificatori può essere vista come la convoluzione tra tutti i codici. Tanto più i codici sono tra loro incorrelati, tanto più il segnale risulta degradato e l'informazione non può essere rivelata da un potenziale intruso, neanche usando una rivelazione di tipo differenziale. Prelevando il segnale dopo l'ultimo codificatore, il diagramma ad occhio risulta chiuso e ciò indica che il segnale è completamente distorto, al punto che bit consecutivi possono sovrapporsi. Al ricevitore dell'utente autorizzato, i dati trasmessi possono essere estratti correttamente usando gli opportuni decodificatori.

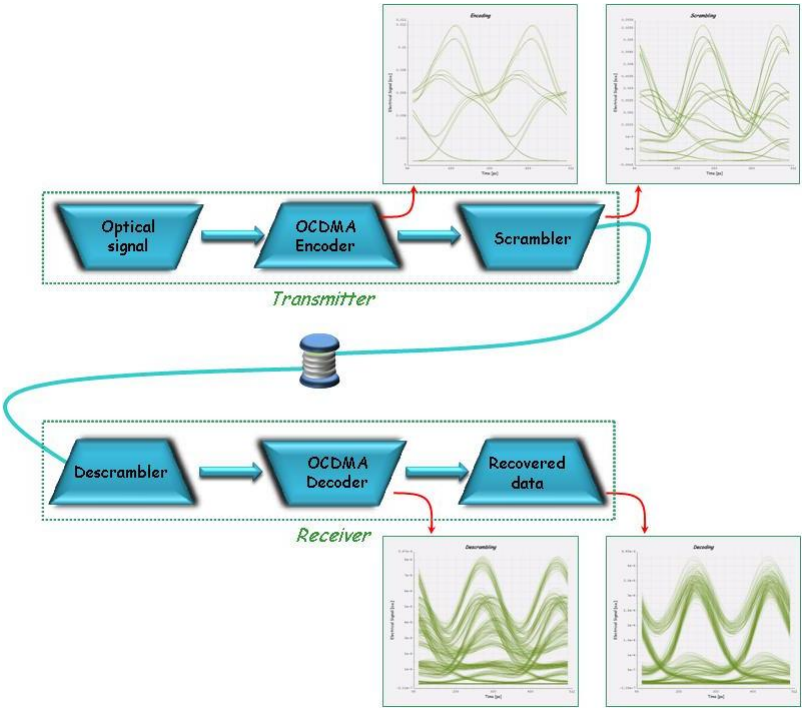


Figura 3: Scrambling con codificatori OCDMA in cascata. Dopo ogni codificatore è riportato il digramma ad occhio del segnale elaborato.

Un tale sistema introduce ulteriori gradi di libertà alla trasmissione per garantire una maggiore confidenzialità, rendendo computazionalmente più difficile per un utente non autorizzato perpetrare un attacco alla sicurezza della comunicazione. Infatti, l'eavesdropper non conosce la lunghezza del codice e il numero di codificatori usati. Anche supponendo, nel rispetto del principio di Kerckhoffs, che egli ne sia a conoscenza, deve comunque provare tutte le possibili combinazioni di tutte le possibili parole di codice usate per i diversi codificatori. Pertanto lo spazio delle chiavi aumenta esponenzialmente con il numero di encoder usati e con il numero delle parole di codice che essi sono in grado di generare.

Sono state effettuate delle simualzioni numeriche per valutare le potenzialità dello scrambling nel dominio ottico. Nel set-up di simulazione, realizzato mediante il software *VPItransmissionMaker*, il segnale viene inviato a due codificatori OCDMA in cascata, poi in una fibra singolo modo ed infine al lato ricevitore due decodificatori ricostruiscono correttamente il segnale. Lo scrambling viene effettuato mediante una elaborazione completamente ottica del segnale. Per la codifica sono stati utilizzati codici di *Kasami* ed i processi di codifica e decodifica vengono effettuati per mezzo reticoli di *Bragg* superstrutturati (SSFBGs) con un profilo ottimizzato mediante apodizzazione. Il profilo degli en/decoder OCDMA viene simulato dapprima mediante il software *Matlab*, per ottenere la risposta voluta, e successivamente vengono inseriti nei moduli di VPI. I codici di *Kasami* derivano dai più noti codici di *Gold*, di cui presentano caratteristiche analoghe e per certi aspetti superiori. Sono codici relativamente brevi ma con elevata cardinalità, perciò permettono di gestire più utenti senza dover ridurre il bit rate di ciascuno. Inoltre l'uso di reticoli di Bragg limita la capacità di decodifica da parte di un utente che non conosca i codici corretti, pertanto anche se in possesso di dispositivi molto sofisticati, la corretta rivelazione della trasmissione richiede molto più tempo e questo aumenta i gradi di libertà del sistema.

Dal momento che in una rete vi potrebbe essere un solo utente a trasmettere in un determinato istante, è bene che la confidenzialità di un sistema non dipenda dall'interferenza da multiplo accesso; di conseguenza la prima analisi fatta ha riguardato una singola trasmissione punto-punto (P2P). Il set-up di simulazione è stato realizzato per affinamenti successivi, testando ogni volta la corretta rivelazione del segnale da parte di un ricevitore in

possesso dei codici corretti. Sono state valutate le prestazioni del sistema in termini di Bit Error Rate (BER), mostrando che non è possibile rivelare correttamente il messaggio senza la conoscenza dei codici utilizzati per elaborare il segnale. Dal confronto dei diagrammi ad occhio dei segnali dell'utente e dell'eavesdropper si vede come il segnale venga distorto senza una corretta rivelazione. Per enfatizzare gli effetti dello scrambling sul segnale, è stata effettuata anche una simulazione mettendo in cascata fino a 4 codificatori: il segnale dopo ogni dispositivo è sempre più distorto ed il diagramma ad occhio ha molti più livelli, pertanto un utente non autorizzato avrà significative difficoltà nel decriptare la trasmissione. Inoltre, è stato analizzato un sistema che riducesse il numero di dispositivi nel trasmettitore e nel ricevitore utilizzando due reticoli di Bragg sovrapposti: le prestazioni risultano simili a quelle ottenute per due reticoli separati e questo permetterebbe una semplificazione dei dispositivi di trasmissione, ma risulta fisicamente più complesso da realizzare.

Successivamente, sono state proposte due differenti configurazioni per un'applicazione multi-utente. Nella prima, ciascun utente è dotato di un codificatore e di uno scrambler; i segnali così elaborati vengono combinati insieme ed inviati in fibra. Le prestazioni del sistema (BER) sono state analizzate considerando uno e due canali interferenti. Si vede che l'interferenza da accesso multiplo (*Multiple Access Interference*, MAI) concorre a degradare il segnale trasmesso e, quindi, a nasconderlo. Dall'analisi dei diagrammi ad occhio in presenza di uno e due canali interferenti si vede come la presenza di altri utenti non ostacoli la corretta rivelazione del segnale da parte dell'utente autorizzato. Nella seconda configurazione proposta, utilizzando la proprietà distributiva della convoluzione, ciascun utente è dotato del solo codificatore, poi i segnali vengono combinati tutti insieme ed a quel punto vengono inviati allo scrambler prima di essere accoppiati in fibra. Questa soluzione riduce il numero dei dispositivi necessari e potrebbe trovare applicazione nelle reti ottiche passive (PON), però risulta meno sicura della precedente poiché si riduce il numero degli scrambler e di conseguenza il numero dei codici usati. Anche in questo caso le prestazioni sono state misurate in termini di BER ed i diagrammi ad occhio mostrano che la presenza di un canale interferente non peggiora significativamente le prestazioni dell'utente autorizzato, mentre un eventuale intruso ha difficoltà a rivelare la trasmissione senza conoscere il

codice. Nel caso di un'applicazione multi-utente il punto critico è la scelta dei codici da utilizzare, poiché non solo sono necessari codici che siano ortogonali tra loro, ma devono essere ortogonali anche le differenti possibili combinazioni.

Nelle reti ottiche di nuova generazione, l'efficienza spettrale è un parametro critico, in quanto le nuove applicazioni, quali ad esempio videoconferenze e giochi real-time, richiedono un'elevata densità di informazione. Alcuni formati di modulazione avanzata, ed in particolare le modulazioni *Differential Phase Shift Keying* (DPSK) e *Differential Quadrature Phase Shift Keying* (DQPSK) vengono utilizzate per incrementare l'efficienza spettrale. Dall'altro lato, la tecnica OCDMA permette di gestire un elevato numero di utenti in una rete condividendo la stessa banda, pertanto diverse soluzioni sono state proposte per incrementare l'efficienza spettrale mediante tale tecnica. La combinazione con formati di modulazione quali la DPSK e la DQPSK concorre ad aumentare l'efficienza spettrale e diminuire il BER, rispetto all'utilizzo di modulazioni OOK o *Duobinary*. In questo caso l'efficienza spettrale è definita come $\eta = KB/\Delta f$, ove $K$ è il numero di utenti simultanei che possono trasmettere con bit rate $B$ e $\Delta f$ è la banda ottica. Anche se il rumore MAI ed il beat noise riducono drasticamente le prestazioni del sistema quando il numero di utenti aumenta, le modulazioni DPSK e DQPSK permettono di diminuire il BER. Pertanto, il numero di utenti che possono accedere alla rete simultaneamente aumenta. In Fig.4 sono mostrati tre diversi schemi ottenuti mediante la combinazione della tecnica OCDMA, con i formati di modulazione OOK, DPSK e DQPSK, rispettivamente.

Il rumore MAI risulta dominante nel caso di codifica incoerente, per la quale sono stati considerati codici ottici ortogonali (*Optical Orthogonal Codes*, OOC). Questi codici sono molto diffusi nelle reti a divisione di codice, perché possono essere generati in modo semplice con dispositivi passivi, costituiti solo da accoppiatori e linee di ritardo. In questo caso, le modulazioni DPSK e DQPSK permettono di migliorare le prestazioni in termini di BER, aumentando il peso dei codici usati; mentre per quanto riguarda l'efficienza spettrale, la DQPSK è la scelta che presenta i risultati migliori.

Il beat noise, invece, risulta dominante nel caso di codifica coerente, per la quale sono stati considerati i codici di *Gold*, largamente utilizzati grazie alle ottime proprietà di corre-

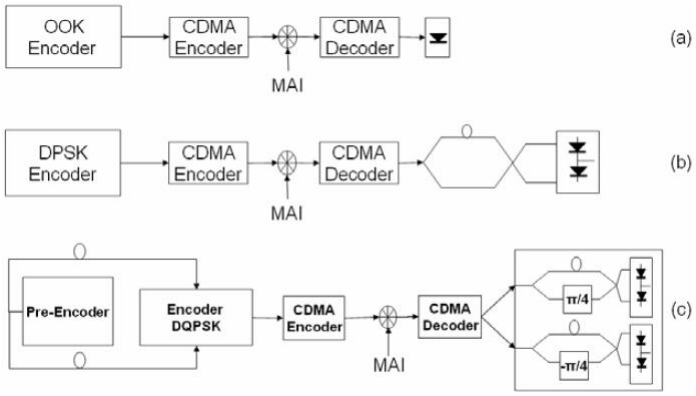


Figura 4: Schemi delle diverse architetture di un sistema OCDMA con differenti formati di modulazione: (a) OOK, (b) DPSK, (c) DQPSK.

lazione. Questi codici possono essere generati utilizzando, ad esempio, reticoli Bragg super strutturati. Anche in questo caso i formati DPSK e DQPSK risultano essere la scelta migliore se si vogliono incrementare le prestazioni del sistema, aumentando il numero di utenti che possono accedere alla rete simultaneamente. Inoltre l'utilizzo della modulazione DQPSK è molto efficace per quanto riguarda la riduzione della banda e l'aumento dell'efficienza spettrale.

La tecnica *Orthogonal Frequency Division Multiplexing* (OFDM) viene spesso usata nelle reti di nuova generazione, poiché offre il duplice vantaggio di mitigare gli effetti della dispersione in fibra e di garantire trasmissioni ad elevato data rate. E' caratterizzata, infatti, da un'elevata efficienza spettrale e da un'elevata tolleranza alla dispersione cromatica ed alla *Polarization Mode Dispersion* (PMD), grazie alla ridotta porzione di banda occupata da ciascun sottocanale che incrementa la robustezza del sistema. Queste caratteristiche permettono di aumentare la distanza raggiungibile prima che si abbiano significative distorsioni nella trasmissione, fino a migliaia di kilometri, con elevati bit rate, senza il bisogno di introdurre compensatori di dispersione. L'elaborazione del segnale nei trasmettitori e ricevitori OFDM utilizza l'algoritmo *Fast Fourier Transform* (FFT), che permette l'uso dei disponibili dispositivi per l'elaborazione digitale dei segnali (*Digital Signal Processing* – DSP). Dopo l'elaborazione, il segnale OFDM viene modulato su una portante ottica e

trasmesso in fibra. Per la ricezione possono essere usati schemi di rivelazione diretta o coerente, a seconda che si voglia un sistema più semplice o più sensibile ed a seconda del dominio di applicazione.

I sistemi a rivelazione coerente (*Coherent* OFDM, CO-OFDM) offrono una virtualmente illimitata tolleranza alla dispersione con un'elevata efficienza spettrale, permettendo di raggiungere grandi distanze; essi però richiedono ricevitori complessi costituiti da oscillatori locali, *Phase-Locked Loop* (PLL) ottici e controllori di polarizzazione. Dall'altro lato, i sistemi a rivelazione diretta (*Direct Detection* OFDM, DD-OFDM) riducono sensibilmente la complessità del hardware dei ricevitori, ma non hanno prestazioni altrettanto elevate. Comunque, le prestazioni ottenibili con i sistemi DD-OFDM risultano essere accettabili e rientrano nei limiti di una correzione dell'errore mediante *Forward Error Correction* (FEC), pertanto possono essere una efficace ed economica soluzione nelle reti ottiche di nuova generazione, in particolare nel caso delle reti di accesso, nelle quali permettono di aumentare il bit rate, grazie ad un incremento dell'efficienza spettrale.

Sfruttando la proprietà delle trasformate trigonometriche, nelle reti ottiche è possibile sostituire la tradizionale trasformata di *Fourier* (*Discrete Fourier Transform*, DFT) con la trasformata *Hartley* (*Discrete Hartley Transform*, DHT), come già dimostrato nelle comunicazioni wireless ad elevato bit rate. In questo modo è possibile ottenere sistemi di trasmissione più economici rispetto alla tecnica OFDM convenzionale.

La separazione delle sotto-bande in frequenza e la loro ortogonalità rimangono inalterate, ma grazie al kernel della DHT, ciascun simbolo della sequenza di informazione viene portato da due sotto-bande simmetriche, aumentando così la diversità in frequenza. Inoltre le trasformate diretta ed inversa di Hartley sono identiche, pertanto lo stesso dispositivo può essere utilizzato come trasmettitore e come ricevitore. La complessità computazionale della DHT è minore di quella della DFT, poiché sono necessarie solo moltiplicazioni reali e ciò risulta in una più semplice e veloce implementazione dell'algoritmo di calcolo. Il fatto poi che la DHT permetta di lavorare su segnali reali semplifica la conversione del segnale OFDM in un segnale ottico per essere trasmesso in un sistema a modulazione di intensità e rivelazione diretta. Inoltre, come nel caso della FFT, anche la DHT può essere eseguita

mediante un algoritmo più veloce, che prende il nome di *Fast Hartley Transform* (FHT).

L'utilizzo della FHT permette di ridurre il numero dei dispositivi elettronici necessari per l'elaborazione del segnale OFDM; infatti, se la sequenza di dati in ingresso viene mappata su una costellazione reale, la FHT inversa (IFHT) fornisce un segnale reale, pertanto solo la componente in fase dovrà essere elaborata, eliminando la componente in quadratura. In questo modo il numero dei convertitori analogico-digitali (DAC/ADCs) viene dimezzato, Fig.5.

L'OFDM basata sulla DHT può essere un'interessante applicazione per il segmento di accesso, in particolare nelle reti ottiche passive (PON), essendo un sistema a più basso costo.

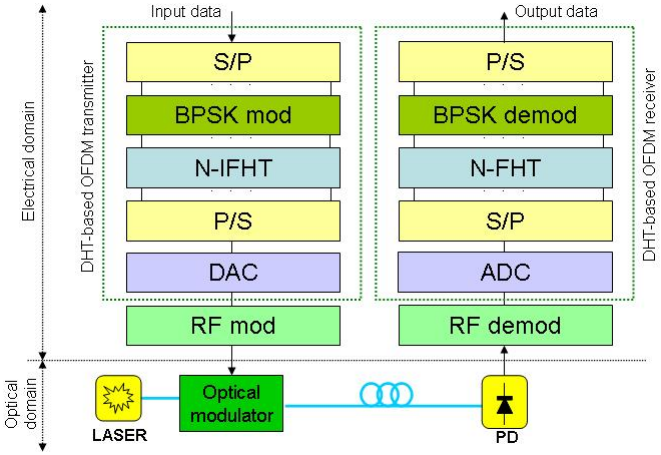


Figura 5: Schema di un sistema di trasmissione OFDM, con elaborazione del segnale mediante FHT.

Recentemente, infatti, l'OFDM è stata proposta come soluzione per le reti di accesso ottiche ed una sempre più diffusa proposta è quella di integrare la tecnica OFDM nelle PON, nota come OFDMA-PON, una tecnica ibrida data dalla combinazione tra OFDM e TDM. In questo modo, oltre ai vantaggi dati dall'introduzione dell'OFDM nelle reti ottiche, è possibile supportare differenti servizi in modo trasparente e allocare la banda tra di essi dinamica,emte, grazie al fatto che le sotto-portanti OFDM possono essere associate a differenti servizi in diversi istanti di tempo ed alcune di esse possono essere riservate per servizi particolari. Inoltre ciascuna sotto-portante può essere modulata in modo indipen-

dente, aumentando così il data rate delle reti già esistenti, grazie ad un miglioramento dell'efficienza spettrale.

A ciascuna ONU viene assegnato un sottocanale, che può essere composto da una o più sotto-bande OFDM, e può implementare schemi di modulazione e di protezione del dato diversi dalle altre ONU. Ogni ONU mappa il proprio segnale sulle sotto-portanti assegnate, mette le altre a zero e completa la modulazione per formare un frame OFDM. Quest'ultimo viene convertito in un segnale OFDM ottico e combinato con quelli provenienti dalle altre ONU, prima di essere inviato all'OLT. Dall'altro lato, l'OLT mappa i segnali da inviare alle singole ONU sulle sotto-portanti date e nei time slots assegnati, poi li converte in frame OFDM. Quando il segnale così costituito raggiunge le ONU, esse sono in grado di estrarre il segnale dalle sotto-portanti a loro dedicate.

In questo modo, le OFDMA-PON raggiungono il duplice obiettivo di fornire maggiore banda e raggiungere maggiori distanze rispetto alle TDM-PON ed inoltre, rispetto alle WDM-PON, di ridurre il numero dei ricevitori nell'OLT e di poter assegnare la banda tra le varie ONU in modo dinamico. Offrono anche la possibilità di aumentare o ridurre il numero delle ONU gestite senza bisogno di modificare l'hardware.

Inoltre una possibile futura applicazione potrebbe essere quella di integrare la tecnica OOFDM (Optical-OFDM) con l'OCDMA per sfruttare al meglio i vantaggi che ciascuna delle due offre. Questo permetterebbe di migliorare le prestazioni nelle reti ottiche passive, in più aprirebbe nuove possibilità nell'ambito delle reti sicure.

Al fine di estendere la trasparenza ottica al segmento di accesso e di utilizzare soluzioni semplici ed economiche, una possibile alternativa alle reti *wired*, può essere l'utilizzo delle reti ottiche *wireless*. Questi sistemi utilizzano fasci laser nell'infrarosso trasmessi in aria, permettendo di sfruttare la banda offerta dalla fibra ottica, sono integrabili con altri sistemi di comunicazione, sono compatibili con qualsiasi protocollo di comunicazione e supportano la tecnologia *Dense Wavelength Division Multiplexing* (DWDM). Inoltre, non sono soggetti ad interferenze e cosituiscono un sistema di comunicazione sicuro grazie all'elevata direttività del fascio laser. I sistemi ottici nello spazio libero (*Free Space Optics*, FSO) costituiscono una valida soluzione nel caso di "*Disaster Recovery*", permettendo di creare

link temporanei ad elevato bit rate, e potrebbero essere una soluzione per il cosiddetto problema dell'*ultimo miglio*, offrendo una connessione veloce per l'utente finale senza bisogno di installare i cavi. Esisitono però dei fattori che ne limitano l'utilizzo, quali l'attenuazione dovuta alle condizioni atmosferiche, la necessità di una linea di vista tra i dispositivi di trasmissione e ricezione e la limitata distanza che possono raggiungere, circa 5Km. La nebbia, in particolare, rappresenta un ostacolo per le comunicazioni ottiche wireless, in quanto la dimensione delle particelle è simile a quella della lunghezza d'onda del segnale ottico, causando un grado di interazione molto elevato. La nebbia può introdurre nel canale di comunicazione un'attenuazione che fino a 300dB/Km.

Realizzando sistemi wireless ottici completamente trasparenti, è possibile eliminare le conversioni elettrico-ottico-elettriche, attualmente utilizzate nei dispositivi commerciali, così da sfruttare le elevate velocità di trasmissione dei sistemi in fibra e realizzando un diretto collegamento con le reti di accesso. Un sistema di questo tipo è stato realizzato e poi sperimentato presso i laboratori dell'Istituto Superiore delle Comunicationi a Roma.

Nel sistema realizzato, il fascio laser viene trasmesso in aria direttamente da una fibra troncata con l'ausilio di un'ottica di lancio, che permette di collimare il fascio su lunghe distanze. Il fascio si propaga nello spazio libero per una distanza di 100m ed in ricezione viene focalizzato direttamente nel core di una fibra singolo modo, utilizzando una lente focalizzatrice ed una lente GRIN, che permette l'accoppiamento del fascio trasmesso nel core della fibra.

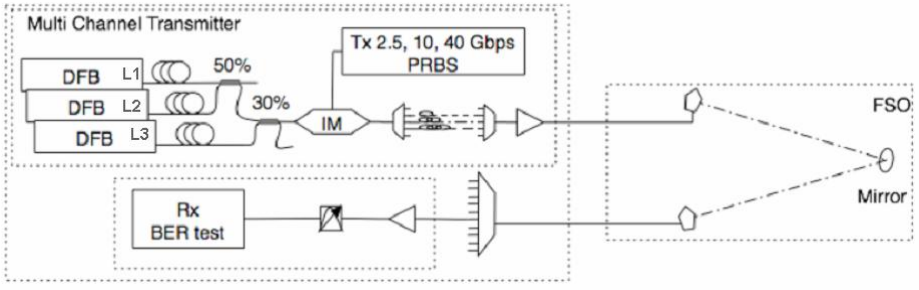


Figura 6: Schema del sistema FSO realizzato.

I dispositivi di trasmissione e ricezione sono stati posizionati in due laboratori attigui,

mentre nel cortile adiacente i laboratori è stato messo uno specchio, ottenendo così una linea di vista "virtuale". Il trasmettitore ed il ricevitore sono stati dotati di dispositivi che permettono movimenti micrometrici per garantire un accurato allineamento di fibre e lenti. E' stato dapprima testato un sistema con Bit rate pari a 2.5Gb/s ed in differenti condizioni, confrontandolo poi con i risultati ottenuti in back-to-back. Successivamente sono state testate due trasmissioni a 10Gb/s e 40Gb/s, rispettivamente. La caratterizzazione del sistema è stata effettuata valutandone le prestazioni in termini di BER e fattore Q; è stato inoltre analizzato l'effetto delle condizioni atmosferiche sull'affidabilità del sistema. Successivamente, per aumentare ulteriormente il bit rate disponibile, è stata anche testata una trasmissione DWDM, come mostrato nel setup di Fig.6, effettuando misure di BER in presenza di due canali interferenti, In entrambi i casi non sono stati riscontrati elevati effetti di interferenza tra i canali. I test effettuati hanno messo in evidenza l'importanza della stabilità meccanica dei dispositivi di trasmissione e ricezione, nonchè la necessità di un corretto allineamento dei suddetti dispositivi. Il sistema proposto risulta comunque integrabile con le attuali tecnologie ottiche per l'accesso, mantenendo elevate qualità di trasmissione.

# Contents

Chapter 1

# Introduction

The frenzied development of networks during recent years, due to the ever-increasing bandwidth demand, has caused a situation characterized by heavy disparities among the different network sections. Fibre optics technology has allowed the construction of long distance links (wide area networks, backbones, information highways) with large available bandwidth and high bit-rates. With the improvement of technology, data rates of the order of hundreds of Gb/s will be reached. In the meantime, new applications requiring more and more bandwidth such as video on-demand, voice over IP, fast internet access and web pages full of multimedia effects have appeared and local area networks (LAN), based above all on Ethernet, have also developed assuring reliability and very high speed. Therefore, the problem nowadays mostly involves the access network, where operating is still expensive and difficult. The so called problem of . The last mile problem, commonly known as the "*last mile bottleneck*", still represents the biggest challenge in the world of modern communication.

The high bandwidth capability of the fibre optic backbone of 2.5Gb/s to 40Gb/s has been achieved by improvements in switching and optical components, and with the implementation of technologies such as wavelength division multiplexing (WDM). The current fibre optic backbone runs to central offices in most population centers. Until now, most the efforts of laying down new fibres has been directed towards extending the fibre optic backbone to new central offices, as opposed to laying fibre directly to the customer. LANs,

on the other hand, are commonly based on high speed fast Ethernet (100Mb/s) or even Gigabit Ethernet (1Gb/s). Therefore, these data networks meet the needs for local connectivity within a single floor or building. However, similarly high data rate connection speeds between buildings either locally or nationwide have become more and more necessary. Consequently, there is a requirement for a high-bandwidth bridge (the "last mile" or "first mile") between the LANs and the MANs (metropolitan area networks) or WANs (wide area networks). Access to the fibre optic backbone for the majority of customers physically located within a mile of the fibre is limited to the current phone or cable TV copper wire infrastructure. Technologies, such as Digital Subscriber Link (xDSL) or cable modems have increased the potential bandwidth over copper to 5 or 6Mb/s over more traditional Integrated Services Digital Network (ISDN) or T-1 (1.5Mb/s) lines. However, these copper-based transmission speeds are still much lower than what is necessary to fully utilize the Gb/s fibre optic backbone. In addition, the ownership of the copper wires requires leasing by other carriers or network service providers [1].

The goal of increased bandwidth can be fulfilled by extending the optical transparency to the last segment of the network. Therefore, there has been an upsurge interest in the introduction of optical technologies in access networks in order to address these disparities and to cope with the demand of wide-area high bandwidth, due to the increasing commercial use of Internet, private Intranets, electronic commerce, data storage and backup, virtual private networks (VPNs), video conferences, voice over IP and so on.

This thesis deals with the analysis of the introduction of optical technologies in the next generation of access networks. The aim of this research is to focus on different aspects that contribute to increasing such networks feasibility and performance. The particular topics investigated were as follows: firstly the level of security to assure high physical layer protection of transmitted data; secondly the use of advanced modulation formats to increase the allowed bit rate and the spectral efficiency, which, in turn, improves the system overall performance; then, finally, the extension of optical transparency to the access network through optical wireless technology.

## 1.1 All-optical Networks

In the optical fiber communication approach, information is transported to one point to another by using light as a carrier and by means of a physical medium able to transmit data at high bit rate over long distances. Therefore, increasing the available bandwidth by the introduction of optical technologies has greatly enhanced the performance of telecommunications networks. The capacity of communication depends on the carrier frequency: The higher the carrier frequency, the larger the available transmission bandwidth. Thanks to the fact that the optical carrier frequency ranges from $10^{13}$ to $10^{16}$Hz, optical fibres have an enormous communication capacity, much higher than copper cables or even millimeter wave radio systems. An additional advantage is that, unlike in the case of coaxial cables, optical communication media are not affected by electromagnetic interferences and suffer from only low transmission loss (0.2dB/km).

The benefits derived from the use of optical technology in communication systems have led to a huge development in optical devices and optical fibre systems, over four generations.

The first generation of optical fibre systems, based on GaAs optoelectronic components, appeared at the end of the 70's and used electromagnetic short wavelength at 0.85m (1st window) and multimode optical fibres. This system capacity was limited by the intrinsic mode dispersion of multimode fibres.

The second generation (80's) used a longer wavelength at 1.3$\mu$m (2nd window) and a single mode fibre whose losses were reduced from 4dB/km to 0.5dB/km. Light emitting diodes (LEDs) or laser diode (LD) were used as light sources. These changes led to an increase in capacity and distance.

The third generation systems use a wavelength of 1.55$\mu$m (3rd window) and dispersion-shifted single mode fibers, so decreasing the loss to 0.2dB/km. A high bit rate of 2.5Gb/s over longer distances, as in the case of long-haul or submarine long-span networks, can be achieved. A InGaAsP LD or a distributed feedback (DFB) LD can be used as a light source.

The fourth generation, for its part, introduces a new type of fibre, namely the non-zero-dispersion single-mode fibre. Moreover uses a wavelength of 1.55$\mu$m and WDM technology.

Optical amplifiers such as erbium-doped fiber amplifiers (EDFAs) and Raman amplifiers are used to increase the transmission distance. The data rate per wavelength is in the range of 2.5Gb/s to 10Gb/s. The trend of the research effort on optical fibre systems is to further improve network performance, by developing ultra-large capacity and ultra-long distance systems.

Optical networks have evolved in parallel with the improvements on optical fibres. For many years, the main goal was to develop technologies to allow the transmission at higher and higher bit rates over increasing distances.

The so-called *first generation optical networks* exploited the advantages of the optical fibres, while leaving all the switching and the processing of the signals to be performed by electronics [2]. The demand for an increase in bandwidth together with the costliness of wiring both prompted the search for a method for increasing the capacity of existing fibres without having to lay new ones. The first approach was to increase the supported bit rate by all optical implementation of multiplexing techniques, such as optical time division multiplexing (OTDM) and wavelength division multiplexing (WDM), in order to overcome the impairments of high-speed electronics. This has led to a large scale expansion of long-haul networks, thanks to the traffic growth. Dense WDM (DWDM) represents the best tradeoff between cost and capacity for backbone networks and also provides benefits to MAN. Subsequently, at the end of 80's, the replacement of electro-optics regenerators with optical amplifiers (erbium-doped fiber amplifier, EDFA, or semiconductor optical amplifier, SOA) introduced further improvements in optical systems.

The *second generation optical networks* are characterized by a reduction of the use of electronics, reaching a higher degree of transparency. This yields to higher throughput and enables optical networks to provide more functionalities, such as switching and routing functions. Moreover, the physical layer of the second generation optical networks supports WDM links and add/drop functions. These networks may offer three kind of services to higher networks layers. The first of these services is a *lightpath* service, applicable in WDM networks, in which a dedicated wavelength is assigned to a connection between two node. The connection can be set up and down upon request (*circuit switched*) or can be *perma-*

*nent*. The second service is a *virtual circuit* service, a circuit switched connection between two nodes with a smaller resource, which makes it possible to manage fixed or statistical multiplexing. Thirdly, there is a *datagram* service, which makes it possible to transmit short packets between the nodes without the necessity of setting up explicit connections [2].

In 1998 ITU-T (International Telecommunication Union-Telecommunication Standardization Sector) introduced the concept of optical transport network (OTN), in order to use WDM wavelength routing and eliminate the effects of electronic bottleneck in the network nodes, thus greatly increasing network transmission capacity and throughput of nodes. WDM-OTN uses optical add/drop multiplexing (OADM) devices and optical cross-connection (OXC) devices in its nodes, so eliminating the optical-to-electrical conversion.

However the traditional OTN has many shortcomings and cannot totally satisfy the requirements of optical networks. Therefore, in 2001, ITU-T defined the architecture for the automatically switched optical network (ASON). The concepts of dynamic switching and cooperation mechanism between the service land transport layer were introduced; thus, optical communication networks, besides being an optical transport network, also include the functions of switching and control. According to the ASON network architecture three planes can be identified: transport plane (TP), control plane (CP) and management plane (MP). ASON supports permanent connections, soft permanent connections and switching connections, including unidirectional point-to-point connections, bi-directional point-to-point connections and bi-directional point-to-multipoint connections. Moreover, ASON guarantees service transparency, broadband services and high quality application, effective protection and recovery mechanisms, real time traffic engineering control and bandwidth management over optical layer, good device interoperability and network scalability [1].

## 1.2 Optical Access Networks

The use of new techniques continually upgrades the performance of OTN. As a consequence, the access network has many problems such as narrow bandwidth, high failure rate and high costs of operation and maintenance. The copper cable is still the main trans-

mission media in access networks and is not able to support new services and applications, especially multimedia and broadband services. Thus, as said previously, the access network has become the bottleneck of communication networks [1].

The current broadband access technologies, such as asymmetric digital subscriber line (ADSL) based on telephone lines and the cable modem (CM) based on common antenna television (CATV), can meet the needs of some services such as Web surfing, email and so on. However, it is not able to satisfy the bandwidth requirements of multimedia services and broadband services, also called triple play, such as high-speed Internet, IP phone and broadcast video, etc.

With ADSL technology, the volume of data flow of uplink and of downlink is asymmetric. Such a volume is basically suitable for applications such as user surfing on the Internet and video on demand (VOD), but is not applicable to interconnecting local area networks (LAN). Deploying ADSL with ATM/Ethernet, internet access services are available. The customer end is equipped with ADSL remote devices and is connected to the digital subscriber line access multiplexer (DSLAM) at the central office by common telephone wires. ADSL remote devices provide the Ethernet interface for the user computers, while DSLAM connects with the Internet service provider (ISP) by ATM (asynchronous transfer mode) or fast Ethernet (FE).

On the other hand, cable modem is another broadband technique with asymmetric uplink and downlink. It is suitable for providing two kinds of services, Internet surfing and VOD. In this case, internet access service can be offered by means of hybrid fiber coaxial cable (HFC), Cable Modem and Ethernet/ATM. The HFC transmits data signal to the subscribers while the cable modem decodes, demodulates and transmits it to a personal computer via an Ethernet port. For the uplink, the cable modem receives the signal from the PC and sends the modulated and encoded signals to the head end devices by HFC. The bandwidth of the cable modem is larger than that of ADSL. How ever, when a cable modem and HFC are used to build up a network, a lot of problems arise in regards to stability, reliability, power supply, operation and maintenance.

In both cases, the bandwidth of the network links is shared among all the users. There-

fore they can not actually offer broadband digital services when the number of users increases, because the bandwidth that is assigned to each user is highly limited. Therefore, optical access network (OAN) represents the trend towards the access network of the future [1]; in particular, optical code division multiplexing (OCDM) technique can be a solution for coping with the problem of shared resources, as will be discussed later.

Optical access networks can be divided into two categories, the active optical network (AON), which uses electrical demultiplexers, and the passive optical network (PON), based on optical demultiplexers. A PON has a simple architecture and has no active elements in the whole link from the source to the destination. It makes it possible to minimize the use of fibre and the number of transceivers by the use of passive splitters/couplers. Hence, PON is a promising technique, reducing operation and maintenance cost, while also being highly transparent. The use of this technology can limit the probability of lines and outdoor devices failing; it also improves the reliability of systems, thanks to the fact that PON can prevent the effect of electromagnetic interference and damage to outdoor devices by thunder. This technology is also suitable for signals with any given format and bit rate. In Fig.1.1 different implementations of PON architecture are shown, called FTTx (fiber to the "x"), where "x" has different meanings depending on where the optical link arrives. The optical link can directly connect an end user or a single building, in which case the network is called "fibre to the home" or "fibre to the building", respectively. Otherwise, if the optical link reaches the cabinet, while the end users are connected by copper cables, the network is known as "fibre to the curb" or "fibre to the cabinet". For all the architectures, a passive optical network is constituted of three main elements: an optical line terminal (OLT), which furnishes the services and sends the signal broadcast to the customer; a passive splitter, which splits the power of the optical signals; and, thirdly, the network interface units (NIU) or the optical network units (ONU), which are the interfaces between the users and the services offered by the network.

PON can be divided into two main groups: TDM-PON, which uses the TDM technology to handle traffic, and WDM-PON, which combines together both techniques of WDM and PON.

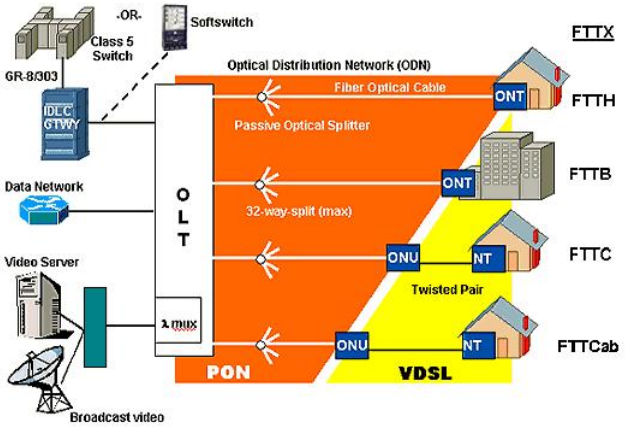


Figure 1.1: FTTx examples: Fibre to the home (FTTH), fibre to the building (FTTB), fibre to the curb (FTTC), fibre to the cabinet (FTTCab), [3].

TDM-PON is a point-to-multipoint architecture and data are broadcast to each ONU by the shared transmission link. The current TDM-PON supports data rates from 155Mb/s to 1Gb/s, which is shared among 8 to 128 users. TDM technology is employed to handle upstream traffic. However the time-share transmission reduces the bandwidth for a single user. In Fig.1.2, the operation principle of a TDM-PON is shown. TDM-PON can be classified as APON (ATM-PON), based on ATM, and EPON (Ethernet PON), based on Ethernet [4]. The former is based on the technology of concentration and statistical multiplexing of ATM; however, its use of fixed length cell makes carrying IP packets a very complex process, consumes considerable time and increases the additional cost of OLT and ONU. EPON, for its part, uses different transmission techniques for data downstream from the OLT to the ONUs and for data upstream from the ONUs to the OLT. The broadcast technique is employed to transmit data downstream from the OLT to multiple ONUs with variable length packets, each one has a header to effectively identify its destination. The traffic is divided into separate signals by the splitter. Each signal carries all the packets directed to the ONUs. When an ONU receives the data signal, it only accepts the packets intended for it and discards the ones directed to the other ONUs. The upstream traffic is managed by the use of TDM technology and each ONU has dedicated time slots. Once the data are coupled into the common fiber, the upstream packets from the ONUs do

not interfere with each other. In comparison with ATM, Ethernet reduces the overhead dynamically, because it is able to carry IP services.

However, in PON systems based on time division multiple access (TDMA), it is difficult to provide bandwidth of Gb/s to all the users. Therefore, TDM-PON is not an effective solution for implementing fibre-to-the-home (FTTH) systems, which cable end-users with fibres and to transport symmetric services with a rate of Gb/s.

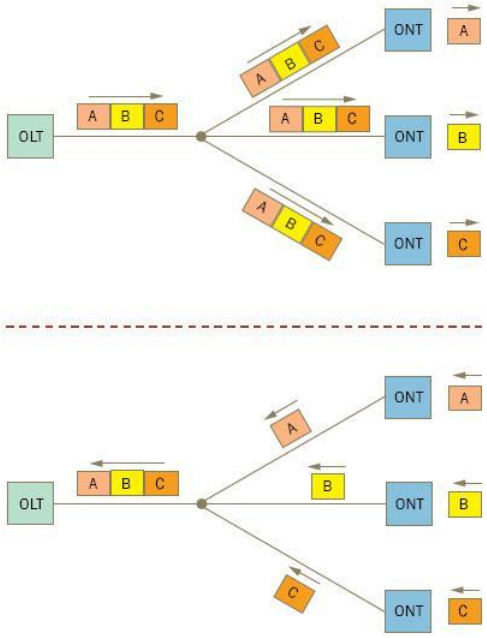


Figure 1.2: TDM-PON principle: downlink (top); uplink (bottom), [4].

An omogeneous combination of WDM techniques and PON yields to the so-called WDM-PON, in which a unique wavelength is assigned to each user, establishing a virtual point-to-point connection between OLT and users [5]. A wavelength mux/demux device at the splitting point can route wavelength channels from the OLT to the proper ONU and backward, Fig.1.3.

Coarse WDM (CWDM) technology can be used in such networks. The wavelength spacing is 20nm and the total usable channels are 18. ITU recommendations define the optical interface standards of CWDM and the total wavelength range from 1270nm to 1611nm. Thanks to the use of the low-water-peak fibres defined by ITU G.652 C&D, the

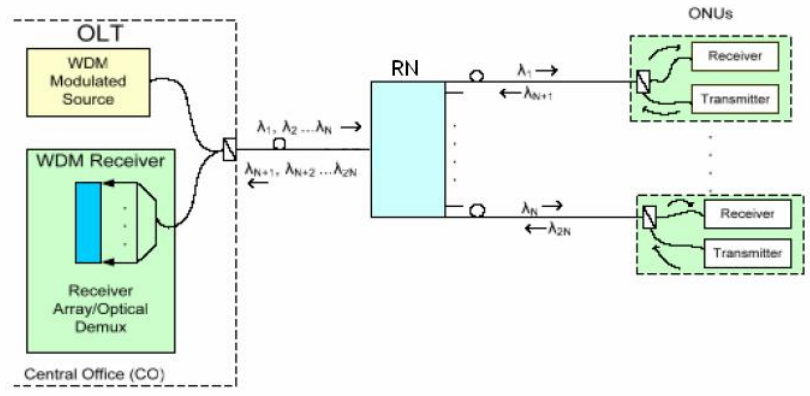


Figure 1.3: WDM-PON architecture, [1].

attenuation in the wavelength range from 1370nm to 1410nm in ordinary single mode fibers is eliminated; this range can be also used in CWDM to achieve broad spectral range transmission. Nonetheless, CWDM has several shortcomings: The transmission distance may be limited when the data rate becomes higher. This is because the dispersion increases with the increase of wavelength; the transport distance and the light separation ratio are limited, since the shorter the wavelength, the greater the channel loss. Another technique can be introduced to offer sufficient bandwidth to more users: Dense WDM (DWDM), in which the wavelength spacing is much smaller than that of CWDM, up to 0.8nm. However, since DWDM-PON needs tunable wavelength devices and temperature control, its cost is higher than that of CWDM-PON. Despite all the advantages over TDM-PON, such as high bandwidth and protocol transparency, some features prevent WDM-PON from large-scale application: It lacks the flexibility to dynamically allocate the bandwidth among multiple services and raises system costs due to requirements for multiple transceivers.

In future optical networks, besides the triple play, the service demand will evolve to high bit rate, i.e. super-high-definition class digital movies, bi-directional medical applications of telediagnosis and surgery, and to customization, such as a wide variety demand of quality of service (QoS). Therefore, an abundant bandwidth will also be necessary in the case of uplink, either on demand or on an always-on basis. Thus, an upgrading scenario of FTTH should be developed into a novel-system of gigabit-symmetric FTTH from the current

FTTH with asymmetry between the uplink and the downlink.

A possible candidate for future Gb/s symmetric FTTH can be the OCDMA technique, a different multiplexing technique other than TDMA (time division multiple access) and WDMA (wavelength division multiple access), which allows the user to share the entire available bandwidth. This technique can implement the multiplexing, switching and add/drop of multi-channel signals over the backbone network and MAN (metropolitan area network) separately, or in a combination of TDM and WDM through the encoding and decoding of the optical signal directly [6]. Moreover, OCDMA can realize the multiple-access networking among many users over LAN (local area network) and the access network.

The Chapter 2 and the first part of Chapter 3 deal with the introduction of OCDMA technique in the access networks. After a wide description of the characteristics of OCDMA, Chapter 2 focuses on an aspect that has gained a lot of interest in the research, the physical layer data security. Since optical technologies are considered as the solution for the next generation networks, physical layer security is a key request in order to avoid information theft from unauthorized users along the path in fibre transmission links. In particular, the level of security of an OCDMA network have been investigated and different solution have been proposed.

Afterwards, in the first part of Chapter 3 the influence of the introduction of OCDMA in combination with different advanced modulation formats on the spectral efficiency of an optical link have been investigated. Spectral efficiency is a critical parameter in optical links, because of the wide demand of high information density services.

To cope with the wide demand of different QoS, another solution can be the introduction of an hybrid technique coming from the combination of OFDM and PON, namely the OFDMA-PON. OFDM sub-carriers can be dynamically assigned to different services in different time slots, therefore the use of OFDM in PON allows the support of various applications in a transparent way and enables dynamic bandwidth allocation among the services [7].

The second part of Chapter 3 deals with the analysis of the optical orthogonal frequency multiplexing (O-OFDM) technique, where an OFDM signal is modulated on an optical

carrier and sent into a standard single mode fibre, achieving high bit rates and mitigating fibre's impairments. The application of O-OFDM in PONs is investigated and a new type of OFDM is proposed, exploiting the properties of trigonometric transforms.

Sometimes, it could happen that establishing wired connections in the last segment of the networks is not convenient and wireless solution could be more suitable. Therefore, optical wireless technology can be individuated as a valid solution to build low cost links faster and to propose a valid alternative to the wired connection for the future FTTH, preserving the entire bandwidth of optical fibres and the optical transparency up to the *last mile* [8].

Chapter 4 deals with the investigation on free space optics (FSO) systems. A transparent wireless optical systems is proposed and experimentally tested in order to extend the transparency to the last mile and to overcome the impairments due the E-O-E (electrical - to optical - to electrical) conversion.

Chapter 2

# Security in OCDMA Networks

## 2.1 Optical Code Division Multiplexing

Optical Code Division Multiplexing (OCDMA) has become a promising technology for truly all-optical communication and for networking based on direct optical signal processing [1]. It combines the advantages of electrical CDMA with the bandwidth predominance of fiber-optic and optical signal processing devices. The advantage of sharing common resources and a more effective use of the available bandwidth, combined with the asynchronous and simultaneous access, make OCDMA attractive for future broadband networks. Passive optical access networks (PON), LAN and MAN, can be based on OCDMA technology.

Code division multiple access (CDMA) technology was introduced in military communications and has been used for a long time, since the late 1970's, in order to resist intended interference and to implement low probability detection. It was a spread frequency technique increasing the robustness of information transmission. Nowadays, CDMA has been widely used in the field of wireless communication, in particular in the third generation wireless communication systems. OCDMA technology realizes multiplexing transmission and multiple access by coding in the optical domain, supports multiple simultaneous transmissions in the same timeslot and the same frequency. Thanks to its easy access and flexible network structure, OCDMA is suitable for access networks. In 1986, Prucnal, Santoro and

Fan proposed a LAN by using optical signal processing [9, 10] and verified the feasibility to implement incoherent OCDMA system by encoding in the time domain. In 1988, Weiner, Heritage and Salehi demonstrated how to spread the femtosecond optical pulse into picosecond-duration pseudonoise bursts. They proposed that frequency domain encoding and decoding of coherent ultrashort pulses could have led to a fast reconfigurable OCDMA network [11]. The spread frequency was achieved by encoding the light spectrum into pseudorandom binary phase codes, by using a grating to separate the spectrum of the femtosecond pulse and of a pseudorandom binary phase mask patterned according to the code. Then decoding the spectrum phase encoded would recover the original pulse [12].

Optical encoding and decoding for incoherent OCDMA uses unipolar codes, which were studied extensively in the earliy years. The research focused on obtaining unipolar codes with good auto- and cross- correlations, such as optical orthogonal codes (OOC) [13, 14, 15] and prime codes (PC) [16, 17]. One-dimensional OOCs possess the ideal correlation properties and have large cardinality (number of code-words), which, is, however, proportional to the length of the time spread (code length) and is approximately inversely proportional to the square of the code weight. Whilst the error probability increases when the code-weight becomes smaller. Furthermore, the data rate for a single user is inversely proportional to the length of the time spread and the number of user is inversely proportional to the data rate for a single user. Therefore, in order to achieve the required bit-rate, the simultaneous number of active users in the network must be reduced. For these reasons, the application of one-dimensional codes to incoherent OCDMA is limited and around 1990, two-dimensional codes [18, 19, 20] were proposed to increase the systems capacity and to improve their performance.

On the other hand, coherent OCDMA uses bipolar codes, employing directly the codes used by RF CDMA communication systems, such as *Gold* codes, *Walsh Hadamard* codes. Then, since the mid-1980's, the research was focused mainly on how to implement bipolar encoding and decoding physically and how to analyze and improve system performance [21, 22]. Temporal phase encoding has been proposed, integrated optics or super structured fibre Bragg gratings [23, 24, 25, 26] being used to realize the optical time-phase

encoders/decoders. After the development of the technology for FBGs, fiber-optic grating has been widely used and has been applied to implement spectral amplitude encoding, spectral phase encoding, temporal phase encoding and the hybrid wavelength-time encoding [27, 28, 29, 30]. A lot of laboratory experiments and field trials of OCDMA systems have been done [31, 32] and showed very good possibilities for the optical access network.

### 2.1.1 Characteristics and classification of OCDMA systems

OCDMA technique provides another dimension for multiple access, other than time- and wavelength domains of well-known multiplexing techniques, such as Time Division Multiple Access (TDMA), Frequency Division Multiple Access (FDMA) and Wavelength Division Multiple Access (WDMA). It allows a more effective sharing of the resources among the users of an optical network, because all users can share the entire available bandwidth, transmitting at the same time and at the same wavelength. This is possible thanks to the use of a code that univocally identifies the sender: each user encodes his data with the code and sends them in the network, multiplexed with other users' signals [13].

Figure 2.1 shows a scheme of a standard OCDMA system: each data sequence is encoded by an optical device that assigns a code to the user and the N encoded signals are multiplexed together using a $N \times N$ star coupler; the resultant signal is sent to the optical network.

In an OCDMA system an encoder and a decoder are necessary for each user, which has a different code (also known as *signature sequence*), independent from the signal that to be transmitted. Each code is composed of a certain number of *chips*, with time duration $T_c$ shorter than the duration $T_b$ of the bit they represent. So each bit of the original signal becomes a sequence of shortest chips due to the encoding process and the spectrum of encoded signal is larger than the original one. This technique is also known as *spread spectrum* and the spreading factor is the rate $T_b/T_c$. The signal sent into the fiber-optic channel is the superimposition of pseudorandom OCDMA signals encoded from multiple users. The signal is broadcast to every node of the OCDMA network and a receiver in each node decodes the signal. The decoder uses the same code to compress again the

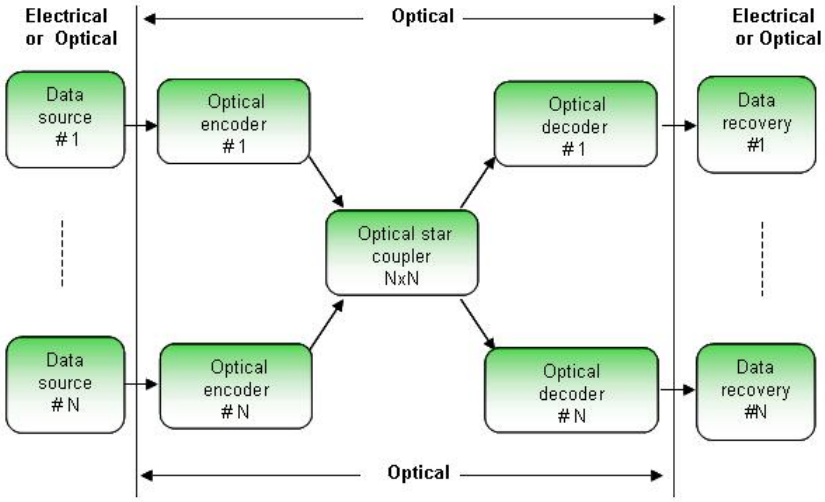


Figure 2.1: Tipical OCDMA system.

spectrum and recover the signal: It evaluates the correlation between the received signal and the code. If the the value of the correlation overcomes a threshold, the original signal is correctly decoded (because the receiver is using the right code), otherwise the original signal is not decoded. This highlights a fundamental characteristic of the codes: they should be orthogonal. Thus, the value of the correlation of an encoded signal with the right code will be maximum. Otherwise the correlation value would be zero, in an ideal case. OCDMA system performance is described by the Bit Error Rate (BER) measurements and is strongly influenced by the multiple access interference (MAI) noise, due to the signals of the other simultaneous users. In incoherent systems MAI noise is dominant, whilst *beat noise* is the main limit for coherent OCDMA systems [33].

OCDMA allows all-optical signal processing using only passive devices, overcoming the impairments due to the use of electronics, and it does not require buffers because of the low delay access. Therefore, it is suitable for passive optical networks (PON). Also, thanks to the all-optical signal processing, OCDMA technique can be used in high-speed transmission, switching and add/drop of data, the third of these depending on traffic variations in the network. OCDMA can also support variable bit-rate and bursty traffic. The users can access the network asynchronously. The network has soft capacity on demand and the

bandwidth can be assigned dynamically, so OCDMA allows a flexible network management and an efficient use of optical network bandwidth. Moreover, the use of the codes improves the monitoring of the quality of service (QoS): this quality of service could be handled in the physical layer by assigning different codes to different services required from the users. OCDMA also improves the security in the network, because the decoder needs the matching code to recover the signal. Therefore, an OCDMA network seems to be secure for information transmission and this characteristic will be further explored in the following sections. In addition, an OCDMA network needs fewer devices than a WDM network does; other advantages are that the equipment being simple and the implementation cost low. Furthermore, OCDMA is highly compatible with DWDM and TDM techniques, and it can be combined with these multiplexing techniques to improve networks capacity, realizing hybrid techniques that can be used to manage different network standards: TDM and OCDMA are suitable for access networks, whilst the combination with WDM is suitable for MAN and backbone networks [34].

Thanks to an intensive research on OCDMA over the past 20 years, many types of OCDMA systems have been proposed. They can be classified by the operating principle or by the encoding domain.

If we classify them in term of encoding domain, they can be divided in three main categories: Direct Sequence (DS) or Time-Spread (TS) OCDMA, if the signal is encoded in the time domain; Spectral Phase Encoded OCDMA (SP-OCDMA), if the signal is encoded in the frequency domain; and there is also a hybrid technique, called Wavelength-Hopping/Time-Spread (WH/TS) OCDMA, in which the signal is encoded in both time and frequency domains, to increase the number of available codes. In this last case, the optical codes are pattern of pulses (chips) with different wavelength and two codewords cannot have two chips with the same wavelength in the same time slot, to assure the orthogonality between all the codes. In an incoherent DS-OCDMA, each pulse representing an information bit is first replicated in W copies, that are delayed and combined together. Consequently, the chip rate is the data rate multiplied for the spreading factor, a parameter related to the code length (the number of the chips in each code). In coherent time-

spreading (TS) scheme, the OC is generated by spreading the coherent optical pulses in time and the phase of the optical carrier is changed according to a specific bipolar signature pattern, similar to that in the electrical field, which has been studied quite extensively for radar and wireless CDMA communication applications. In the SP-OCDMA, the spectral components of the data pulse have been first separated and then the phase of each component is changed by a phase mask, so ultra-short broadband pulses are necessary. Fig.2.2 shows an example of both systems.

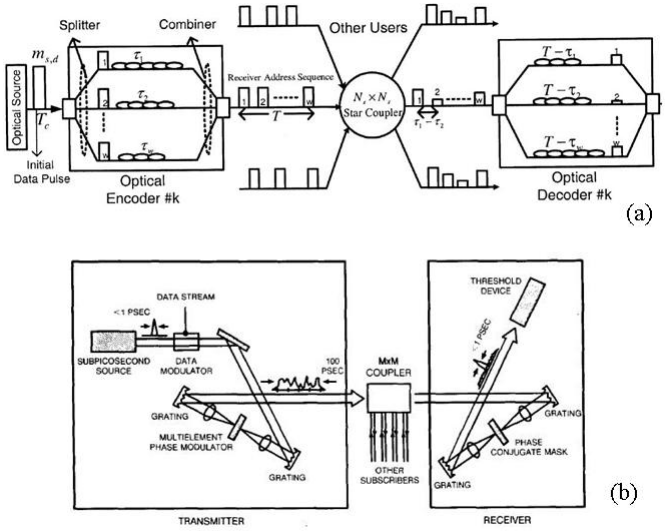


Figure 2.2: (a) DS-OCDMA scheme, [35]; (b) SP-OCDMA scheme, proposed by [36].

Sorting OCDMA systems according to the amount of resources of time and wavelength, they can be divided into one-dimensional (DS- AND SP-OCDMA) and two-dimensional systems (WH/TS OCDMA).

Another classification of the OCDMA techniques can be proposed, depending on the kind of codes used and on the nature of the superimposition of the optical signal [1]: they can be divided into incoherent and coherent systems. The former uses unipolar codes, so employs the presence or the absence of light signal to represent the binary "1" and "0" respectively, and the light signals are detected with the square-law devices at the receiving terminals. This form of signal addition is the superimposition of light powers. This kind of OCDMA system may use incoherent light sources, such as amplified spontaneous emission

(ASE) and light-emitting diode (LED). On the other hand, a coherent system uses bipolar codes and exploits the coherent property of light. The phase of optical signals is encoded and detected at the receiving terminals. In this case, the form of signal addition is the superposition of light signal amplitudes. This kind of OCDMA needs to use ultra-short broadband light pulse sources. Fig.2.3 summarizes the PCDMA classification.

The OC en/decoders are the critical components in OCDMA systems implementations. A lot of different devices can be used to realize OCDMA encoding, depending on the application domain and the kind of codes. Techniques that have been proposed include fiber-optic delay lines (FODL) [9, 13, 37], planar lightwave circuits (PLC) [38, 39, 36], spatial light modulators (SLM) [40], arrayed-waveguide grating (AWG) [41], fiber Bragg gratings (FBG) [28, 42, 43, 25], holographic device [44], and micro-electromechanical systems (MEMS) [45]. In Figure 2.3, their applications for different schemes are also shown. For example in the case of incoherent DS-OCDMA, optical fiber delay lines or FBGs can be used, instead PLC and super structured Fibre Bragg Gratings (SSFBG) can implement Coherent DS-OCDMA, where controlling the optical paths in the order fractions of optical wavelength is required to guarantee the optical pulses are coherently interfering with each other during the signal processing and PLC can satisfy this critical requirement. However, PLC can not easily generate OC of hundred chips, because of the physical constraint of the silica substrate and design complexity, which will result in an inability to generate a large number of OCs, leading to poor system scalability. For example, the FBG might be a powerful alternative. Instead, in the case of SP-OCDMA gratings and phase masks are necessary to separate the different spectrum components of the signal and add different phases to each component. Moreover arrayed waveguide gratings (AWG) or tunable FBGs can be used to realize Frequency Hopping encoding.

### 2.1.2 Optical Codes

To implement OCDMA communication and networking, codes with good performance are required. Choosing a set of code parameters, a family of codes can be constructed that should satisfy the following conditions:

- all codewords should be identified from their shifted versions;
- all codewords should be distinguished from all the other codeword and their shifted versions;
- each codeword has high autocorrelation peak and low autocorrelation sidelobes;
- the crosscorrelation between all the codewords is low.

If all the previous conditions are satisfied, each family has as many codewords as necessary, corresponding to the number of users that can access the network at the same time, and good enough auto-/cross correlation functions so that the interference between the users (multiple access interference, MAI) can be suppressed effectively by decoding the signals.

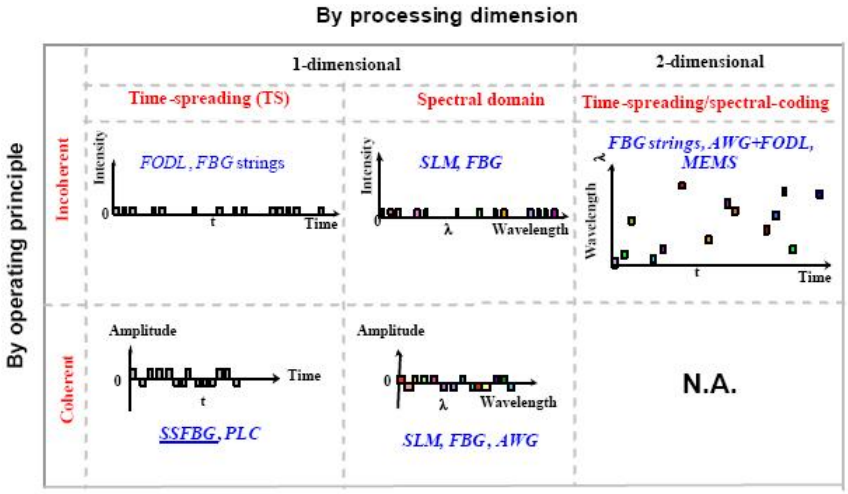


Figure 2.3: Classification of OC generation techniques, [25].

As for different OCDMA systems, optical codes families can be classified according to their operation principle as incoherent or coherent schemes, or according to their processing dimensions. Figure2.3 shows these classifications.

Regarding the processing dimension, OCs can be processed either in the time and the frequency domain in $1-D$ schemes or in both domains simultaneously in $2-D$ schemes [19, 20].

The incoherent techniques, which is based on optical-power-intensity, processes OCs in a unipolar $(0, 1)$ manner, but has disadvantages such as small code size, low optical power and bandwidth efficiency, and poor correlation property [15, 16, 17]. The binary 1 and 0 are represented by the presence or the absence of light signal, so incoherent OCDMA systems can not denote and detect the negative components in bipolar codes. Therefore, the bipolar codes of the electrical wireless CDMA can not be applied, they can only use unipolar codes. Unipolar codes should have very large cardinalities and very good auto- and cross-correlations: Each codeword should have autocorrelation peaks as high as possible and autocorrelation sidelobes as low as possible, in order to guarantee that the systems can be conveniently synchronized when the users access the network; at the same time, the cross-correlation functions must be as low as possible to reduce MAI. Usually, for this kind of codes the best autocorrelation sidelobes and cross-correlation functions are 1, thus the unipolar codes are called quasi-orthogonal.

On the other hand, coherent techniques, which work on a field-amplitude basis, process OCs in a bipolar $(-1, +1)$ manner by encoding the phases of optical signals, all optically; thus, they are superior to incoherent techniques in the overall performance [36, 37, 46]. Bipolar codes from the electrical wireless CDMA can be directly used, such as m-sequences, Gold codes, *Walsh-Hadamard* codes. Due to the presence of negative components in bipolar codes, the cross-correlation functions between any two codewords can be close-to-zero, which makes MAI very small and thus the system performance can be greatly improved and the number of network nodes can be increased. However, pulse-phase encoding with bipolar codes requires ultrashort coherent optical pulse sources, which are susceptible to the fibre-optic nonlinearities and dispersion. For the case of spectral amplitude and phase coding, the number of subscribers in a system and the system performance are limited by the resolution of optical gratings and masks.

In the earlier days, mostly one-dimensional unipolar codes were deeply studied and they were mainly optical orthogonal codes (OOC), a well-known class of codes proposed by *Salehi* in 1989 [13, 15]. An OOC family is a set of $(0, 1)$-sequences,characterized by four parameters $(N, W, \lambda_a, \lambda_c)$, where $N$ is the code length (number of chips), $W$ is Hamming-

weight (number of 1 in the code sequence), $\lambda_a$ and $\lambda_c$ the auto- and cross-correlation constraints respectively, in particular $\lambda_a$ is the value of autocorrelation sidelobes, whereas $\lambda_c$ the crosscorrelation value. If $\{x_n\}$ and $\{y_n\}$ are two distinct binary unipolar sequences belonging to the same code family, the auto- and crosscorrelation function properties can be defined as follows:

$$\begin{aligned} R_{xx}(m) &= \sum_{n=0}^{N-1} x_n x_{n+m} = \begin{cases} W & m = 0 \\ \leq \lambda_a & 1 \leq m \leq N-1 \end{cases} \\ R_{xy}(m) &= \sum_{n=0}^{N-1} x_n y_{n+m} \leq \lambda_c \qquad 1 \leq m \leq N-1\,. \end{aligned} \tag{2.1}$$

The auto- and cross-correlation functions determine the recognition properties of the codes and consequently the performances of the system. The autocorrelation constraint of OOC guarantees that each signature sequence is different from its cyclic shift and this property enables the receiver to implement synchronization, i.e., to find the beginning of its message and locate the boundaries of the codeword. On the other side, the cross-correlation guarantees that each signature sequence is different from cyclic shifts of other signature sequences and this property enables the receiver to identify its message in presence of interference from other subscribers. Thus, the cross-correlation is very helpful for the receiver to achieve synchronization in the presence of multiple subscribers and track its message after synchronization. Therefore, the autocorrelation constraint only contributes to synchronization, while the crosscorrelation affects synchronization and operation, as well [47].

If the autocorrelation constraint is properly relaxed under the premise of satisfying the requirements of system performance, that is, let the autocorrelation constraint $\lambda_a$ be greater than the cross-correlation constraint $\lambda_c$, the cardinality of OOC can be increased greatly. When $\lambda_a > \lambda_c$ the family of codes is called the constant-weight asymmetric OOC, whereas in the particular case of $\lambda_a = \lambda_c = \lambda$ the codes are called constant-weight symmetric OOCs. Otherwise, an $(N, W, \lambda_a, \lambda_c)$-OOC is said to be variable-weight OOC when $W$ is not a constant. Therefore, variable-weight optical orthogonal codes can be seen as the generalization of the constant-weight OOC. When this codeword is assigned to a subscriber as address code, the quality of transmission service of the user with larger weight codeword

is higher. Thus, an OCDMA network can offer flexible and diversified services to many kinds of users and multiple transmission media, satisfying multiple performance requirements from different users and services.

The number of codewords in an $(N, W, \lambda_a, \lambda_c)$-OOC is called cardinality of the code and it has been demonstrated to be (Johnson upper bound [1])

$$M \leq \left\lfloor \frac{(\mathrm{N}-1)\ldots(\mathrm{N}-\lambda)}{\mathrm{W}(\mathrm{W}-1)\ldots(\mathrm{W}-\lambda)} \right\rfloor, \tag{2.2}$$

where $\lfloor \cdot \rfloor$ indicates the integer part of the real number. In the case of $\lambda_a = \lambda_c = \lambda = 1$, the upper bound becomes

$$M \leq \left\lfloor \frac{\mathrm{N}-1}{\mathrm{W}(\mathrm{W}-1)} \right\rfloor \tag{2.3}$$

From the set-theoretical perspective, an $(N, W, \lambda_a, \lambda_c)$-OOC, can be alternatively viewed as a family of $w$-sets of integers $modulo - n$ [15], in which each $w$ set corresponds to a codeword and the integers within each $w$ set specify the positions of nonzero chips (i.e., 1 chip) of the codeword.

Given a OOC family $C = (N, W, \lambda_a, \lambda_c)$, it is possible to obtain other code families, such as $C' = (N, W, \lambda'_a, \lambda'_c)$ with $\lambda'_a \geq \lambda_a$ and $\lambda'_c \geq \lambda_c$, or $C'' = (tN, tW, t\lambda_a, t\lambda_c)$ by concatenating t copies of the codewords belonging to C.

Another family of unipolar codes is the *Prime Codes*. Each sequence of this family has length $N = P^2$, where $P$ is a prime number. Each codeword consists of $P$ sequences with equal length $P$, containing one single pulse ("1"), so the code weight is $W = P$. P is the autocorrelation peak value, whilst the maximum value of autocorrelation function side lobes is $\lambda_a = P - 1$ and the maximum value of the crosscorrelation is 2 [17, 48]. The prime code cardinality is $M = P$. To increase this parameter, it is possible to include in the code set shifted versions of the codewords. The drawback is the increasing of the crosscorrelation peak; furthermore it is possible to use these codes only with synchronous decoding scheme. Another family with the same properties of prime codes, but characterized with a simplified encoding/decoding architecture is the $2^n$ *Prime Code* with weight $W = 2^n$ [49]. Another family with larger cardinality and $\lambda_c = 1$ is the $2^n$ *Extended Prime Code* [50]. In this

case the code length is $L = P(2P - j)$, with $j$ belonging to a *Galois Field*, $GF(P) = 0, 1, \ldots, P - 1$. The code set is obtained by prime sequences consisting of subsequences of length $2P - 1$ with one single pulse (1) and $2P - 2$ zeroes.

On the other hand, coherent bipolar codes are short code sequences, with a larger code recognition parameter [21]. The codewords are $\{1, -1\}$ sequences. Many bipolar codes are borrowed from multiple access techniques in wireless systems, such as the *Pseudorandom Noise sequences* (*PN-sequences*), obtained as the output of a shift register. In the most common use, the *maximal-length sequences* are PN-sequences, characterized by good correlation properties. They can be generated by the feedback-shift-registers (shown in Fig. 2.4(a)) and have the maximal period, therefore, they are called the *maximal linear feedback-shift-register sequences*. The period of an *m-sequence* is not only associated with the number of stages of the shift-register, but is also related to the linear feedback logic. When an r-stage shift-register is employed, the period of the generated *m-sequence* is $n = 2^r - 1$. The linear feedback logic is determined by a primitive polynomial of degree $r$, Eq.2.4:

$$f(x) = \sum_{i=0}^{r} c_i x^i \tag{2.4}$$

A primitive polynomials $f(x)$ of degree $r$, must satisfy the following three conditions:

1. $f(x)$ is an irreducible polynomial: it can no longer be decomposed into smaller factors.

2. $x^n + 1$ can be exactly divided by $f(x)$, where $n = 2^r - 1$.

3. $x^q + 1$ cannot be exactly divided by $f(x)$, where $q < n$.

An *m-sequence* generator can be built as long as a primitive polynomial is found. The number of *m-sequences* with the period of $n = 2^r - 1$ is the same as the number of the r-stage primitive polynomials. The number of the r-stage primitive polynomials is

$$|C| = \frac{\phi(2^r - 1)}{r} \tag{2.5}$$

where $\phi(2^r - 1)$ is an Euler number: the number of integers (including 1) that are relatively prime to and less than $2^r - 1$.

$$\phi(2^r-1)=\begin{cases}2^r-2, & \text{if } 2^r-1 \text{ is a prime number,}\\ (p_1-1)(p_2-2), & \text{if } 2^r-1=p_1p_2, \text{ for } p_1p_2 \text{are prime numbers.}\end{cases} \tag{2.6}$$

An m-sequence has the following properties:

- The period of the *m-sequence* generated by an r-stage shift-register is $2^r-1$.
- The probability of appearance of 1 and 0 in an m-sequence is approximately the same and the number of $1s$ is only one more than the number of $0s$ in an *m-sequence*.
- Generally, a subsequence of $1s$ or $0s$ in an *m-sequence* is called a run. There are totally $2^r-1$ runs in an *m-sequence*, where the number of runs for length 1 is 1/2 of the total runs and the number of runs for length 2 is 1/4, etc. There exist a consecutive 1 run for length r and a consecutive 0 run for length $r-1$.

Moreover, when the logical "0" and "1" in an *m-sequence* take the values of "1" and "$-1$" respectively, the cyclic autocorrelation function of the *m-sequence* is

$$R_{xx}(\tau)=\sum_{i=0}^{n-1}x_ix_{i+\tau}=\begin{cases}2^r-1 & \tau=0\\ -1 & 0<\tau\leq n-1\end{cases} \tag{2.7}$$

where $X=(x_0,x_1,\ldots,x_{n-1})$ is any codeword of a *m-sequence* and $n=2^r-1$. So the autocorrelation function takes only two values.

And, let $X=(x_0,x_1,\ldots,x_{n-1})$ and $Y=(y_0,y_1,\ldots,y_{n-1})$ be any two *m-sequences*, their crosscorrelation is

$$R_{xy}(\tau)=\sum_{i=0}^{n-1}x_iy_{i+\tau} \qquad 0\leq\tau\leq N-1. \tag{2.8}$$

Although *m-sequences* have ideal autocorrelation property, it is difficult to find a general method to predict the behavior of their cross-correlation functions. It has been demonstrated that only very small sets of *m-sequences* can have good cross-correlation properties.

By combining a couple of *m-sequences* with a bit-by-bit $modulo-2$ addition under the control of a synchronizing clock, a *Gold sequence (or Gold code)* can be obtained. The two generators have the same period and rate and, also, the period of the combination

code is the same. Although the *Gold code* is obtained by the $modulo-2$ addition of two *m-sequences*, it is a non-maximal linear shift-register sequence. The scheme is shown in Fig.2.4(b)

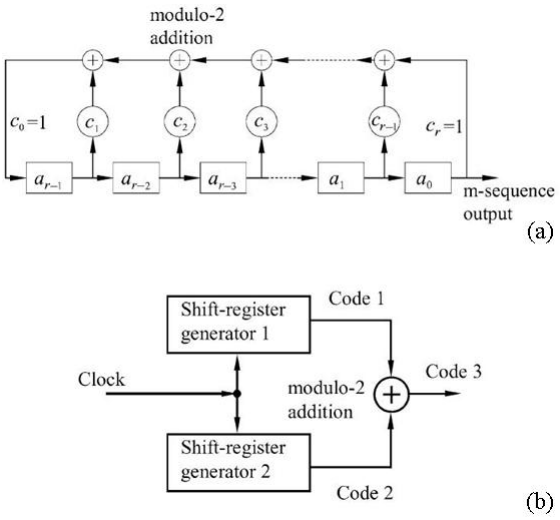


Figure 2.4: (a) r-stage linear feedback shift-register: m-sequence generator; (b) Gold code generator, [1].

$2^r - 1$ Gold codewords can be generated by varying the relative shifts of two preferred *m-sequences* with the period $n = 2^r - 1$.

- The cardinality of *Gold codes* with period $n$ is

$$|C| = 2^r - 1 + 2 = 2^r + 1 \tag{2.9}$$

- *Gold codes* have three valued autocorrelation and crosscorrelation function with values $\{-t_r - 1, -1, t_r - 1\}$, where $t_r = 2^{\lfloor (r+2)/2-1 \rfloor}$. $\lfloor x \rfloor$ denotes the largest integer of less than or equal to $x$.

Therefore, a *Gold code* set has many more codewords than *m-sequence* and its crosscorrelation property is also greatly improved by picking two preferred *m-sequences* to generate *Gold code*, but their autocorrelation functions are slightly worse than those of the *m-sequences*.

Another well known family of bipolar codes is the *Walsh-Hadamard* codes. It consists of the row vectors of a *Walsh* code matrix arranged according to the order of *Hadamard*. The elements of this *Walsh* matrix are $\pm 1$ and the matrix can be rapidly generated from the following recursion relation:

$$\mathcal{H}_{2n} = \begin{bmatrix} H_n & H_n \\ H_n & -H_n \end{bmatrix}$$

and the recursion starts from $H_1 = 1$. Using the recursion expression, we can deduce the code matrices for $n = 1$ and $n = 2$, e.g.:

$$\mathcal{H}_2 = \begin{bmatrix} 1 & 1 \\ 1 & -1 \end{bmatrix}$$

$$\mathcal{H}_4 = \begin{bmatrix} 1 & 1 & 1 & 1 \\ 1 & -1 & 1 & -1 \\ 1 & 1 & -1 & -1 \\ 1 & -1 & -1 & 1 \end{bmatrix}$$

It can be seen that $H_{2n}$ is a $2^n \times 2^n$ square matrix consisting of $\pm 1$ elements. Each matrix row is a codeword, therefore the code cardinality is $M = 2^n$. Each codeword is orthogonal to the others, i.e. the inner product is equal to zero

$$S_{jk}(m) = \frac{1}{N} \sum_{i=0}^{N} H_j(i) H_k(i) = 0 \tag{2.10}$$

where $H_j(i)$ is the i-th element of the j-th row of the *Hadamard* matrix. Therefore, the autocorrelation function value of a *Walsh-Hadamard* code obtained by a *Walsh* matrix of $n \times n = 2^i \times 2^i$ dimensions is equal to $n = 2^i$ and its cross-correlation function value equals 0:

$$H_j(i)(H_k(i))^T = \begin{cases} 2^i & j = k \\ 0 & j \neq k \end{cases} \tag{2.11}$$

This property does not keep valid under temporal shifts. Moreover, the autocorrelation has not a *delta*-shaped peak, due to the non-uniformity of the spectrum, because the energy compacts into a discrete set of frequency components.

Another family of code that will be used in the system presented in Sec.2.4.2, is the family of *Kasami* codes.

*Kasami* codes are bipolar codes and have similar characteristics as Gold codes, but with a larger number of code words. A set of *Kasami* sequences can be constructed from a composite of a preferred *m-sequence* with its properly decimated version. If the considered *m-sequence* has length equal to $N = 2^n - 1$ (with $n$ an even number), where $n$ is primitive polynomial degree, or even the shift register length, the generated *Kasami* sequence will have the same period.

According to the construction of the code, two different group can be defined: the small set and the large set of *Kasami* codes.

The first one comes from the combination between the preferred *m-sequence* with its decimated version $a' = a[q]$, where

$$q = 2^{n/2} + 1$$

Consequently, the period of the sequence $a'$ will be equal to $2^{n/2} - 1$. By a $q$-times repetition of $a'$ a sequence $b$, with period $2^n - 1$ is obtained: $b = a'q$. The sum (mod2) of $a$ with $b$ and with $2^{n/2} - 2$ translations of $b$ will form a new set of sequences:

$$S_{KS} = \{a, a \oplus b, a \oplus Tb, \ldots, a \oplus T^{(2^{n/2}-2)}b\}$$

Counting all the sequences that form this set, i.e $a$, $b$ and all the translations of $b$, the number of code words in the small set of *Kasami* is $2^{n/2}$, so that this number represents the cardinality of this group.

This family of code has crosscorrelation values taken from the set:

$$\{-s(n), -1, s(n) - 2\} \quad s(n) = 2^{n/2} + 1$$

These values are smaller than the values obtained for *Gold* sequences with the same value of $n$. Therefore, the small set of *Kasami* codes improve the crosscorrelation properties, but the number of available code words is smaller.

In order to increase the cardinality of this family of codes, another group can be considered: the large set. As in the previous case, the period of each sequence is $N = 2^n - 1$

(with $n$ an even number). The advantage with respect to *Gold* codes is a larger cardinality, but, on the other hand, the disadvantage respect to the small set is an increased value of the crosscorrelation function.

A sequence of the large set is obtained by a $N$ period *m-sequence* $a$ with two decimated sequences:

$$b = a[2^{(n+2)/2} + 1] \quad c = a[2^{n/2} + 1]$$

By the sum of three sequences $a$, $b$ and $c$, with translations of $b$ and $c$. If $n = 0(mod4)$:

$$S_{KL} = \{a, a \oplus T^{k'} b^{(j)}, a \oplus T^m c, b^{(j)} \oplus T^{m'} c, a \oplus T^{k'} b^{(j)} \oplus T^m c\}$$

$$\begin{array}{cc} j = 0, 1, 2 & k' = 0, \ldots, (2^n - 1)/3 - 1 \\ m = 0, \ldots, 2^{n/2} - 2 & m' = 0, \ldots, (2^{n/2} - 1)/3 - 1 \end{array}$$

If $n = 2(mod4)$:

$$S_{KL} = \{a, b, a \oplus T^k b, a \oplus T^m c, b \oplus T^m c, a \oplus T^k b \oplus T^m c\} \begin{array}{c} k = 0, \ldots, 2^n - 2 \\ m = 0, \ldots, 2^{n/2} - 2 \end{array}$$

The number of sequences that can be obtained with the large set is:

$$\begin{cases} M = 2^{3n/2} + 2^{n/2} - 1, & n = 0(mod4) \\ M = 2^{3n/2} + 2^{n/2}, & n = 2(mod4) \end{cases}$$

The crosscorrelation function ha five values:

$$\{-t(n), -s(n), -1, s(n) - 2, t(n) - 2\}$$

where $s(n) = 2^{n/2} + 1$ (as for the small set), $t(n) = 2^{\lfloor (n+2)/2 \rfloor} + 1$, which is the crosscorrelation formula of the *Gold* codes.

A direct comparison of the correlation bounds for *m-sequence*, *Gold* codes and *Kasami* codes indicates that the the latter are optimal, since they posses lower periodic crosscorrelation peaks. However, the occurrence frequencies of $-1$ crosscorrelation is more for *Gold* than *Kasami* sequences and the higher the probability of a $-1$ crosscorrelation the better is the code [72]. So Gold code are on one hand better than the *Kasami* codes (due to higher occurrence frequency of $-1$ crosscorrelation) and on the other hand they are worse

than *Kasami* codes because of their higher peak cross-correlation values and the smaller number of available code words for the same selected code length.

Thanks to all the above features and the number of available families of codes, OCDMA techniques have been always addressed as a secure transmission, because the receiver needs the matching code to reveal correctly the transmitted encoded signal. This aspect will be analyzed in the following sections.

## 2.2 Overview on Security

All the precautions to avoid information theft in a network are included in the term security of communications. A security attack compromises the security of information, and it is possible to distinguish two different kinds of attack: passive attacks, where the transmission is only intercepted or monitored to reveal the message or to control traffic streams, and active attacks that modify data streams, repeating or modifying the message transmitted. Examples of this two kinds of attack on data security are shown in Fig.2.5.

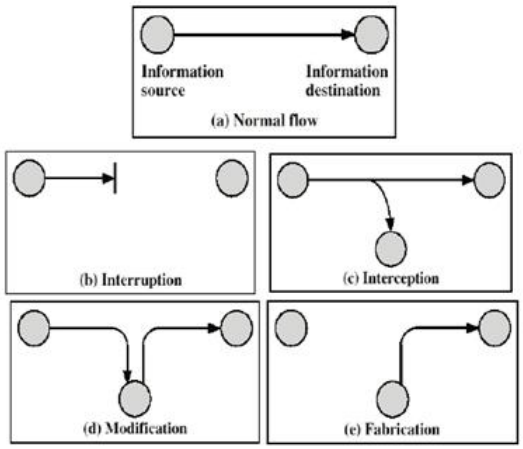


Figure 2.5: Possible kind of attacks.

On the other hand, security mechanisms are techniques to control, prevent or recover a communication system from such attacks. Ciphering, digital signature, authentication are examples of security mechanisms.

Evaluating the security of a communication technique it is important to define what kind of security in under consideration. Among all, the most common are confidentiality, integrity and availability.

- Confidentiality assures that only an authorized user can receive the information, which is protected from unauthorized accesses.
- Integrity assures that data could be sent and modified only from authorized user by allowed procedures. It verifies that the content of the transmitted message has not been modified or created from unauthorized users.
- Availability assures that all hardware and software resources of a network are always available for authorized users, so they can access to all the data and all the resources even after attacks from unauthorized users or after uncontrollable phenomena.

Data confidentiality is probably the most known kind of security in communications and it is also the most sought, thanks to the fact that realizing an high confidential system, data could be transmitted in the network without risks of eavesdropping.

The assumptions used in a security analysis can strongly affect the degree of security that the analysis shows and it is important to define rigorously the initial hypothesis and the parameters that estimate the security level. According to the Kerckhoffs' principle, which basically states that the security of a cryptosystem should depend only on the secrecy of the key and not of the cryptographic algorithms, a security analysis assumes that potential adversaries are technologically sophisticated, have significant resources and know a great deal about the signals transmitted [51, 52].

### 2.2.1 Security in OCDMA

Optical Code Division Multiple Access is always addressed as potential secure technique, thanks to the fact that many users can share the same optical resources and all the transmitted signal overlay both in time and frequency domain, showing noise-like waveform [53]. Furthermore, the use of codes to encode/decode the signals and to identify the user seems to assure an high degree of security to the system. For these reasons, among the three

most known type of security cited in Sec.2.2, OCDMA is addressed as a technique that can potentially provide confidentiality and availability protections.

The assumptions in an OCDMA security analysis are chosen in agreement with the Kerckhoffs' principle, so that the eavesdropper could know the ciphering mechanism, e.g. the data rate of the signal transmitted, the wavelength, the type of encoding, and the structure of the codes, but not the particular code that a single user employs.

Moreover, it is reasonably easy for a user to change the codes if his code is compromised, whereas the other parameters are difficult to change quickly, because they need hardware or software redesign of the system. Therefore depending on the secrecy of hard-to-change parameters for data confidentiality is poor security practice and it is better to rely on parameters that could be changed quickly [52].

As said in the previous section, the initial hypothesis and the chosen parameters can strongly affect the results of a security analysis, so also in the case of OCDMA it is important to define which parameters must be considered. The most important are the code space, the code word, the modulation used and the signal tapping [51].

**Code space:** the number of codes that each user could use. Since each user is identified by a particular code and he uses it to separate his signal from the others, it is difficult for an eavesdropper to correctly reveal the signal without any knowledge of the code, especially if a lot of users are transmitting at the same time. The simplest kind of attack is called Ciphertext Only Attack and in this attack the eavesdropper tries all the code words in a recursive way. Therefore for this kind of attack, also known as Brute Force Attack, a large number of different code assures a certain degree of security: larger is the number of available code words, larger is the number of the trials needed and the time they require. The code space can vary a lot depending on type of encoding: in case of DS-OCDMA sometimes the brute force attack is not hampered by the code space for a given code length; instead the SP-OCDMA and the Frequency Hopping have a larger code space with the same given code length.

**Code word:** in order to increase the difficulty of the detection of the code word, it is important to vary the used code word frequently. The frequency of variation depends

on the potential attacker ability of detecting the signal and the code word. But the disadvantage of this strategy is that the keys exchange between the transmitter and the receiver must be updated frequently.

**Signal tapping:** an eavesdropper may tap signals in different locations within a network. He may enter in an user terminal or tap the signal from the fibres in the network, but for the purpose of eavesdropping it is better to tap isolated signal, avoiding the MAI noise. Since each user terminal in an OCDMA network receives the multiplied signal from all the other users, entering in the terminal does not give to the eavesdropper an isolated signal. Therefore it is better for him to tap a fibre in the network infrastructure, this gives more opportunities to tap an isolated signal.

**Modulation:** the choice of the modulation can affect a lot the confidentiality level assured by OCDMA. The most used is On Off Keying modulation (OOK), a light pulse is sent to represent a bit 1 and no pulse to represent a bit 0. Albeit this modulation allow the use of simple optical transmitters and receivers, it is vulnerable to relatively simple techniques of eavesdropping. Recently, it has been demonstrated that OCDMA transmissions with this modulation technique are vulnerable to a standard power detection [54], so an eavesdropper could reveal the signal transmitted without any knowledge of the code, if he could tap an isolated signal. In this case, there is no need for the eavesdropper to break the coding scheme or steal the code, because the power detector output contains the user's data stream. A solution could be to send the same amount of energy for each transmitted bit by using a code for bit 1 and a different code for bit 0. This approach is known as 2-code keying. It has the disadvantage of increasing the MAI noise when there are simultaneous users and it has still a certain degree of vulnerability.

Therefore, considering security as an inherent characteristic of OCDMA technique is not a correct assumption, because it depends on all the parameters cited before [51, 52]. When multiple users send simultaneously information with different codes, it is very difficult for an eavesdropper to intercept the correct data, without knowing the code. But it could

happen that a single user would be active in the network and in this case OCDMA cannot guarantee the security.

Many theoretical and practical studies have been done with the aim of increasing confidentiality in OCDMA techniques. Since it has been demonstrated that in a spectrally phase-coded OCDMA for a single-user system employing on-off keying (OOK) the waveform can be detected using a simple energy detector, code switching scheme have been proposed. But also in these conditions, the system shows a certain degree of vulnerability. In this scheme the information is hidden for an eavesdropper using a simple energy detector, but further studies have demonstrated that it is vulnerable to a scanning with a narrow band-pass filter and also to a DPSK detection [55, 56].

The security performance of OCDM has been carefully analyzed [52, 56, 60, 61] and in the following Sec.2.3 and Sec.2.4, other solutions to increase the confidentiality of an OCDMA network will be studied.

## 2.3 Security of an all-optical multiport encoder/decoder

Passive optical networks (PON) are the most promising and cost-effective solution for next generation access networks (NGAN). But due to their simple topology, data confidentiality is one of the major issues in these networks, in fact downstream information travels broadcast from the optical line terminator (OLT) to all the connected optical network units (ONU), so a malicious user can intercept data directed to another user. Most recommendations for PONs do not specify any encryption mechanisms for transmissions and even where specified they are only for downstream. On the contrary it has been demonstrated that the possible presence of dirty connectors, because of which the power reflected allows to an eavesdropper to observe the traffic from the ONU, makes encryption necessary also in upstream transmissions [57]. PONs using electronic and optical code division multiple access (CDMA) have been experimentally demonstrated [6, 58, 59].

A schematic of a PON using an OCDMA transmission is shown in Fig.2.6, where the OLT uses a laser source, a data modulator and an optical encoder; the cryptographic system assigns two optical codes to each user in the case of a bit-ciphering scheme, or a set of

optical codes to encode a stream of bits in the block-ciphering scheme. The ONU recognizes the signal using a matched decoder, a photodetector and an optical hard thresholder; time gating may be used to enhance system performance.

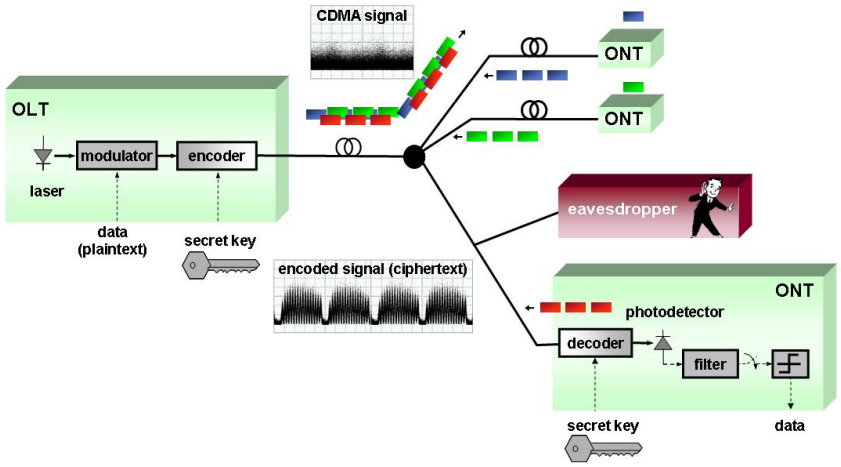


Figure 2.6: Scheme of a passive optical network with OCDMA ciphering transmission.

OCDM has the advantage to encrypt data at a very high data date and its transmission confidentiality is mainly related to the number of different codes that can be generated and processed; however, the increase of code cardinality implies that a larger number of encoders/decoders (E/D)s is necessary at both ONU and OLT sites to generate different codes and the system implementation becomes unfeasible.

Moreover, OCDMA systems are often considered potentially secure because multiple users simultaneously transmit encoded signals and MAI noise helps in hiding the transmitted message, nevertheless their vulnerability must be analyzed considering the worst-case condition, that is assuming the eavesdropper able to intercept isolated signals, avoiding the MAI noise, as shown in Fig.2.6. Therefore, in this section, security performance of point-to-point (P2P) optically encoded transmission will be analyzed, in terms of data confidentiality against *brute-force code searching*, *known-plaintext* and *chosen plaintext* attacks. According to *Kerckhoffs'principle*, the condition that the eavesdropper could know everything about the OCDM encoding technique, in terms of data and chip rates, code length, modulation formats, wavelengths..., except for the particular code of a known code

family that the user is employing [51], will be considered.

To realize the analyzed coding schemes, different configuration of the multiport E/D, carefully studied in [62, 63], will be presented. The multiport E/D is a planar device with an arrayed waveguide grating (AWG) configuration and has N input and N output waveguides, as shown in Fig.2.7. The two slab couplers, with effective index $n_s$, are in a Rowland circle configuration, with radius $R$; $d$ is the pitch of the arrayed waveguide grating, and $\theta_i$ and $\theta_o$ are the diffraction angles at the input and output waveguides, respectively. Each waveguide of the array that interconnects the two slab couplers has a different length equal to $L + j\Delta L$, with $j = 0, 1, \ldots, N-1$. Therefore, the $N$ copies of the input pulse, generated by the first slab, experience a different delay due to the different paths in the arrayed waveguide grating and they are recombined by the second slab region.

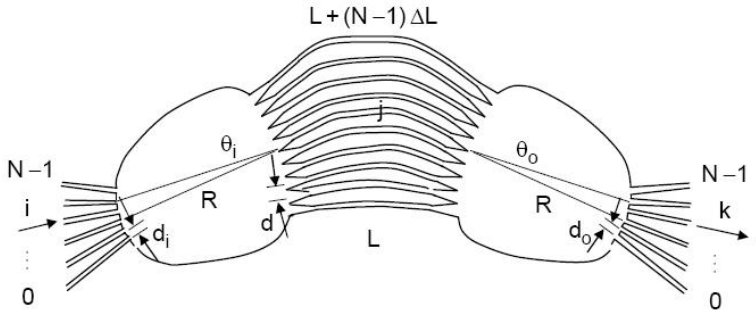


Figure 2.7: AWG architecture.

The AWG-based device is not used as a frequency multiplexer in a spectral coding scheme, but it generates PSK codes on a single wavelength, using a time-spreading technique. When a single short laser pulse, of a duration of about 2ps, is sent into one of the encoder input ports, the input slab coupler makes $N$ copies of the laser pulse, with phases given by the Rowland circle configuration. The optical pulses travel through the grating arms with different delays. So the code chips obtain different phases and are recombined by the output slab coupler to generate $N$ different PSK codes at the device output ports (Fig.2.8(a)). Each PSK code is composed of $N$ optical chips and the differential path delay in the grating is chosen larger than the input pulsewidth, so that the chips in the optical code do not overlap. The decoding process is performed by the same device (Fig.2.8(b)),

forwarding the code into one of the decoder input ports and measuring the cross-correlation signals (CCP) at its outputs: the autocorrelation peak (ACP) detected at one port identifies the code. The cross-correlation between two codes is small, due to their orthogonal property, so the ratio between ACP and CCP is high enough to recognize the code even in presence of MAI noise. The orthogonal property of the codes stems from a frequency domain analysis: each code corresponds to a different frequency channel that does not overlap with the others, so that the cross-correlation between two codes is small.

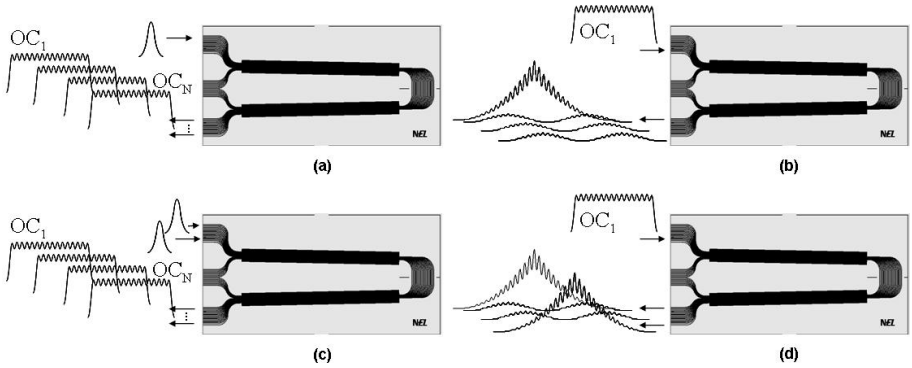


Figure 2.8: Multiport encoding/decoding device: one-dimensional AWG-based (a) encoder and (b) decoder; multidimensional AWG-based (c) encoder and (d) decoder.

The impulse response of the AWG-based E/D device between the $i$-th input waveguide and the $k$-th output waveguide is

$$h_{ik}(t) = \sum_{j=0}^{N-1} \exp\left[-\pi\iota\frac{n_s d}{\lambda}(2j - N + 1)(\sin\theta_i + \sin\theta_o)\right] \times \delta\left(t - n_s\frac{L + j\Delta L}{c}\right), \quad (i, k = 0, 1, \ldots, N-1) \quad (2.12)$$

where $\iota = \sqrt{-1}$, $\delta(t)$ is the Dirac delta, $L$ is the smallest waveguide length, and $\theta_i$, $\theta_o$ are the diffraction angles in the input and output slabs, respectively. The diffraction angles can be related with the input/output waveguides pitches $d_i$ and $d_o$, and the slab focal length $L$, as follows

$$\sin\theta_i \cong (2i - N + 1)\frac{d_i}{2R} \qquad \sin\theta_o \cong (2i - N + 1)\frac{d_o}{2R} \quad (2.13)$$

The chip interval, or the time distance between two consecutive pulses in each code, is $\Delta\tau = n_s\Delta L/c$ and it equates with the inverse of the free spectral range (FSR) of an AWG

multiplexer/demultiplexer.

In a standard E/D configuration, the code cardinality coincides with both the number of ports and the code length, i.e. the number of chips in each code. However, the key space is not large enough to guarantee secure transmission, since an exhaustive code search can break the system confidentiality in a small amount of time. To increase the cardinality it is possible to use the multi-port E/D in a different configuration, sending $n$ laser pulses into $n$ different encoder input ports. In this way it is possible to realize a n-D encoding and the n-dimensional codes generated are a coherent sum of $n$ PSK codes. The multi-dimensional configuration has been described in [64]. A set of $n \leq N$ laser pulses are sent simultaneously into $n$ input ports of the encoder to generate $n$-dimensional codes that are a coherent sum of $n$ PSK codes. These codes can be detected by the same decoder, measuring $n$ ACPs at its output ports. The position of the ACPs among the decoder outputs unequivocally identifies the code. Fig.2.8 (c) and (d) represent the encoder and decoder for a multidimensional AWG-based device, respectively.

If the number of input pulses is fixed to $n$, the number of different codes that the E/D can be generate/process is $\begin{pmatrix} N \\ n \end{pmatrix}$ and coincides with the number of different combinations of $n$ ACPs and $N-n$ CCPs. Using $n = N/2$ laser pulses, the maximum number of codes that can be generated is $\begin{pmatrix} N \\ N/2 \end{pmatrix}$.

The PSK codes generated by a multi-port E/D are direct-sequence codes, composed of $N$ chips with the same amplitudes and different phases of values $j2\pi/N (j = 0, 1, \ldots, N-1)$, where each code corresponds to a different frequency subband. The frequency spectrum of two PSK codes is shown in Fig.2.9(a), and it is possible to observe that the codes correspond to two different frequency channels. The intensities of the auto- and cross-correlation signals are shown in Figs.2.9 (b) and (c), respectively, and are quite similar. The ratio between the auto- and cross-correlation peaks is about 10dB, which is high enough to recognize the code in the presence of MAI noise.

A multi-dimensional code is generated by summing $n$ PSK codes, by sending $n$ laser pulses to the encoder input ports simultaneously. Since different PSK codes corresponds

to different frequency subbands, with 10GHz channel spacing, the spectral contents of the multi-dimensional codes are composed of $n$ frequency channels, as shown in Fig.2.10(a). Figs.2.10 (b) and (c) show their auto- and cross-correlation signals detected at the matched and unmatched ports, respectively.

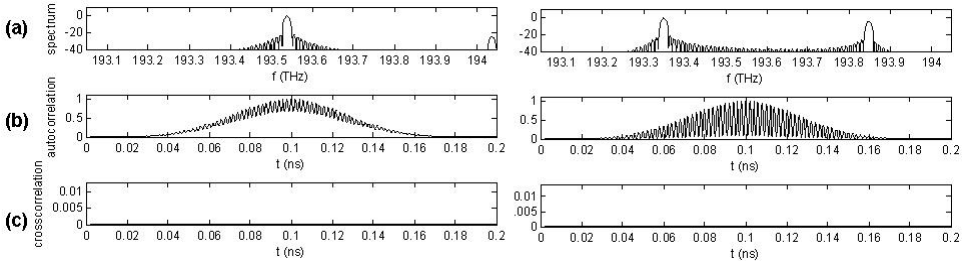


Figure 2.9: (a) Spectrum, (b) autocorrelation signal detected at the matched port and (c) crosscorrelation signal detected at an unmatched port of two unidimensional PSK codes generated by an encoder with $N = 50$ ports that is fed with $n = 1$ laser pulse.

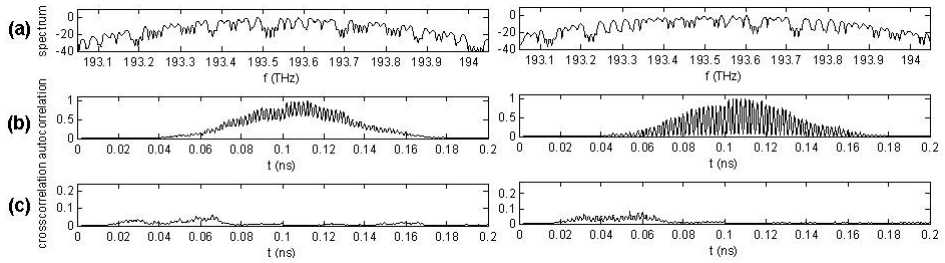


Figure 2.10: Two multidimensional codes generated by an encoder with $N = 50$ ports that is fed with $n = 25$ simultaneous coherent laser pulses in a random configuration: (a) spectrum, (b) autocorrelation signal detected at one of the $n = 25$ matched ports and (c) crosscorrelation signal detected at one of the $N - n = 25$ unmatched ports.

This device with different configurations could perform bit- and block-ciphering techniques, realizing signal encryption at physical layer. In all numerical simulations, the eavesdropper will be considered able to test $10^7$ codes per second. This number has been taken as a reference from standard cryptography literature [65], even if, with the present level of optical technology, it is quite unlikely to test ten million optical codes in a second, therefore the obtained numerical results are an upper bound for optical network security.

### 2.3.1 Bit-coding systems

With bit coding a one-to-one correspondence between bits and optical codes is established, because each bit from each user is encoded with the code word. This encryption scheme can be designed to be computationally secure against brute-force code searching attacks, by increasing the number of codes, but it is completely vulnerable against known-plaintext and chosen-plaintext attacks.

As said in Section 2.2.1, on-off keying (OOK) data modulation is extremely vulnerable, as it can be broken by power detection; therefore, a two-code keying (or code shift keying (CSK)) transmission, where both mark and space are encoded [66], will be considered in the following discussion.

In a multidimensional encoding scheme, as the one of Fig.2.11, where, for the sake of simplicity, the first $N/2$ ports of the encoder are used to transmit the logic $'0'$ and the remaining ports are used for the logic $'1'$. The laser pulses are switched between two $1 \times n$ splitters according to the bit value.

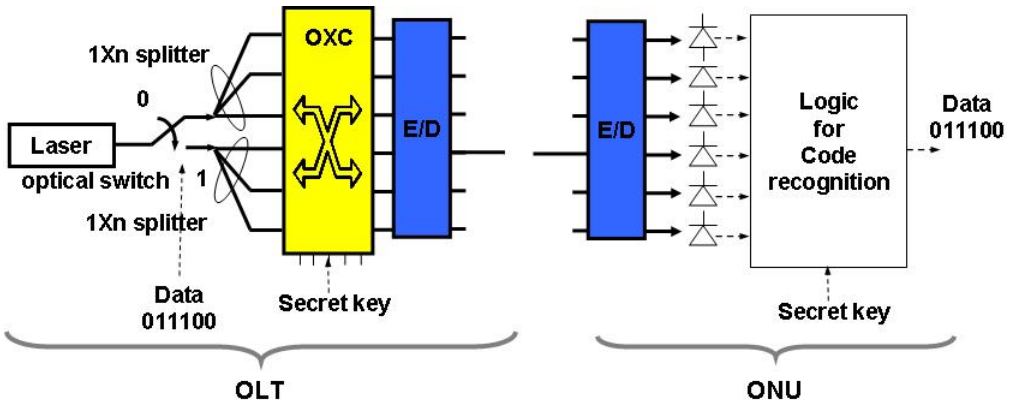


Figure 2.11: OLT and ONU architectures for bit-cipher transmission using multidimensional codes.

The optical cross connect (OXC) is driven by the secret key and connects the splitter outputs to $n$ input ports of the encoder, selecting a $n$-dimensional code. At the ONU terminal, the $n$ ACPs detected at the decoder output ports identify the $n$-dimensional code and an electronic logic circuit converts this information into the received bit. The number

of codes that can be generated/processed by a E/D in a multi-dimensional configuration is very high: as an example, a multi-dimensional E/D with $N = 100$ ports and $n = 50$ input pulses, can generate more than $10^{29}$ codes.

In Fig.2.12, network security, in term of number of years required to find the matched code, is plotted, considering that $n = N/2$ ports are used to encode marks, and the remaining ones are used for spaces. The total number of codes is $\begin{pmatrix} N \\ n \end{pmatrix}$ and the confidentiality is evaluated by dividing this number by $10^7$ codes/s, which is the number of codes that an eavesdropper can test in a second.

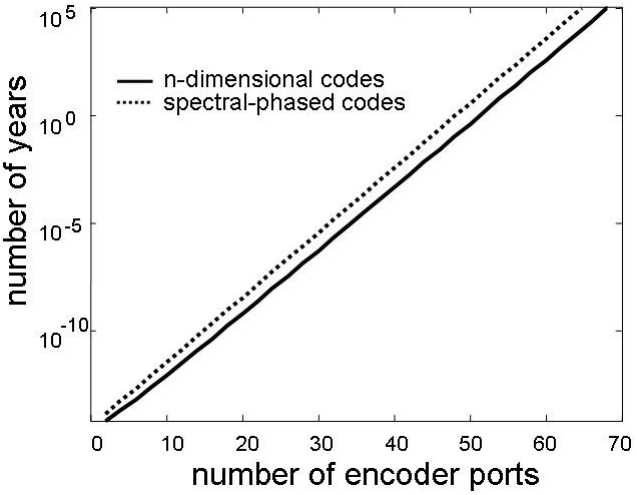


Figure 2.12: System confidentiality as a function of the number of encoder/decoder ports, in the case of $n$-dimensional codes (continuous line) and spectral-phased codes (dotted line).

The system is computationally secure for a large value of $N$, but an eavesdropper that possesses the decoder can easily intercept the code; furthermore, a spectral analysis of the received signal, using an optical spectrum analyzer (OSA), can also identify the code, because the $n$-dimensional codes are superpositions of different non-overlapping frequency subbands. Therefore, in order to increase network confidentiality, it is necessary to introduce more degrees of freedom.

A possible solution is the introduction of a set of phase shifters at the encoder input

ports: by changing the phases of the coherent laser pulses that are used to generate a $n$-dimensional code, a spectral-phase code is obtained.

Two pseudo-random binary phase code, with phase shifts of 0 or $\pi$, in two random combinations, are generated and are applied to $n = N = 50$ coherent laser pulses, sent into the encoder input ports. The matched and unmatched decoded signals are reported in Figs.2.13 (a) and (b), respectively. It is possible to observe that since all the encoder (and decoder) ports are used, the matched signals coincide with the input laser pulses, and this feature is very attractive in asynchronous OCDM schemes since a delta-like shaped auto-correlation signal can be used to reduce both MAI and beat noise effects.

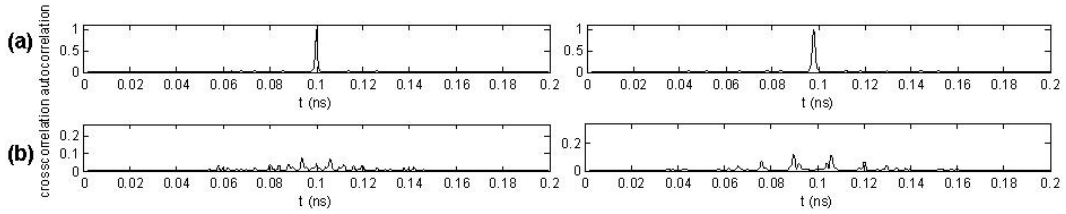


Figure 2.13: (a) Autocorrelation signal detected at the matched ports and (d) crosscorrelation signal detected at an unmatched port of two spectral phase code, generated by an encoder with $N = 50$ ports that is fed with $n = N = 50$ simultaneous coherent laser pulses with phases 0 and $\pi$, in a random configuration.

The OLT and ONU architectures are shown in Fig.2.14: the first $N/2$ ports of the encoder and decoder are used for the logical "1", and the remaining ones for the "0". In this case, the secret key corresponds to the sequences of $N$ phases that can have values 0 and $\pi$. Therefore, the number of all possible keys is $2^N$, dividing this number by $10^7$ codes/s, the number of years required to break the network security is obtained and is plotted in Fig.2.12 [73]. The two optical spectral-phase codes coincide with the secret key, and an eavesdropper has to test many different phase shift configurations in order to intercept the code. Therefore, it is possible to say that this encoding scheme is completely based on the physical domain and the increased confidentiality is related to the fact that the code cannot be detected without knowing the secret combination for phase distribution.

In a standard spectral encoding technique, each phase transition produces a dip in

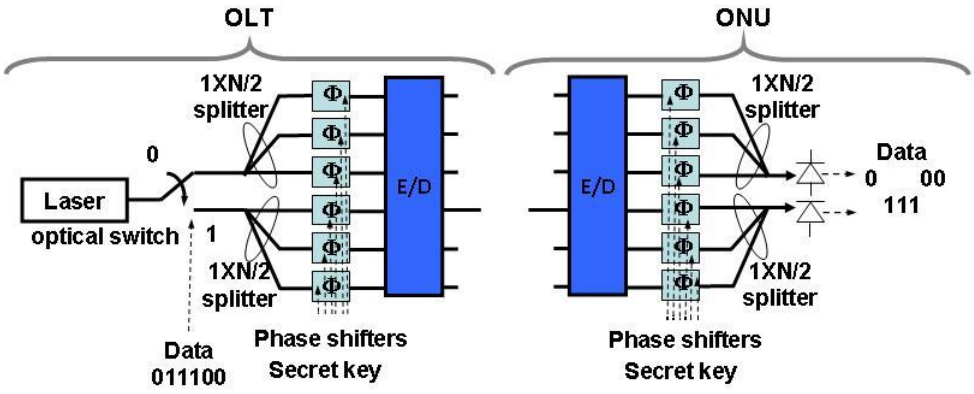


Figure 2.14: OLT and ONU architectures for bit-cipher transmission using spectral phase codes.

the spectrum of the encoded data and this represents a serious vulnerability in spectral-phase encoded signals. In fact, it has been demonstrated that from the measured filtered spectral data an adversary can easily recover the transmitted bits [56]. Whereas, all different codes generated at the output ports of the multi-port E/D present the same spectral dips, and therefore a simple spectral analysis based on the presence of dips does not allow an adversary differentiate a "0" from a "1".

### 2.3.2 Block-coding systems

Block ciphering is a technique widely used in electronic cryptography, where a sequence of $m$ bits is encoded into a different codeword. It is possible to extend it to the optical field, with the aim of increasing the degree of confidentiality against all kind of attacks. A block-cipher scheme presents an higher degree of confidentiality with respect to bit-cipher, not only against brute-force code searching attacks, but also against known-plaintext and chosen-plaintext attacks.

A possible block-cipher scheme is shown in Fig.2.15 and it is equivalent to $M$-ary transmission [67], where a stream of $m$ bits from a single user is encoded into $M = 2^m$ codewords: the serial bit stream from each user is mapped into a source alphabet with $M$ determinations, that is associated with a different code. As in the previous system, two different cases

will be considered: 1-dimensional codes and multidimensional-codes. In both of them, the pulse repetition rate of the laser is not equal to the user bit rate, but is reduced by a factor of $m$. The security relies on the logic of assigning a different code to each bit sequence and not on the optical code itself. Block-ciphers are in general more secure than bit-ciphers, because the adversary cannot discover this correspondence just by making some guesses. The number of possible secret keys coincides with all possible permutations of $n$ bits, i.e., $2^n!$.

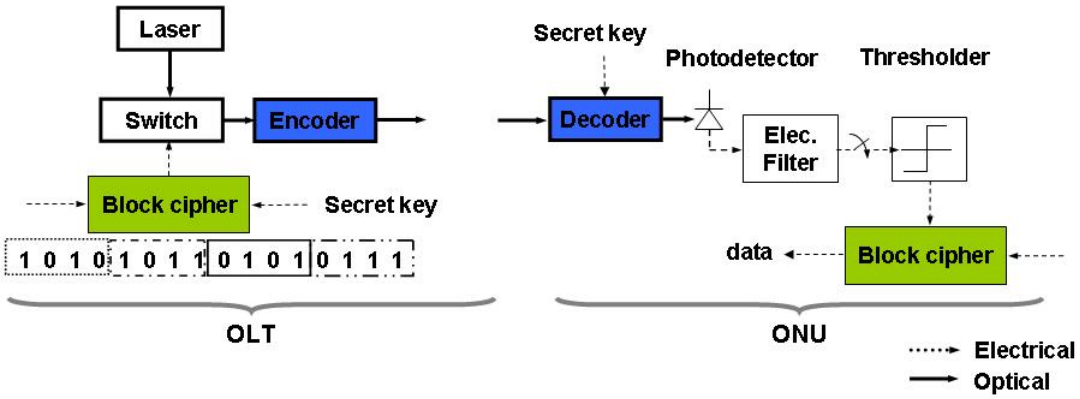


Figure 2.15: OLT and ONU architectures for block-cipher transmission.

In the case of Fig.2.15, the system transmits a standard 1-dimensional PSK code that is detected at the matched port of the decoder. The electronic logic circuit associates a different code with each transmitted bit sequence.

Given an optical multi-port E/D with $N$ ports, the maximum length of the bit sequence that can be encrypted is $log_2 N$. The time required to break this block-cipher transmission is $N!/10^7$s, as shown in Fig.2.16 [75].

To increase the bit sequence length, and therefore system confidentiality, it is possible to use multi-dimensional codes. In this case, as shown in Fig.2.17, the input laser pulse is split into $N$ copies that are forwarded to the encoder input ports, depending on the switch fabric status. Therefore the electronic signal that drives the switch fabric is the secret key that assigns a different multi-dimensional code to each $n$-bit block. This scheme enlarges the number of codewords to $M = 2^N$, so that an E/D with $N$ ports is able to encrypt

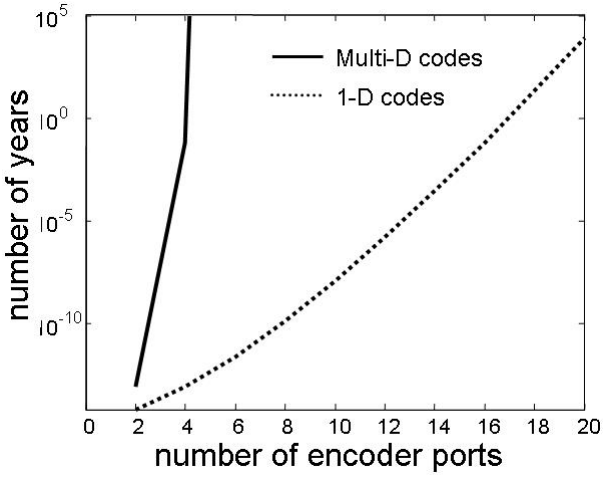


Figure 2.16: Block-cipher confidentiality versus the number of encoder/decoder ports $N$: (dotted line) block-cipher using 1-dimensional codes, (continuous line) block-cipher using multi-dimensional codes.

a sequence of $n = N$ bits, and the time required to break the confidentiality is $2^N!/10^7$, as shown in Fig.2.16. Furthermore, by choosing $n < N$, it is possible to enhance system confidentiality by using two or more multi-dimensional codes to encrypt the same sequence of bits.

In a block-ciphering system the secret key is the logic to assign an optical code to a given bit sequence. Therefore the number of different secret keys is very large, even though in actual electronic encryption schemes not all the possible secret keys are used.

### 2.3.3 Comparison of bit and block techniques

In Fig.2.18, a quantitative comparison between the bit and block ciphering techniques is shown, considering two different kind of attack [74]: in the first case the simplest ciphertext only attack (COA), the exhaustive key search attack, is evaluated; in the second one the chosen plaintext attack is considered, in which the adversary has access to the encryption function and can encrypt any plaintext message, trying to determine the key.

In Fig.2.18(a), the number of trials needed to break the security with exhaustive key search attack is shown and is evaluated as a function of the number of the E/D ports $N$.

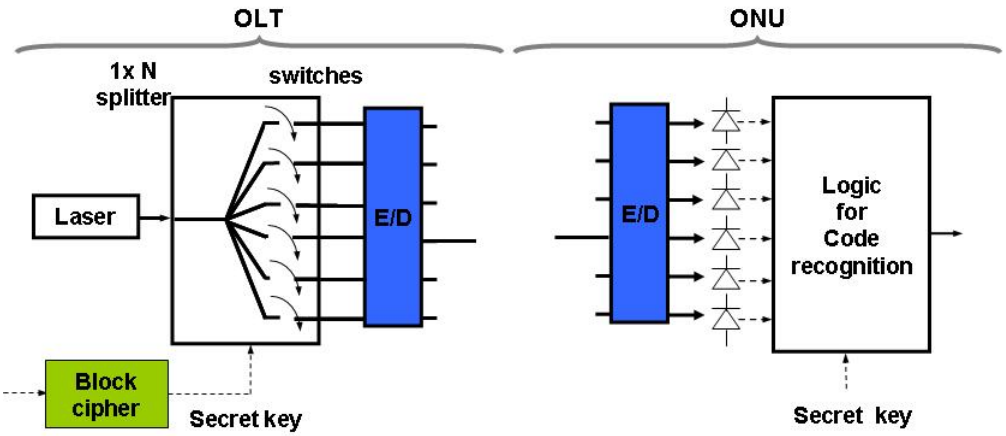


Figure 2.17: (a) OLT and ONU architectures for block-cipher transmission ($M$-ary transmission) using multi-dimensional codes.

An average number of trials equal to $K/2$ is considered, where $K$ is the number of secret keys that each coding technique could generate. As said before, the number of secret keys is equal to $K = 2^N$ in the case of bit-ciphering, with spectral-phase codes and it is equal to $K = N!$ for block-ciphering in the case of 1-D codes or $K = 2^N!$, in the case of $n$-D codes.

For the second kind of attack, the chosen plaintext attack, the lower bound security parameter of modern cryptanalysis is the number of plaintext bits that a potential eavesdropper needs to know for breaking the confidentiality. In a bit-ciphering scheme, just a single bit allows the adversary to intercept the data; in block-ciphering scheme, instead, the number of message bits required are $(N-1)log_2N$, for 1-D codes, and $N(2^N-1)$ for n-D codes, as shown in Fig.2.18(b).

## 2.4 Optical scrambling-based OCDMA

Another solution to increase the confidentiality in OCDMA networks is the use of optical scrambling, that can be implemented with simple and off-the-shelf devices.

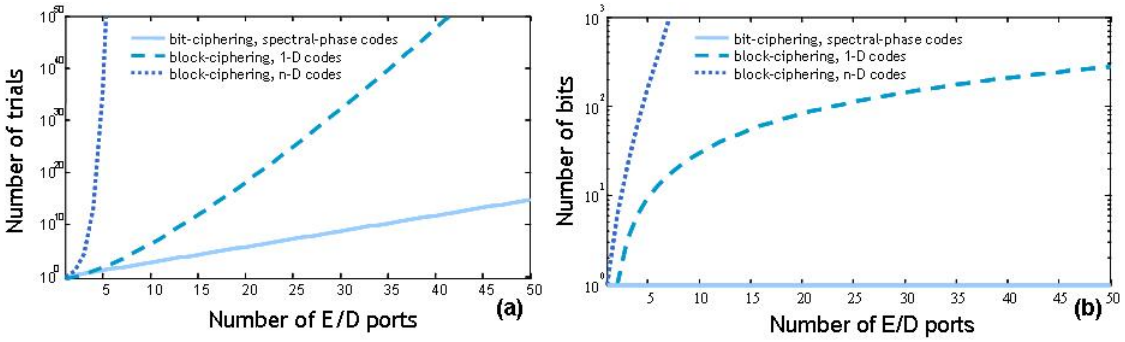


Figure 2.18: (a) Number of trials to break the confidentiality in a COA attack. (b) Number of bits needed to break the confidentiality in a CPA attack.

### 2.4.1 Scrambling technique

Electronic scrambling is an approach developed for data security. A common application is image information hiding. The digital image scrambling transforms image into chaos state and the information contained in the new state will lose the meaning of the original images, thus security of image or data can be guaranteed. The technology can be implemented in frequency or spatial domain. The former provides larger security, but the implementation is more complex. A proposed method to scramble digital images is based on Discrete Cosine Transform (DCT) with a three step procedure. The final scrambling is obtained decomposing the original image for its first variable by $1 - D$ DCT, then the coefficients are modulated by chaotic sequence, and afterwards the same procedure is applied to the second variable. This make an exhaustive search not enough to decrypt the image correctly. In Fig.2.19 an example of digital image scrambling is shown. After the scrambling for the first variable, the image is indecipherable (Fig.2.19(b)), and if the process continues on the second variable the image is even more indiscernible (Fig.2.19(c)). But after an inverse operation the image is correctly recovered (Fig.2.19(d)) [68].

In telecommunications, scrambling is usually carried out by the addition of components to the original signal or by the changing of some important components in order to make extraction of the original signal difficult. A well known technique is Self-Synchronizing scrambling, that can be interpreted as a multiplication of the source bit stream by $x^d$,

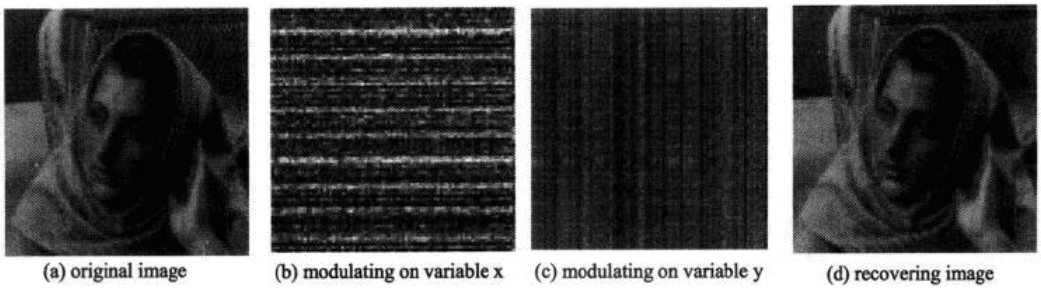


Figure 2.19: Example of digital image scrambling.

where $d$ is the degree of scrambling polynomial, and $modulo-2$ division by the scrambling polynomial. To recover the source stream the received bit stream is $modulo-2$ multiplied by the scrambling polynomial. The equations 2.14 and 2.15 represent the transmitted signal after scrambling and the recovered signal [69].

$$t(x) = \frac{s(x)x^d}{d(x)}, \tag{2.14}$$

where $t(x)$ is the transmitted signal, $s(x)$ a continuous source bit stream and $d(x)$ the scrambling polynomial of degree $d$.

$$u(x) = \frac{r(x)d(x)}{x^d} = \frac{(t(x) \oplus e(x))d(x)}{x^d} = s(x) \oplus \frac{e(x)d(x)}{x^d}, \tag{2.15}$$

where $u(x)$ represents the decoded sequence, $r(x)$ represents the received bit stream and $e(x)$ is a possible error pattern.

The scrambler could be seen as a device that encodes the message at the transmitting side and makes the message unintelligible at a receiver not equipped with an appropriately descrambling device (in the case of the previous cited technique, without the unscrambling polynomial).

Using the scrambling, the eye diagram of the signal transmitted is closed and indicates that the signal is fully distorted, so an eavesdropper could not reveal the signal through a simple differential detection. Therefore this technique is gaining research interests in optics to increase the confidentiality of optical networks and it could be seen as a solution to overcome the vulnerabilities of OCDMA techniques.

In optical communications, the scrambling could be realized with the introduction of the "entropy" infusion, by using encoded random frameless noise, combined with the variation of the phases of each chip in the codes, for encoded data or noise (Fig.2.20). In this case, the scrambler is realized by an encoder representing a diagonal matrix, that changes the relative phases of the chips, and a monomial matrix that identifies the codes used to transmit the signal [70].

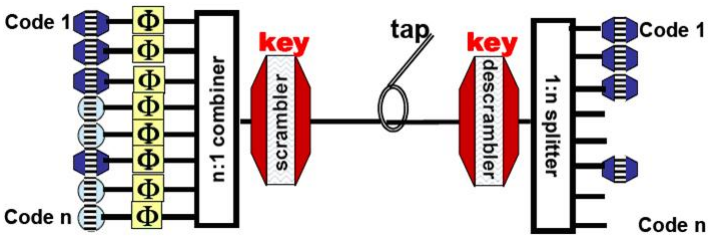


Figure 2.20: System schematic for the OCDM-based photonic encryption, [70].

Another proposed solution to realize the scrambling with a fully optical method is to exploit the different delays between the modes propagating in a multi-mode fibre (Fig.2.21). The scrambling and unscrambling are achieved using two different multi-mode fibre segments with proper refractive index profile designs. The first multi-mode fibre introduces modal dispersion to fully distort the input data signal. On the receiving side, the multi-mode fibre provides the same amount of inverse modal dispersion to compensate the mode delay and to rebuild the signal [71].

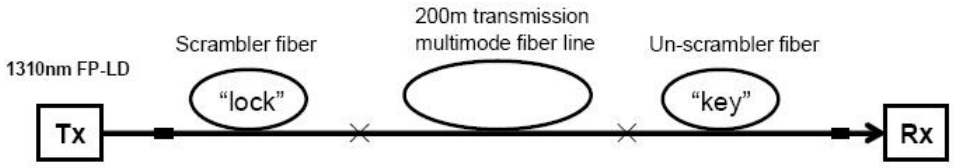


Figure 2.21: Scheme of the setup for the passive optical scrambling, [71].

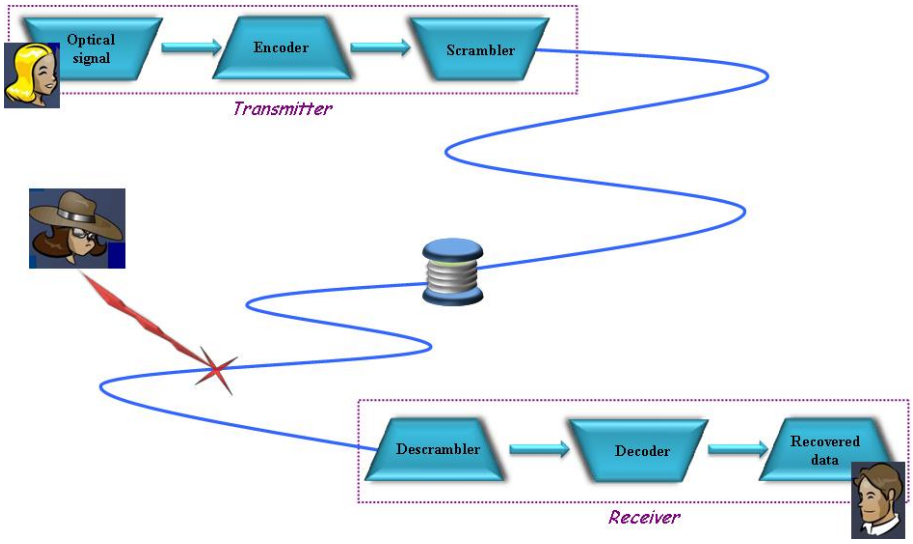


Figure 2.22: General schematic of an optical scrambling system with OCDMA encoders.

### 2.4.2 Optical scrambling system with OCDMA encoders

In this paragraph, an optical scrambling system, realized by a cascade of OCDMA encoders, will be discussed. This would lead to a system simple, feasible and consistent with the current optical technologies, since the used devices are well known. In this system the scrambling is accomplished by introducing one or more additional encoders in cascade with the primary OCDMA encoder. In Fig.2.22 a general schematic of the system with only one additional encoder is shown. By the use of scrambling the degrees of freedom in the encoding process are increased, increasing accordingly the decryption complexity. Since only one user could be active in a network and the confidentiality level assured should not depend by conditions not related with the system itself [51], that is, for example, the multiple access interference, as a starting point of the analysis a single point-to-point (P2P) transmission will be considered, that can be intercepted by an eavesdropper anywhere on the transmission link, but before the decoder.

#### Theoretical analysis

First, some theoretical consideration can be done. Introducing the scrambling, the degrees of freedom of a system are increased, making more difficult for an eavesdropper to perpe-

trate, i.e., a brute force attack. Thanks to the multilevel eye diagram, a potential attacker cannot decipher the transmission with power or differential detection, so the only way for deciphering the transmission is to guess the used codes. To enumerate valid codes he needs to know the code length and the number of encoders, because the total length that he can reveal is the sum of the length of each code used in each encoder. In the proposed system, code length detection is complex for an eavesdropper tapping the signal after the second encoder, because a signal encoded by a cascade of multiple encoders is fully distorted to the point that consecutive encoded bits overlap. As an example in Fig.2.23 the pattern of three consecutive encoded bits is shown: after encoding and scrambling is not possible to distinguish the waveform representing each bit [79].

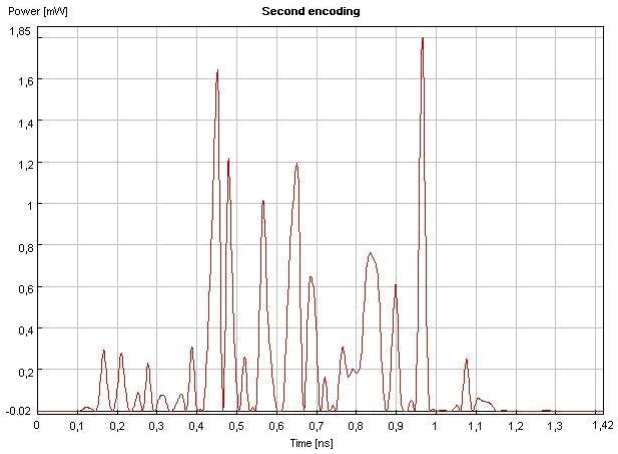


Figure 2.23: Pattern of a set of three consecutive one bits after encoding and scrambling.

However, it is not a good practice to base the security level of a system on conditions unrelated with the system itself, like potential adversaries abilities or hard to change parameters, or in other words the parameters that need hardware or software redesign of the system [51]. Therefore, in the analysis it has been assumed that the eavesdropper is technologically sophisticated and is able to discover the code length and how many encoders have been used. Even if he has this knowledge, the system has still a high degree of freedom, because to perpetrate a brute force attack, he should do a large number of trials. In fact, to correctly decipher the transmission the eavesdropper must test not only all the available code words but also all the possible combinations between these words.

To generalize this idea, it is possible to calculate the number of tests as a function of all the possible combinations with repetition between all the code words (Eq.2.16).

$$trials = \frac{(N+K+1)!}{K!(N-1)!}, \tag{2.16}$$

where $N$ is the number of available code words and $K$ represents the number of used encoders. Combinations with repetition have been considered because, in theory, a user could use the same word for encoding and scrambling. This yields the curves of Fig.2.24, in which it is shown that there are a lot of possible combinations and the number rises quickly with the increasing of the number of code words and of the number of the encoders used. As a consequence also the difficulty of deciphering of the eavesdropper rises.

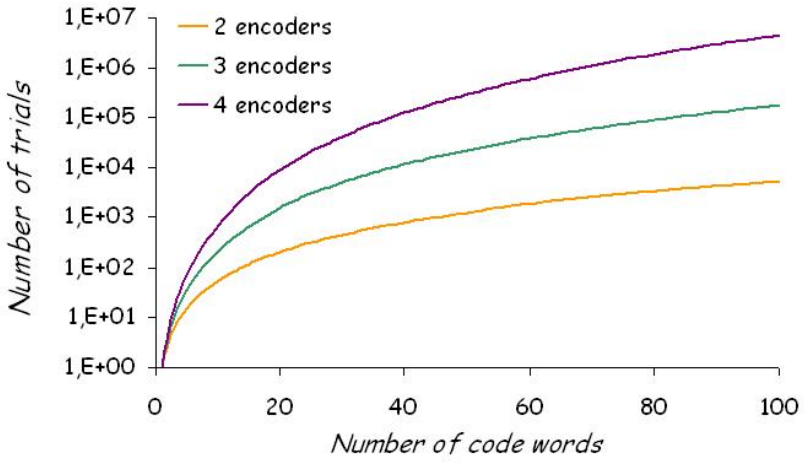


Figure 2.24: System confidentiality as a number of trials necessary to break the security.

If the eavesdropper knows the code total length and the number of encoders, an additional degree of freedom can be added by using encoders of unequal code length. This provides the additional difficulty that he does not know how this length is distributed over the different codes, e.g., if he discovers a total length of 29 chips, it is still unknown if the user has two codes of 15 chips each, or one code of 2 chips and another of 28 chips, etc. The consequence of this additional degree of freedom would be an even larger number of possibilities and an increasing in the difficulty of detecting the signal.

### P2P transmission

The simulation setup is developed by the means of the software *VPITransmissionMaker*, realized by *VPIphotonics*™ [76]. The numerical simulation setup is shown in Fig.2.25: the scrambling is achieved by introducing one additional encoder in cascade with the primary OCDMA encoder. At the transmitter end, a data signal is sent into two consecutive OCDMA encoders: the first realizes the encoding and the second realizes the scrambling. Then at the receiver side two decoders rebuild correctly the original signal. The data sent is a 16*ps* pulsewidth Gaussian pulse, with 1W peak power, at a data rate of 5Gb/s and the used codes are 15 chips *Kasami* codes, with 2.3mm chip length.

The encoding/decoding processes rely on phase shifted *Super Structured Fibre Bragg Gratings* (SSFBGs) with an optimized apodization profile to assure a better orthogonality between codes, facilitating the correct user recognition, and above all to make necessary a perfect match of the codes in coding and decoding processes [77]. Moreover the use of FBGs limits the processing ability of an eavesdropper, so even if he would have a very sophisticated optical equipment, the correct detection would require a lot of time.

In the simulation setup, the encoder and the scrambler are performed with a block (the block called *measured* in Fig.2.25) that implements an optical filter based on a transfer characteristic read from a file. The file is written with the software Matlab® and contains the features of the codes (the wavelength and the real and imaginary parts of the spectrum)[1]. To compensate the losses introduced by the use of SSFBGs, an optical amplifier was added to the system. Then, to improve the quality of the signal depicted, an optical filter was connected before each scope and also an electrical filter with a bandwidth of 3.5 GHz was considered. Moreover, to make the transmission more similar to real traffic, noise was added and a PRBS signal drives the Gaussian pulse generator. After each stage a scope is connected to monitor the signal at any point along the transmission path.

In Fig.2.26, the eye diagrams of the signal after each device in the transmitter are shown. After the scrambler, it is possible to see that the signal is fully distorted because the eye

[1]The profile of SSFBGs that realize the encoding is simulated by the Matlab application *Optmistic* realized by P.Teixeira.

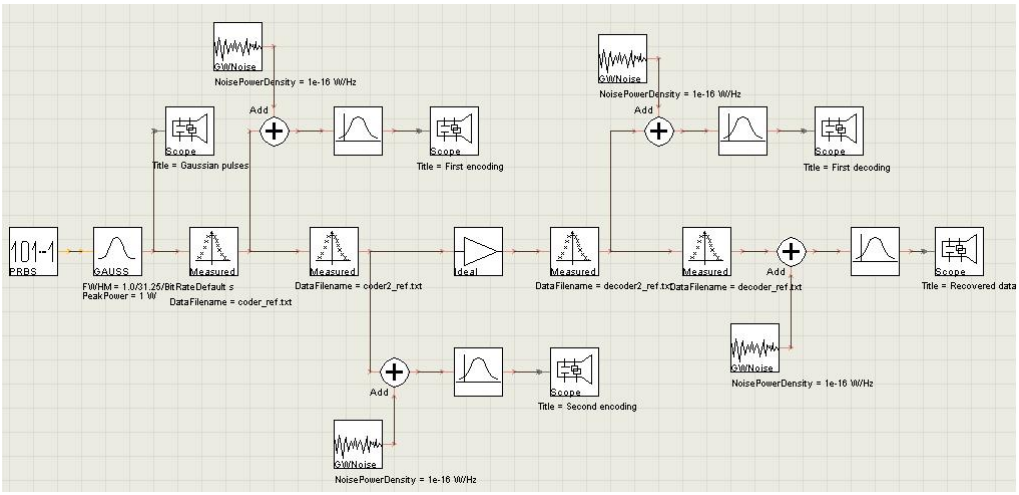


Figure 2.25: Numerical simulation setup with two encoders.

diagram, even if not totally close, has many levels. So, thanks to this fact an eavesdropper cannot decipher the transmission with simple power or differential detections [78]. While

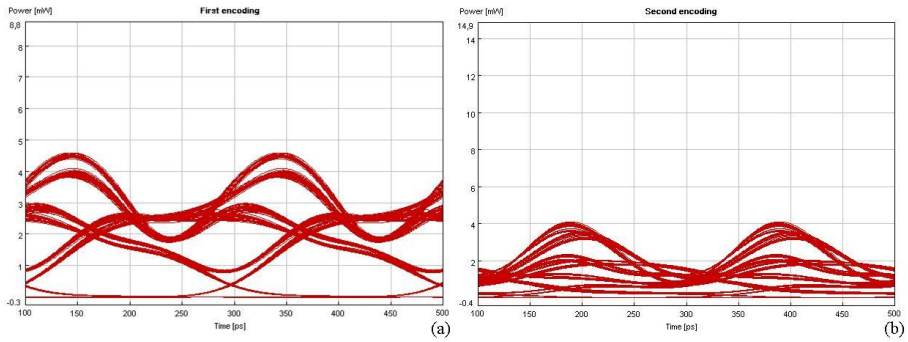


Figure 2.26: Eye diagrams of the signal at the transmitting side.

in Fig.2.27 the eye diagrams of the signal in the descrambling process are shown. If the receiver has a matching decoder, the data are correctly recovered, as indicated by the open eye.

To test the performance of the system realized, BER measurements have been performed using the setup of Fig.2.28 [80]. In this setup the transmitter is connected with the user's receiver and with the eavesdropper's receiver to compare the performance of both of them. A sweep attenuator module has been used to change the power received and a power meter

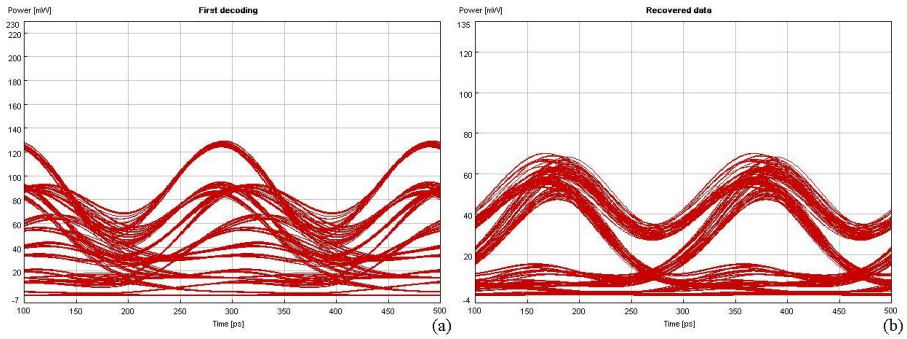


Figure 2.27: Eye diagrams of the signal at the receiving side.

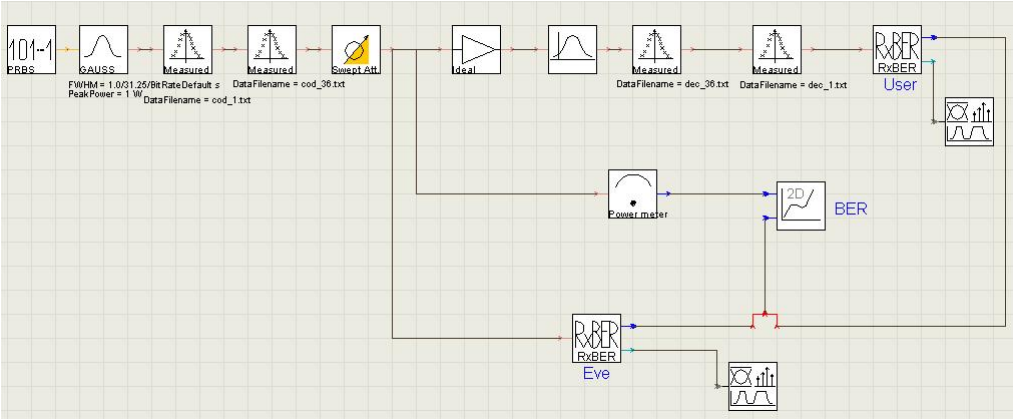


Figure 2.28: Numerical simulation setup for BER measurements.

has been used to measure it. The data sent is a PRBS signal with a data rate of 5Gb/s and 1W peak power.

The user's receiver is composed of the matching decoders of the encoders used in the transmitting side to reveal correctly the transmission and with a receiver module, which permits to calculate the BER. Moreover an optical amplifier module has been used to compensate the losses introduced by the two modules that simulate the SSFBGs decoders. Instead, for the eavesdropper's receiver only the receiver device have been used. These two different configurations for the receivers are chosen to compare the performance of the latter with the user's ones and to test if the transmission can be recovered even without a matching decoder.

The BER measurements (Fig.2.29) show a large difference in performances between the

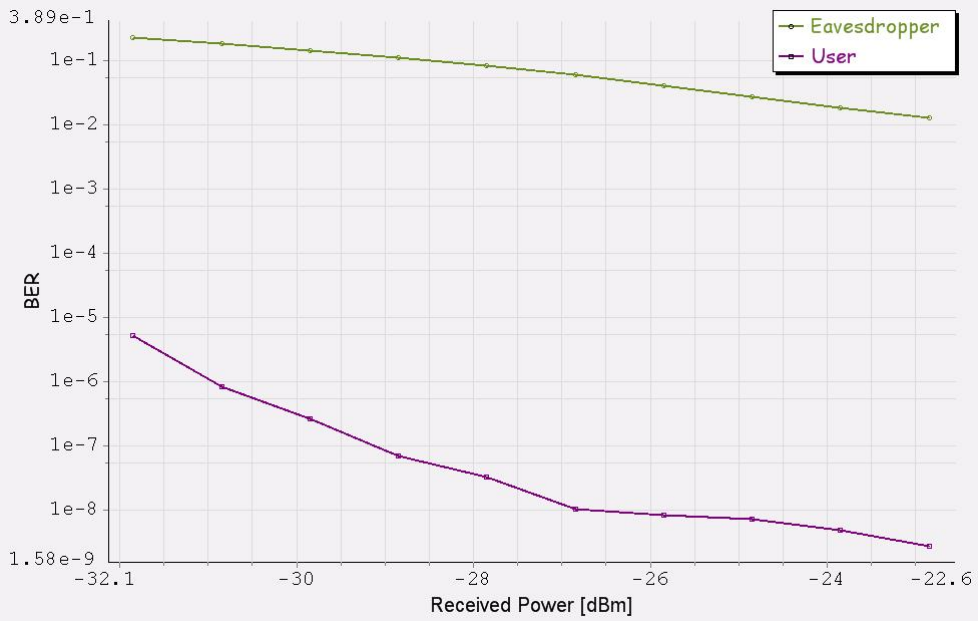


Figure 2.29: BER measurements for a back-to-back transmission.

user with the matching decoder (violet curve) and the eavesdropper without the decoder (green curve). The BER value for the eavesdropper ranges between $10^{-2}$ and $10^{-1}$. This means that the eavesdropper is not able to reveal correctly the transmission without the decoder and he must guess the used code words and try all the combinations, as modeled in the theoretical analysis. In Fig.2.30 the eye diagrams of both eavesdropper and user at a received power of $-26$dBm, where the value of user's BER is in between of $10^{-9}$ and $10^{-8}$, are reported. Even in this case, it is possible to notice that without the descrambling process the eye diagram has many levels, so the signal is fully distorted.

A further improvement of the setup entailed the system shown in Fig.2.31, where system perfomance are investigated for a signal transmitted over a 20km fibre channel. A Distributed FeedBack (DFB) laser module, with a central frequency of 193.4THz and average power of 1W, is externally modulated by a PRBS signal at 5 Gb/s. At the transmitting side the signal is still scrambled by two different phase-shifted SSFBGs encoders in cascade configuration, using 15 chips *Kasami* codes, after the scrambling the signal is sent over a 20-km fibre link. At the receiving side, three different configurations have been considered

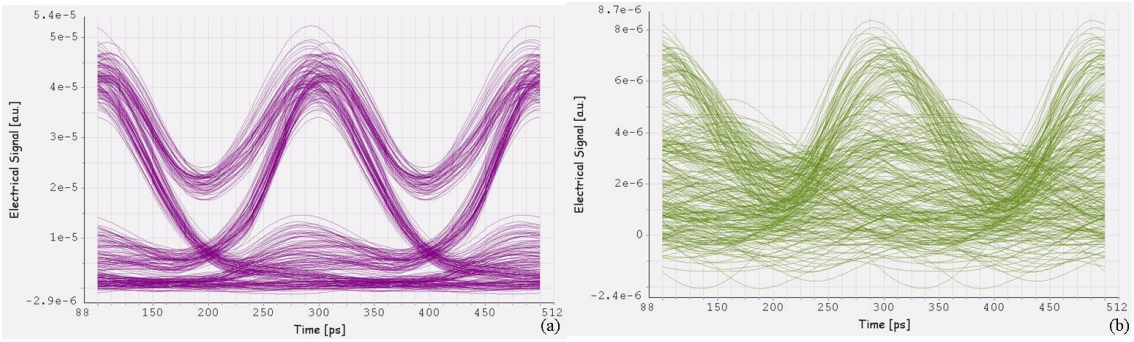


Figure 2.30: Eye diagrams of (a) the eavesdropper and of (b) the user for a received power value of $-26dBm$, in the case of back-to-back transmission.

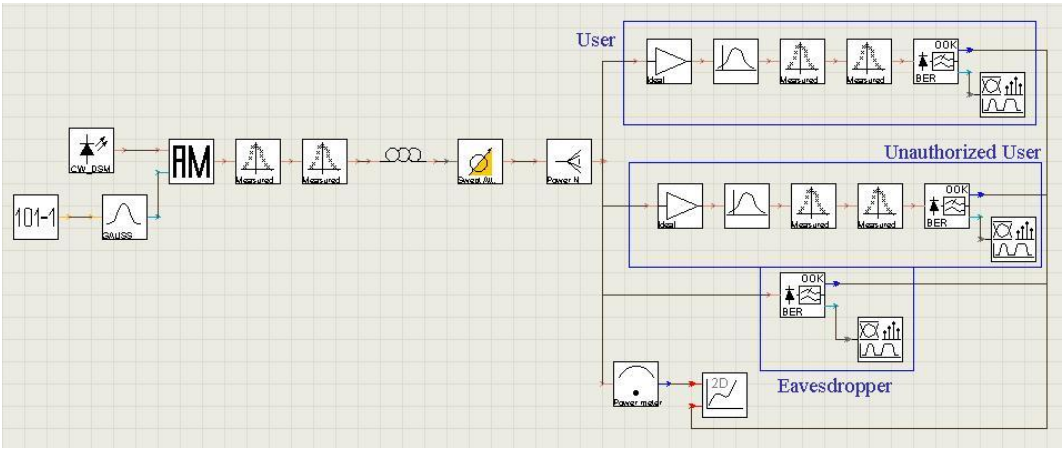


Figure 2.31: Numerical simulation setup for BER measurements with 20km fibre link and three receivers.

in order to compare their performance: an authorized user equipped with two decoder modules set with the matching codes, a potential eavesdropper equipped only with a receiver and an unauthorized user, which could be seen as another potential attacker, equipped with the decoders, but set with wrong codes. In all the receivers an optical amplifier, to compensate the losses introduced by the encoders, and a BER tester.

In Fig.2.32(a),(b) and (c) the eye diagrams detected by the authorized user, a potential eavesdropper and an unauthorized user, respectively, are shown. The eye diagram of the authorized user is open and the signal is correctly recovered after 20km of fibre. Instead,

the eye diagrams of the other two receivers are multilevel in the first case or totally closed for the latter, and this means that the signal is fully distorted and the receivers cannot detect correctly the signal, even by using differential detection.

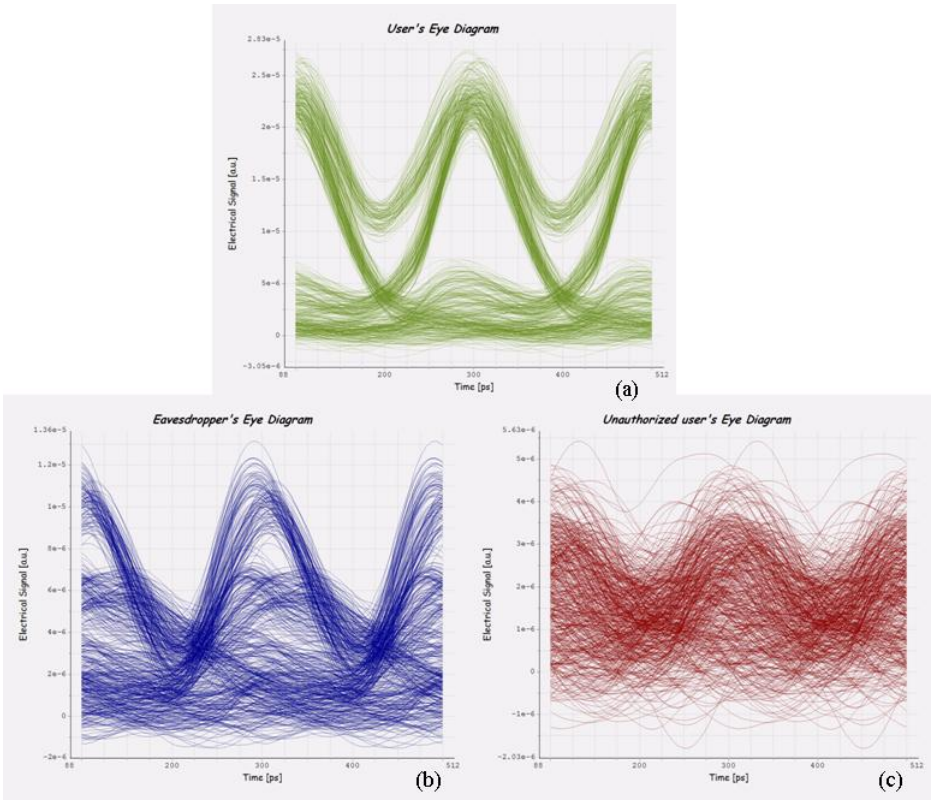


Figure 2.32: Eye diagrams (a) of the intended user, (b) of a potential eavesdropper, and (c) of an unauthorized user, for a transmission over 20km fibre channel.

Also the BER simulation of Fig.2.33 shows a large difference in performance between the authorized user (green curve with rhombuses), the eavesdropper (blue curve with circles) and the unauthorized user (red curve with squares). In the last two cases, the signal cannot be distinguished by the noise, so that the receivers are not able to detect the transmitted data.

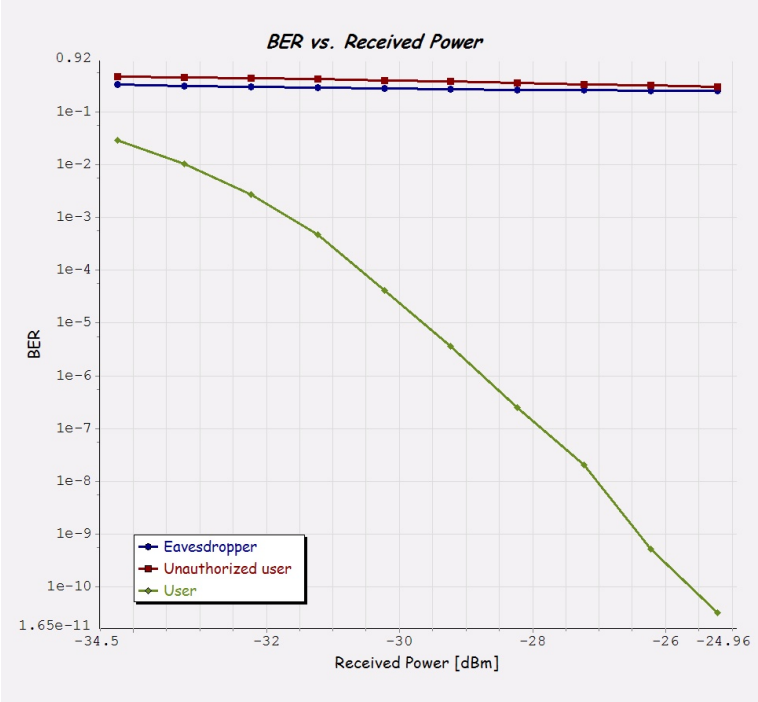


Figure 2.33: BER measurements of a P2P transmission over 20km fibre link for the authorized user (green curve with rhombuses), the eavesdropper (blue curve with circles) and the unauthorized user (red curve with squares).

### Multiple encoders

To increase the security level, making the signal more distorted, it is possible to add more OCDMA encoders [79]. As demonstrated in the theoretical analysis, if more encoders are added in cascade with the first one, the difficulty in deciphering the transmission for a potential attacker increases. So, to show the effect of multiple encodings on the signal, a setup with a cascade of four OCDMA encoders was realized. Each encoder uses different 15 chips *Kasami* codes. A scope is connected after each encoding block to visualize the effect of each further scrambling process on the signal.

In Fig.2.34 the eye diagrams of the signal after one, two, three and four encoders are reported to show that after each additional device the signal appears even more distorted and the eye diagram has more levels. The signal transmitted is a PRBS signal at 5Gb/s.

An eavesdropper tapping a signal encoded with a cascade of four devices will have

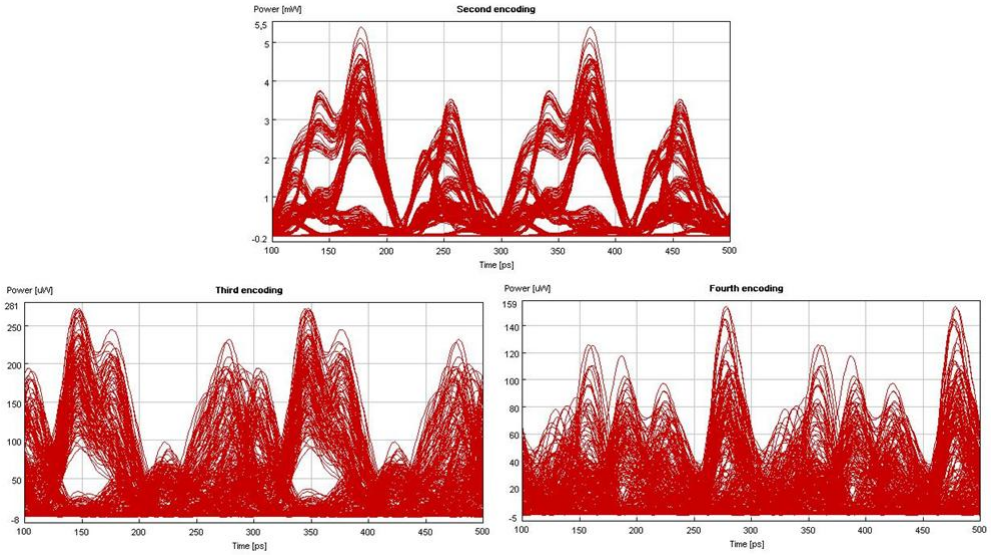


Figure 2.34: Eye diagrams after multiple encoders.

significant difficulty in deciphering the transmission. But on the other hand this solution will lead to a more complex transmitter, because each user will need a larger number of devices for the transmitter and for the receiver.

### Superimposed encoders

In order to reduce the number of devices at the transmitting and receiving sides, another system could be proposed. In this system two SSFBGs are superimposed [78], thus it could be possible to use only one device to encode and to scramble the signal. The setup realized to simulate this system is shown in Fig.2.35. In this setup only one block *measured* was necessary and the characteristic of two superimposed SSFBGs is passed to it from a file.

Also in this case after the scrambling the signal is fully distorted, but with the matching device the transmission can be correctly recovered, as shown in Fig.2.36. This system is more simple because each user needs only one device to encode and to scramble and only one to descramble and to decode, but the physical realization of the model should be investigated more in detail.

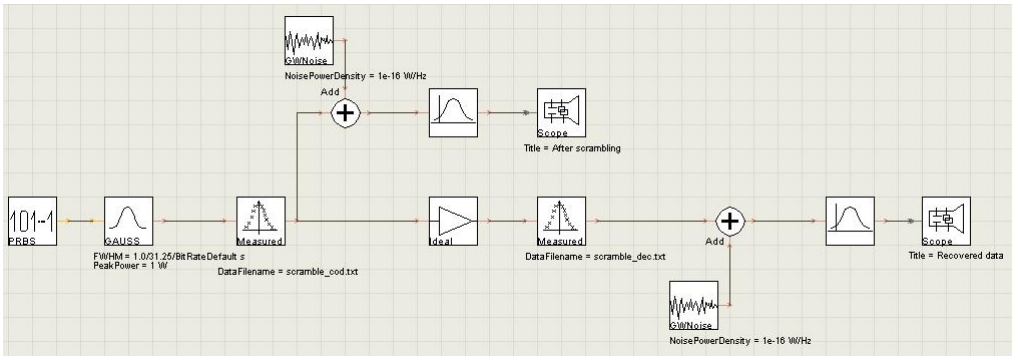


Figure 2.35: Numerical simulation setup for optical scrambling with two superimposed OCDMA encoders.

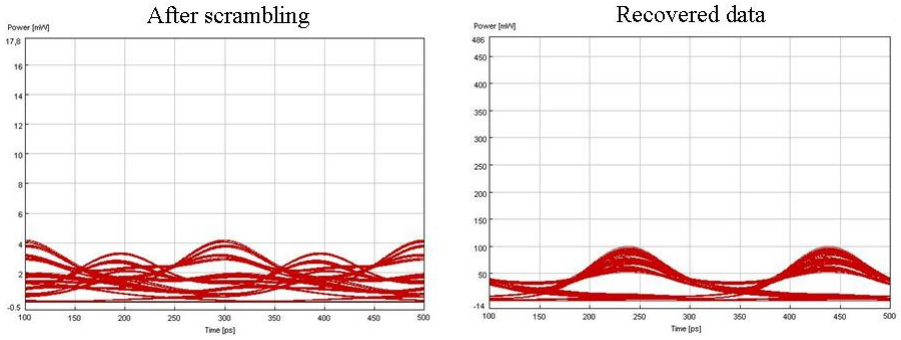


Figure 2.36: Eye diagrams after multiple encoders.

### Multiuser configuration

Afterwards, two multiuser configurations of the optical scrambling-based OCDMA system were realized. In the first configuration, each user is equipped with an encoder and a scrambler, then all the scrambled signals are combined together and sent in the fibre link. Therefore, each data signal from each user is convolved with two codes so that the impulse response of the encoder chain is the convolution between the codes. The more the codes are uncorrelated, the more the encoded signal is degraded and no information can be theft from unauthorized users, even using differential receivers. At the intended receiver side, the information is correctly extracted using the matched decoders.

A critical point in this application is the choice of the codes, because to allow a correct detection of the signal by the intended user, the orthogonality must be assured not only

between each code word, but also the convolution between two codes of an user must be orthogonal to the convolution of two other codes of another user in the network. In order to investigate the properties of the codes used in the proposed system, the autocorrelation of two of the codes, the correlations between the codes used in each transmitter and the correlations between the channels have been calculated and are shown in Fig.2.37 and in Fig.2.38 (a) and (b), respectively. From the analysis of the obtained values it is possible to conclude that the chosen codes are suitable for the application in a multiuser configuration.

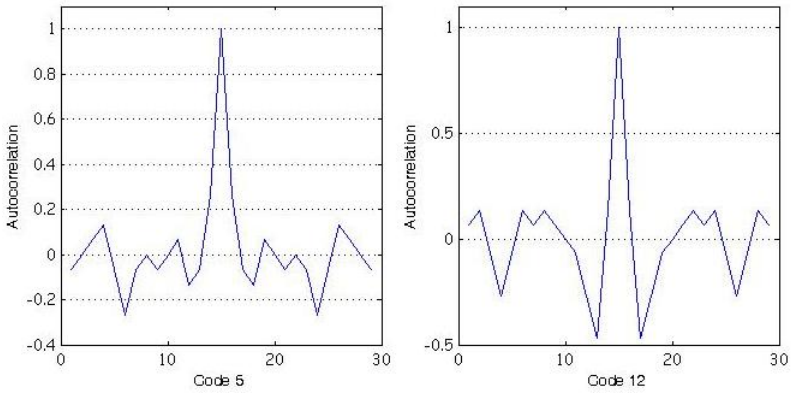


Figure 2.37: Autocorrelation of two codes of the *Kasami* family.

The schemes used for the numerical simulations are shown in Fig.2.39 and in Fig.2.40, that represent the transmitting and receiving side, respectively. A Distributed FeedBack (DFB) laser module, with a central frequency of 193.4THz and average power of 1W, is externally modulated by a 5Gb/s signal; two filter modules simulate the two encoders that generate 15-chip *Kasami* codes. The encoded signals from three users are combined together and transmitted over 80-km single-mode fibre link (Fig.2.39).

The receiver is composed of two matching decoder modules, an optical amplifiers and a bit error rate (BER) tester. Possible tapping attacks are simulated by two other receivers, equipped with an optical amplifier and a BER tester, but without any decoder or with a wrong decoder respectively (Fig.2.40). The system performance has been investigated with one and two interfering channels, to test the interference effects between the channels.

The eye diagrams of the received signal, considering one and two interfering channels, are shown in Fig.2.41(a) and 2.41(b), respectively. In both cases the eye is adequately open

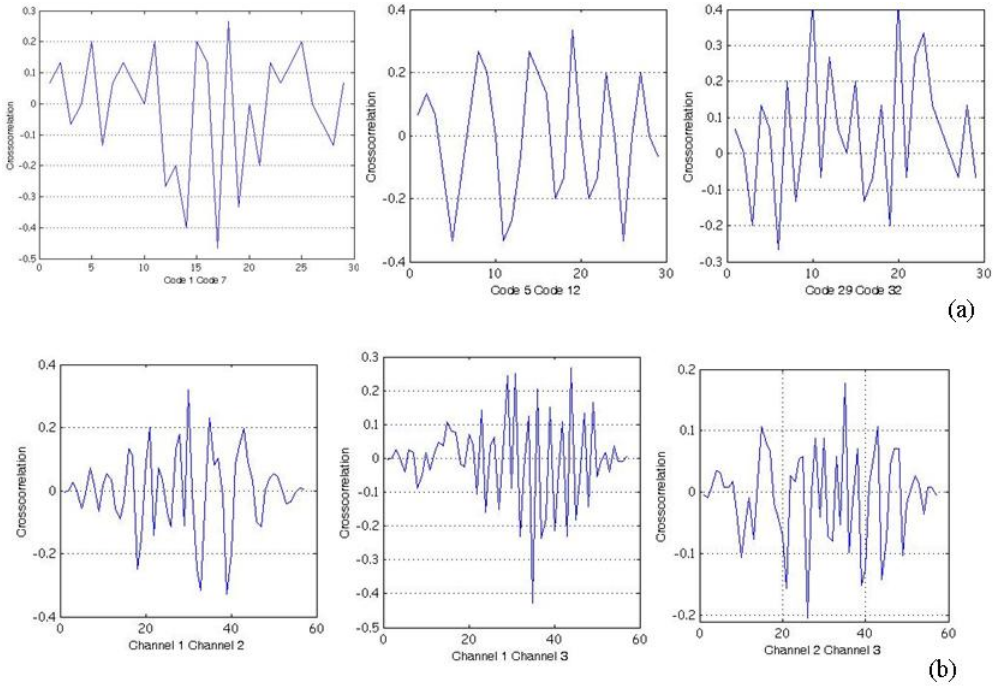


Figure 2.38: (a) Crosscorrelation between the codes used in each transmitter. (b) Crosscorrelation between the signals resulting by the convolution of the codes used in each channel.

and the introduction of another OCDMA channel does not affect the transmission. Instead, the eye diagram measured for the eavesdropper is shown in Fig.2.41(c); it has many levels, leaving the signal fully distorted, and this prevents a malicious attacker from sifting the transmission without using of the matching codes. The multiuser access interference (MAI) noise helps in hiding the message, but on the other hand, the presence of other users does not affect too much the detection of the signal by the authorized user.

To compare the performance of authorized and unauthorized users in the case of two interfering channels, BER measurements have been performed, Fig.2.42. As in the P2P application, three kinds of receivers have been considered: the intended receiver equipped with two decoder modules set with the matching codes, the eavesdropper equipped only with a receiver and the unauthorized user, which could be seen as another potential attacker, equipped with the decoders, but set with wrong codes. From the analysis of the BER

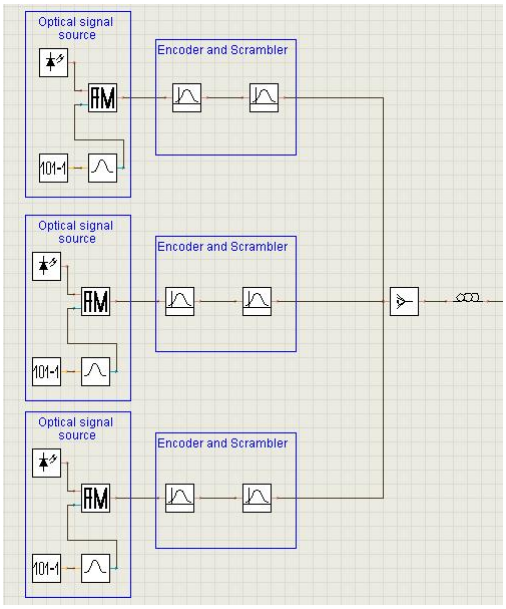


Figure 2.39: Transmitting side of the numerical simulation setup for the multi-user configuration.

curve, it is possible to observe that the BER for the eavesdropper and for the unauthorized user is very high so that they are not not able to detect any received signal. Moreover, in Fig.2.43 a comparison between the eye diagrams detected by the three receivers, when two interfering channels are considered, is shown.

The second configuration for a multi-user application is based on the distributive property of the convolution, so, at the transmitting side, the signal from each user is encoded one time by a single encoder, then all the signals from all the users are combined together by a combiner. The multiplexed OCDMA signal is then scrambled using another encoder. This solution reduces the number of the devices necessary to scramble the signals and it could find application in a passive optical networks (PON) scenario. The rest of the devices is the same as in the previous configuration. In this case, one interfering channel is considered.

The numerical simulation setup for the transmitting side of this configuration is shown in Fig.2.44. Two asynchronous users are simulated by two DFB laser modules, externally modulated by a 5Gb/s signal. Also in this case, the central frequency is 193.4THz and

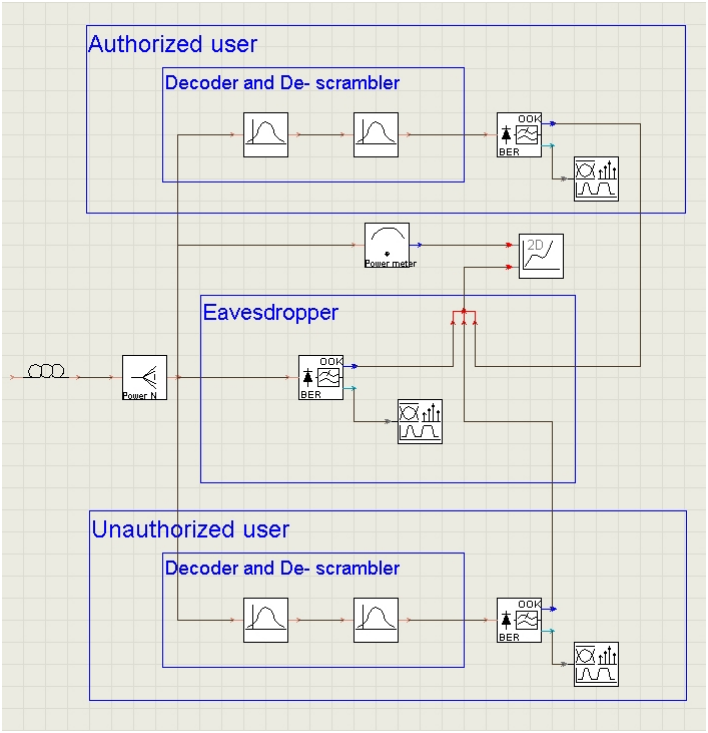


Figure 2.40: Receiving side of the numerical simulation setup for the multi-user configuration.

the average power is 1W. Each transmitter is equipped with one module to encode data with a 15-chip *Kasami* code. Then a combiner adds all the signals together, and after that, another OCDMA encoder scrambles the resulting signal. Scrambled data are sent into a single mode $80-km$ fibre link. At the receiver side, an authorized user is simulated with an optical amplifier, two decoder modules set with the matching codes that allow the correct revelation of the data, descrambling and decoding the received signal, and a receiver module. On the other hand, two potential attackers are simulated in two different ways, one with an optical amplifier and a receiver module, another with an optical amplifier and the decoders with wrong codes. The numerical simulation setup for the receiving side is equal to that illustrated in Fig.2.40 for the previous configuration.

To evidence the scrambling effect, the eye diagrams measured after the combiner and after the scrambler are shown in Fig.2.45(a) and 2.45(b), respectively. It is evident from Fig.2.45(b) that the scrambling makes the signal fully distorted so that the decryption is

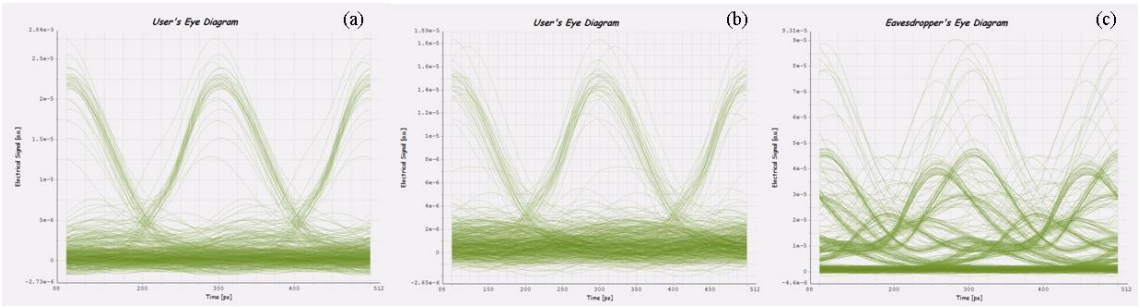


Figure 2.41: Eye diagrams of the detected signal with one (a) and two interfering channels (b). (c) Eye diagram detected by the eavesdropper.

difficult, even using differential detection. It is important to notice that the eye diagram in Fig.2.45(b) represents also the eye diagram of an eavesdropper tapping the signal at any point along the link after the scrambler. In Fig.2.46(a) the eye diagram at the receiving side for the authorized user is shown: with the matching codes the signal is correctly recovered. Whilst in Fig.2.46(b) and (c) respectively, the eye diagrams for an eavesdropper and for an unauthorized user are shown: in both cases, the signal is dipped into the noise and it is not possible to detect it correctly.

In order to test the performance of this configuration, BER measurements have been done and are shown in Fig.2.47.

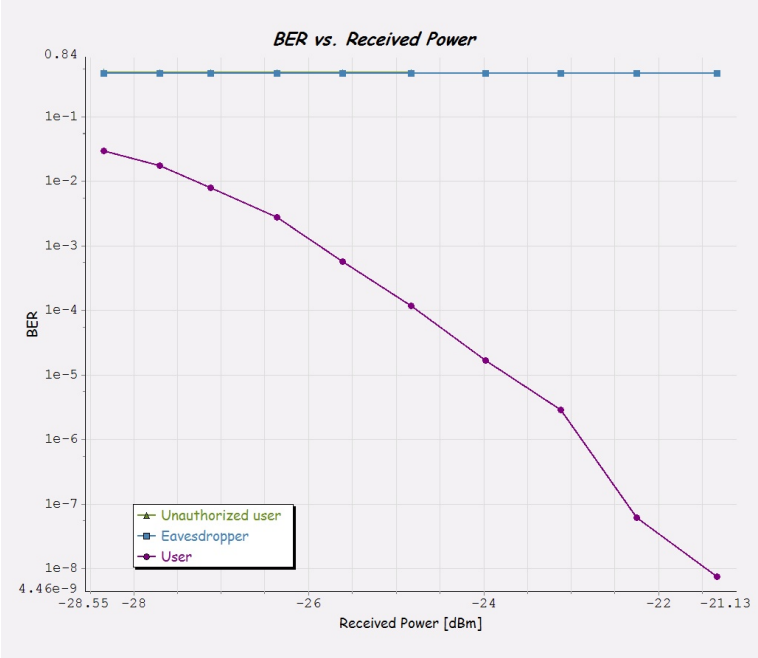


Figure 2.42: BER measurements in the case of multiuser configuration, considering two interfering channels, for the authorized user (violet curve, with circles), for the eavesdropper (blue curve, with squares) and for the unauthorized user (green curve, with triangles).

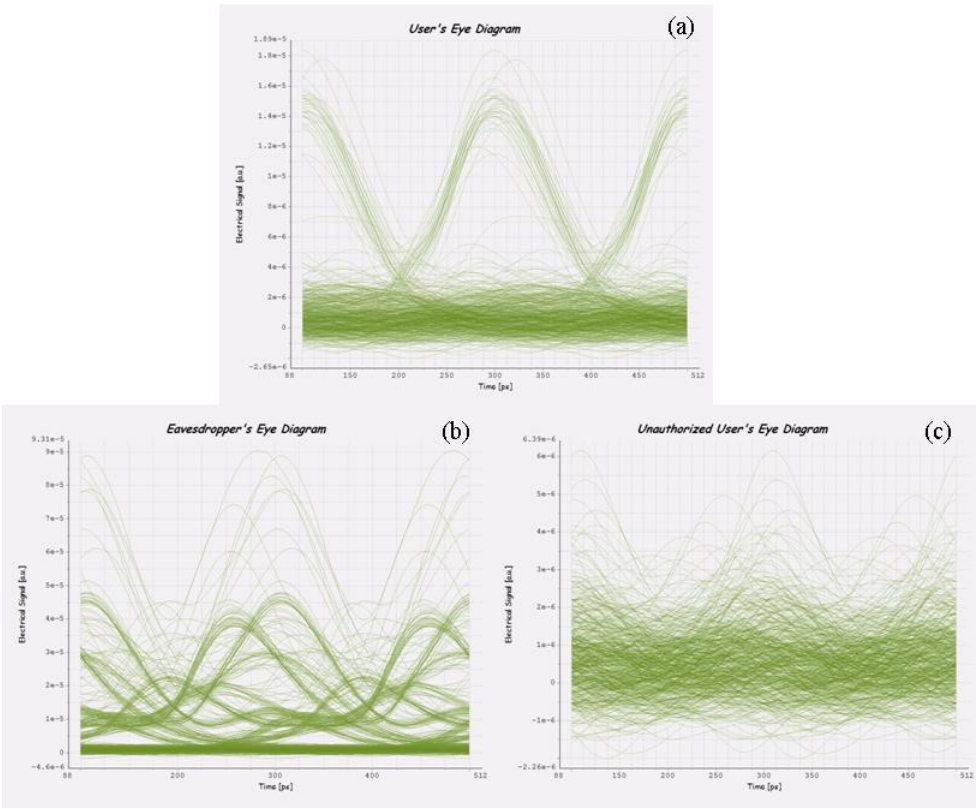


Figure 2.43: Eye diagrams of (a) the authorized user, (b) the eavesdropper and (c) the unauthorized user, in the case of two interfering channels.

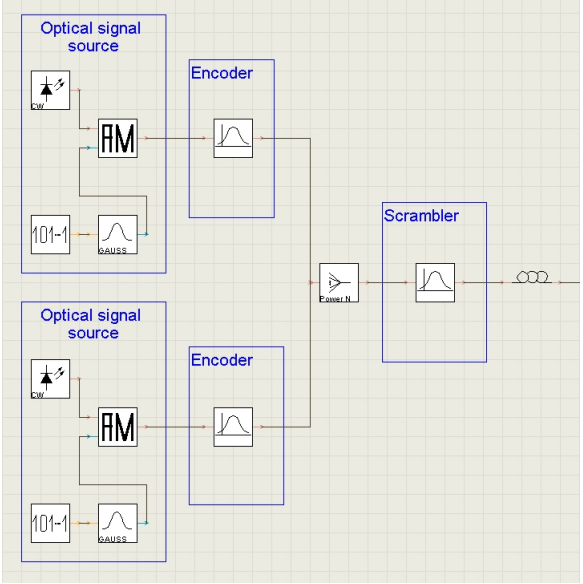


Figure 2.44: Transmitting side of the numerical simulation setup for the channel scrambling configuration.

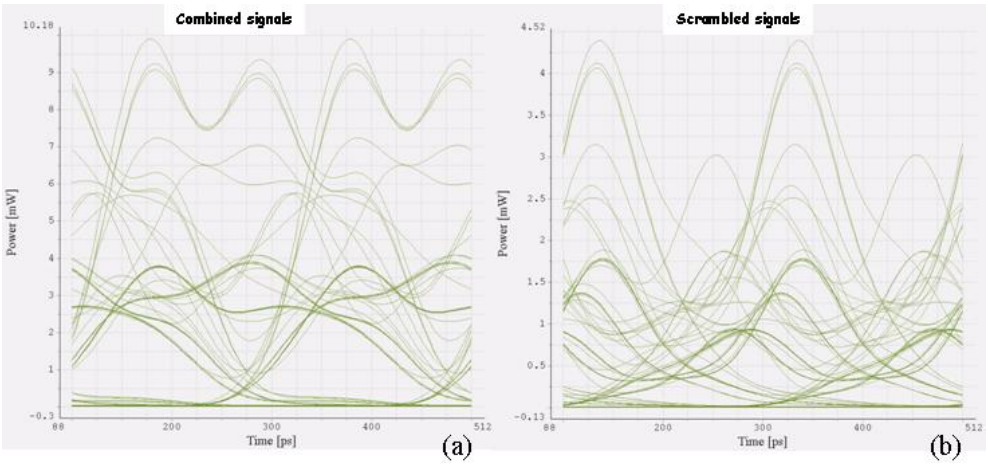


Figure 2.45: Eye diagrams of the combined signals (a) and of the scrambled signals (b).

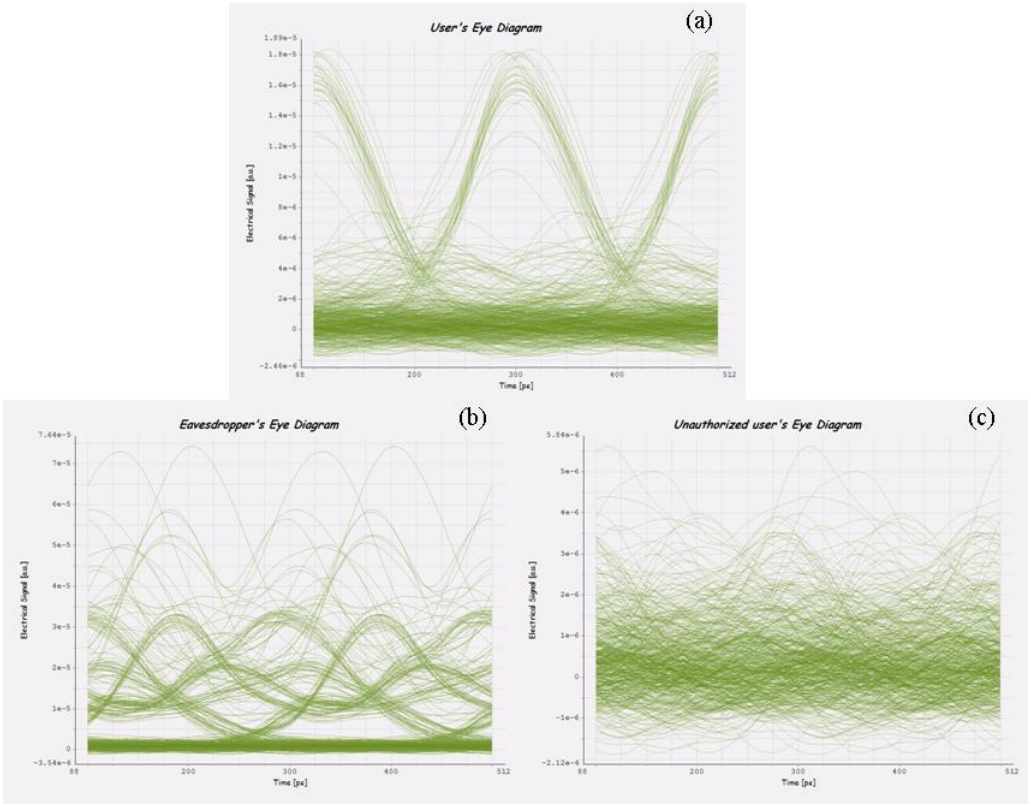


Figure 2.46: Eye diagrams of (a) the authorized user, (b) the eavesdropper and (c) the unauthorized user, for channel scrambling configuration.

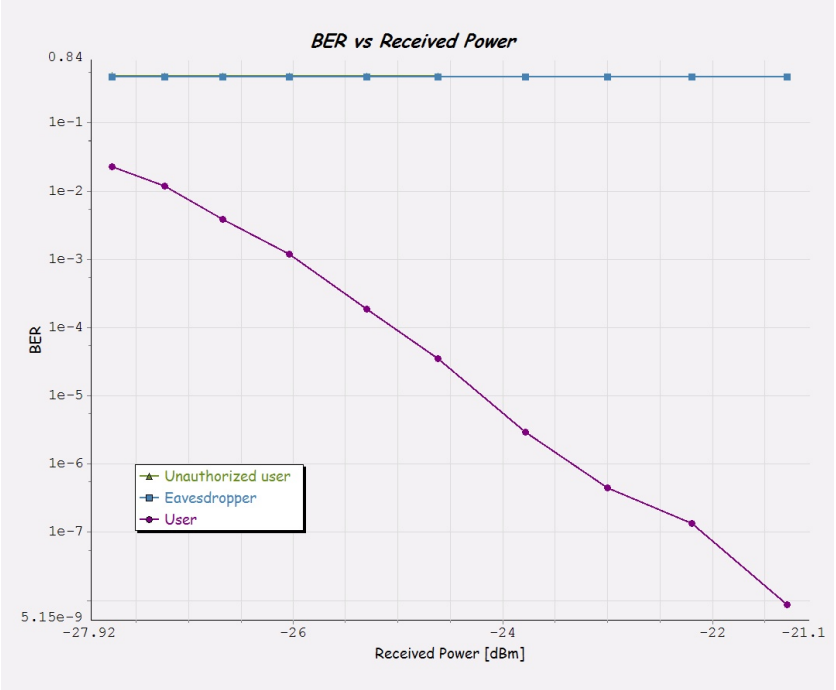


Figure 2.47: BER measurements in the case of channel scrambling configuration, considering one interfering channel, for the authorized user (violet curve, with circles), for the eavesdropper (blue curve, with squares) and for the unauthorized user (green curve, with triangles).

Chapter 3

# Advanced Modulation Formats in Access Networks

## 3.1 OOK, DUOBINARY, DPSK and DQPSK modulation in OCDMA networks

The use of advanced modulation formats have been investigated in OCDMA networks in order to increase the performance, in particular differential phase shift keying (DPSK) [84] and differential quadrature phase shift keying (DQPSK) [85] have been used to reduce the multiple access interference (MAI) and beat noises in coherent OCDMA, increasing the spectral efficiency.

Spectral efficiency is one of the most critical parameters in an optical link, since new IP-based applications, such as video-conferences and real-time games, require high information density. On the other hand, OCDMA transmission offers extraordinary network capabilities, allowing a large number of users to share the same bandwidth. In this case, the spectral efficiency is $\eta = KB/\Delta f$, where $K$ is the number of simultaneous users transmitting at a bit rate $B$ and $\Delta f$ is the optical bandwidth.

It has been demonstrated that the use of DPSK and DQPSK can increase the spectral efficiency to 0.41 b/s/Hz and 0.87 b/s/Hz, respectively [84, 85].

MAI and beat noises drastically reduce the system performances when the number

of users increases, but the introduction of DPSK and DQPSK modulation can be used to enhance the BER. Therefore, advanced modulation formats increase the number of simultaneous users that can synchronously access the network, thus enhancing the spectral efficiency and systems performance.

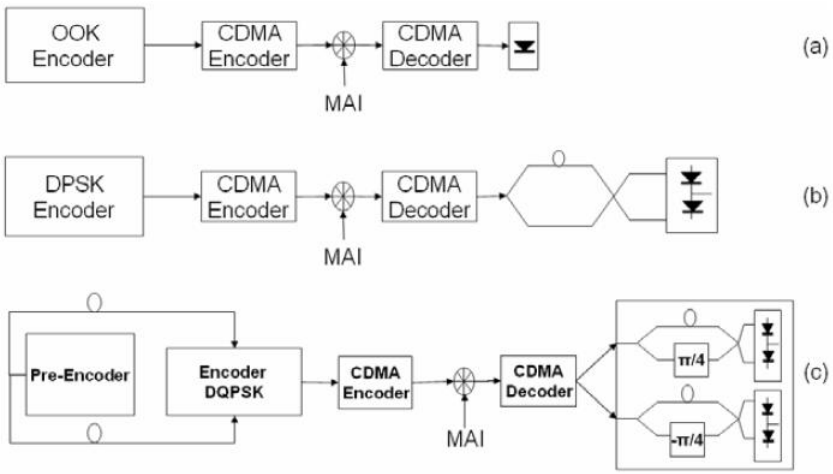


Figure 3.1: OCDMA architecture using (a) OOK, (b) DPSK, (c) DQPSK modulation formats.

In Fig.3.1 three different OCDMA architectures are illustrated, where before the encoder, the signal is modulated by using different advanced modulation formats such as OOK, DPSK, with balanced detection, and DQPSK. The analysis of the effect of advanced modulation formats on OCDMA transmission will be done in term of BER and spectral efficiency, considering both incoherent and coherent encoding techniques.

First, incoherent techniques will be analyzed, considering OOCs, already described in Section 2.1.2.

In the case of OOK modulation, and using an optimal threshold, the BER can be evaluated as [13]:

$$BER_{OOK} = \frac{1}{2}\mathrm{erfc}\left(\frac{Q}{\sqrt{2}}\right) \tag{3.1}$$

$$Q = \frac{A_g W}{\sqrt{4\sigma_1^2}} \tag{3.2}$$

$$\sigma_1^2 = (K-1)A_g^2\frac{W^2}{2F}\left(1-\frac{W^2}{2F}\right) + \sigma_{th}^2 \tag{3.3}$$

where $W$ is the code weight and $F$ is the code length. Moreover, $A_g$ is the peak power of a single chip, $K$ is the number of users and $\sigma_{th}^2$ is the thermal noise variance, that is dominant in a PIN photodiode.

The BER curve, calculated with Eq.3.1, for an OCDMA transmission using OOK modulation is shown in Fig.3.2, using a code with 200 chips length and considering different code weights.

In the case of DPSK modulation, with balanced detection, the formula for BER calculation becomes

$$BER_{DPSK} = \frac{1}{4}\left(1 + \text{erfc}\left(\frac{-A_g W - (K-1)A_g\frac{W^2}{2F}}{\sqrt{2\sigma_1^2}}\right) + \text{erfc}\left(\frac{A_g W - (K-1)A_g\frac{W^2}{2F}}{\sqrt{2\sigma_1^2}}\right)\right) \tag{3.4}$$

where the symbols have the same meaning as in the previous case: $W$ code weight, $F$ the code length, $A_g$ the peak power of a single chip, $K$ the number of users and $\sigma_{th}^2$ the thermal noise variance. Also in this case the BER calculations is shown in Fig.3.2, for a code chip length of 200 and variable code weights.

Finally, the BER for DQPSK modulation can be evaluated as

$$BER_{DQPSK} = 1 - (1 - BER_{DPSK})^2 \tag{3.5}$$

and it is shown in Fig.3.2 as well.

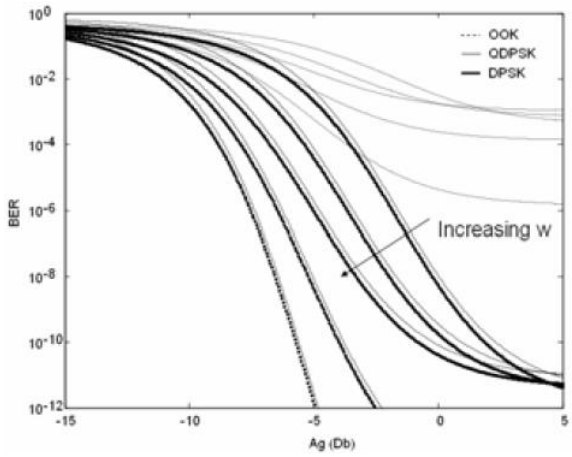


Figure 3.2: BER for OOC codes with OOK, DPSK and DQPSK modulation formats.

Due to the MAI noise, BER for standard OOK modulation is always larger than $10^{-6}$, whereas both DPSK and DQPSK reduce the BER to about $10^{-10}$ by increasing the code weight [86].

Afterwards, following the theoretical model of [87], the spectra for a pseudo random bit sequence (PRBS) and a single-user OCDMA transmission have been calculated as

$$\Phi(f) = \frac{1}{T_c}\Phi_B(f)|E_i(f)|^2 \tag{3.6}$$

where $T_c$ is the bit (or chip) interval and

$$\Phi_B(f) = \Phi_{OOC}(f) * \Phi_{Mod}(f) \tag{3.7}$$

is evaluated as the convolution between the power spectral densities of the OOC code and of the PRBS modulated signal, respectively.

The PRBS modulated signal has a bit rate of 10Gbit/s, whereas, for the OCDMA signal, the user bit rate is 50Mbit/s and the chip rate is 10Gbit/s. In Fig3.3 a comparison between the power spectra of a PRBS modulated signal using DUOBINARY, OOK, DPSK and DQPSK and the power spectra of OCDMA encoded signal using the same modulation formats are shown. The OCDMA encoding do not alter the frequency spectrum, so that DQPSK halves the bandwidth of DPSK modulation.

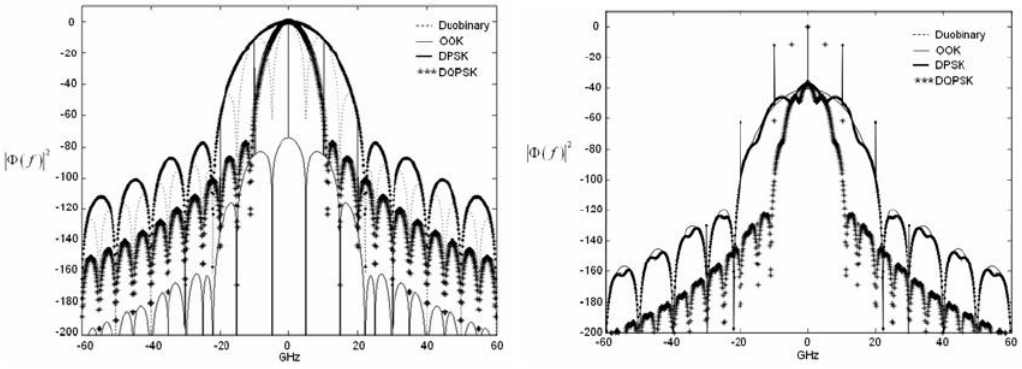


Figure 3.3: (left) Power spectra of a PRBS modulated signal, using duobinary, OOK, DPSK and DQPSK modulations; (right) power spectra of OCDMA encoded PRBS signal.

In the case of coherent codes, beat noise is the dominant noise source, and using a

Gaussian approximation for the probability density function [88], we obtain

$$BER = \sum_{i=0}^{K} \binom{K}{i} 2^{-(K-1)} \frac{1}{2} \left[ \left( 2 - \frac{1}{W} \right) P_{e10}(i) + \frac{1}{W} P_{e01}(i) \right] \tag{3.8}$$

where $W$ and $K$ have the same meaning as in the previous calculations, or, the code weight a nd the number of users, respectively. Moreover, $P_{e10}(i)$ is the probability of making an error detecting a mark when a space has been transmitted and $P_{e01}(i)$ is the probability of making an error detecting a space when a mark has been transmitted. In the case of OOK transmission they are represented by the following expressions

$$\begin{aligned} P_{e10}(i) &= 1 - \frac{1}{2} \left[ \text{erfc} \left( \frac{I_{th}(i) - m_1(i)}{\sqrt{2\sigma_1^2}} \right) \right] \\ P_{e01}(i) &= 1 - \frac{1}{2} \left[ \text{erfc} \left( \frac{I_{th}(i) - m_0(i)}{\sqrt{2\sigma_0^2}} \right) \right] \end{aligned} \tag{3.9}$$

where $I_{th}$ is the threshold and $m_1(i) = A_g + A_g \frac{i}{F}$, $m_0(i) = A_g \frac{i}{F}$, $\sigma_1^2 = \sigma_{MAI}^2 + \sigma_{beat1}^2 + \sigma_{th}^2$, $\sigma_0^2 = \sigma_{MAI}^2 + \sigma_{th}^2$.

For DPSK modulation, the use of an optical thresholder, or an optical time gating is mandatory; in this case, it is

$$BER = \sum_{i=0}^{K} \binom{K}{i} 2^{-(K-1)} \left( \frac{1}{W} P_{e10}(i) \right) \tag{3.10}$$

with

$$P_{e10}(i) = \frac{1}{2} + \frac{1}{2} \text{erfc} \left( \frac{-m_1(i)}{\sqrt{2\sigma_1^2}} \right) \tag{3.11}$$

The BER calculation in the case of OOK, DPSK and DQPSK modulations are shown in Fig3.4, considering different number of users and using Gold codes of 511 chips. If DPSK and DQPSK modulations are used, it is possible to multiplex up to 10 users.

While in Fig.3.5 the power spectral densities of single-user OCDMA modulated signals, using DUOBINARY, OOK, DPSK and DQPSK modulations, are shown. Since in this case a chip rate of 640Gchip/s and an user bit rate of 1.25Gbit/s have been considered, the spectrum of Fig.3.5 is wider than the corresponding of Fig.3.3. It is possible to observe that only DQPSK reduces the bandwidth and increases the spectral efficiency [86].

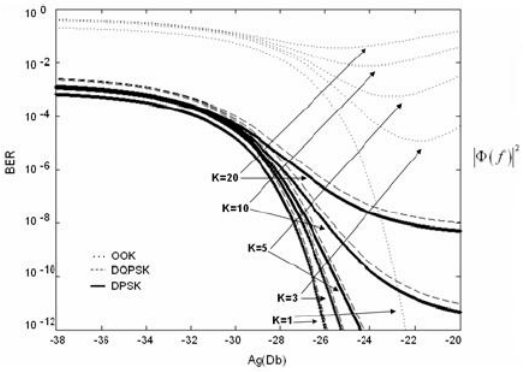


Figure 3.4: BER performance of 511-chip Gold code for OOK, DPSK, DQPSK modulation formats and different number of users.

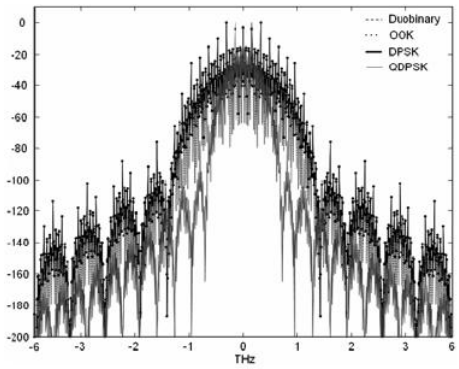


Figure 3.5: Power spectral density of a single-user OCDMA modulated signal.

## 3.2 Optical OFDM

Optical Orthogonal Frequency Division Multiplexing (Optical OFDM) is a promising technique for next generation high-speed data transmission, to achieve a data rate of 100Gb/s per optical carrier [89], because it allows to mitigate the fiber transmission impairments and to provide high data rate transmission. The low bandwidth occupied by a single OFDM channel increases the robustness against chromatic dispersion (CD) and polarization mode dispersion (PMD) and allows to extend the attainable distance to thousands of kilometers, before significant distortion [90, 91], without the need for dispersion compensation. For example, in Ref.[89], a high data rate transmission (42.7Gb/s) for 640km, without any dispersion compensator, has been demonstrated.

Signal processing in the OFDM transmitter/receiver utilizes the efficient algorithm of FFT, which enables the use of available digital signal processing (DSP) devices. After being generated by electrical signal processing, the OFDM signal is modulated onto a single optical carrier and sent into the fiber.

To detect the transmission, either direct-detection (DD) or coherent detection (CD) schemes can be used, trading simplicity against increased sensitivity. CO-OFDM systems achieve a virtual unlimited fiber dispersion tolerance, with high spectral efficiency and large transmission distances; however they require complex receivers composed of local oscillators, optical phase locked loop (PLL) and polarization controllers. On the other hand, DD-OFDM systems reduce considerably the hardware complexity of receivers, but yield to a system performance decrease compared to coherent ones. Due to the fact that the electrical OFDM signal is quasi-analogical with zero mean and high peak-to-average ratio, the majority of the optical power is wasted in the optical carrier (i.e. an additional DC value of the complex baseband signal) resulting in low receiver sensitivity. However, the performance of DD systems are acceptable and satisfy FEC limit; moreover DD-OFDM eliminates the difficulties associated with receiver end phase noise and frequency offset correction, so that conventional DFB or directly modulated lasers (DML) can be used without severely degrading the transmission performance [104]. Therefore, DD systems could be a resilient and cost effective solution for future optical networks.

In the case of intensity modulation, the bandwidth efficiency can be increased by suppressing one of the sidebands, resulting in OOFDM with single-sideband (SSB) transmission [90].

A possible implementation of a optical DD-OFDM system with optical single-sideband (OSSB) transmitted signal is proposed in Ref. [90] and it is shown in Fig.3.6.

In the OFDM transmitter, blocks of parallel input data are modulated by Quadrature-Amplitude Modulation (QAM), then each QAM data channel is sent to an input of the inverse-FFT (IFFT) module, to generate a dense comb of OFDM sub-carrier frequencies. The IFFT produces a complex-valued time domain waveform containing a superposition of all of the sub-carriers. This waveform is modulated onto an RF-carrier, $f_{RF}$, using an I-Q

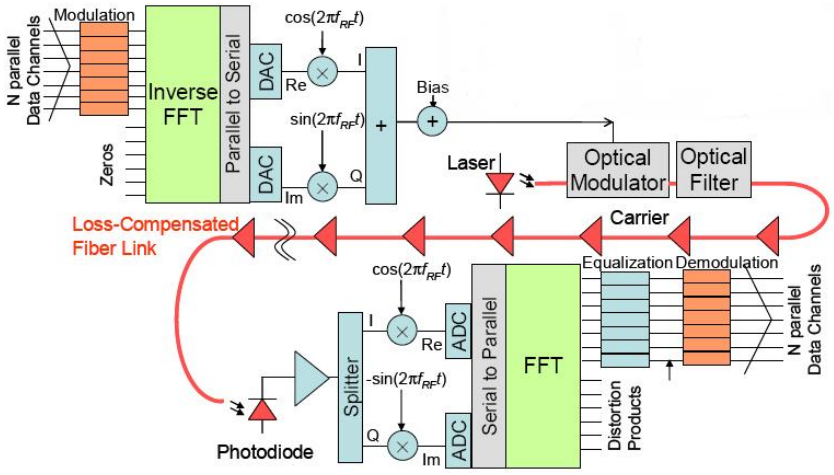


Figure 3.6: Block diagram of an optical OFDM system with direct detection, [90].

modulator, producing a real-valued waveform comprising a band of sub-carriers displaced from DC. Afterwards the processed signal is modulated onto an optical carrier using a linear optical modulator and, before to be sent into a single mode fiber, the output of the optical modulator is filtered to remove all frequencies other than the upper side-band (or lower sideband if preferred) and an attenuated optical carrier. The optimum receiver sensitivity is obtained when the power in the optical carrier equals the power in the upper sideband.

After propagation through the fiber link, the signal is sent to the photodiode that converts it onto an electrical waveform. This is converted to I and Q components, which are then converted to OFDM sub-carriers using a FFT. If the transmitter and receiver FFT windows are synchronized in time, the FFT acts as a set of closely-spaced narrowband filters. In a real system, a cyclic prefix is added to each transmitted block after the IFFT, so that the relative delays between the received OFDM sub-carriers, due to fiber dispersion, can be compensated without destroying the orthogonality of the OFDM sub-carriers. In the frequency-domain, each channel is equalized to compensate for phase and amplitude distortion due to the optical and electrical paths. This is easily achieved by using a separate complex multiplication coefficient for each channel, that can be determined by training the system with a known data sequence or by introducing pilot channels to the OFDM band

to estimate the dependence of optical phase on frequency. After equalization, each QAM channel is demodulated to produce N parallel data channels that can be converted into a single data channel by parallel to serial conversion.

The modulation on the RF carrier, that produces a gap in the spectrum between the optical carrier and the OFDM signal, has two goals: it displaces the signal band from the region where second-order intermodulation products due to photodetection fall and allows a non-brickwall (i.e. realizable) optical filter with 5GHz wide passband-stopband transitions to be used to suppress the carrier.

The OFDM technique makes the system robust against channel dispersion and enhances the corresponding spectral efficiency, moreover it makes easy phase and channel estimation in a time-varying environment. However, it also presents some intrinsic disadvantages, such as high peak-to-average power ratio (PAPR) and sensitivity to frequency and phase noise [92].

### 3.2.1 OFDM principles

OFDM belongs to a broader class of multicarrier modulation (MCM) in which information data is carried over many lower rate sub-carriers. Serial high-speed data are transmitted by dividing them into blocks, modulated with QAM or PSK schemes, and using Fourier transform techniques to encode the data on separate sub-carriers in the frequency domain. Therefore, modulation and demodulation of a high number of carriers can be realized by standard digital signal processing. Data is carried by varying the phase or the amplitude of each sub-carrier.

OFDM is a special case of the frequency division multiplexing technique, where digital or analog data is modulated onto a certain number of carriers and transmitted in parallel over the same transmission medium. Thanks to the parallel data transmission, each channel occupies only a small frequency band, so that signal distortions originating from frequency-selective transmission channels (i.e., fiber dispersion in the case of optical communications) are minimized. For conventional FDM, the spectral efficiency is limited by the selectivity of the bandpass filters required for demodulation, while OFDM is designed such that the

different carriers are pair wise orthogonal. Therefore, OFDM is characterized by a very high spectral efficiency and, consequently, for the sampling point the inter-carrier interference (ICI) is suppressed although the channels are allowed to overlap spectrally.

Orthogonality is achieved by placing the different RF-carriers onto a fixed frequency grid and assuming rectangular pulse shaping, so that the maximum of one sub-channel coincides with the minimum of the adjacent one, as shown in Fig.3.7. The OFDM signal can be implemented as the output of a discrete inverse Fourier transform that has parallel complex data symbols as input; in this way system complexity is drastically reduced.

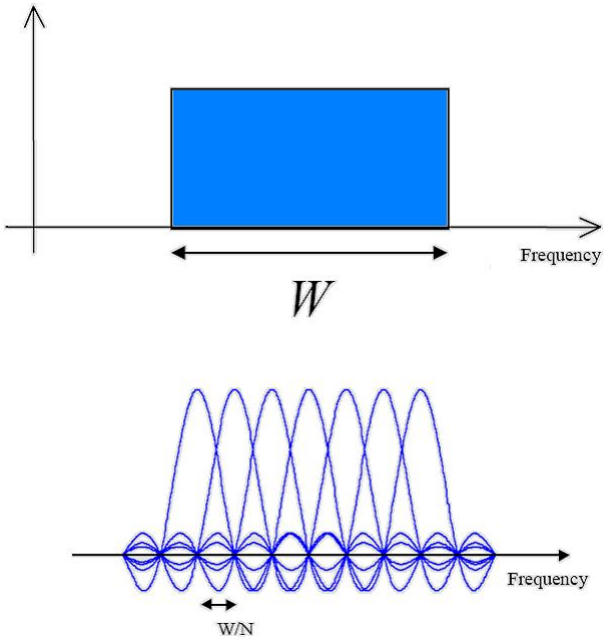


Figure 3.7: Sub-channels of an OFDM signal, [95].

It is possible to observe by Fig.3.7 that the available spectrum is divided into many narrow bands, each of them with a spectrum equal to $\sin(x)/x$. The difference between adjacent channels is $\Delta f$, so each subband can be individuated by $f_k = f_0 + k\Delta f$ and the overall bandwidth $W$ of the $N$ modulated carriers is $N\Delta f$. The frequencies of each sub-channel are chosen so that an integral number of cycles are included in a symbol period. Signals are mathematically orthogonal. The signaling interval becomes $T_s = 1/\Delta f$.

In Fig.3.8 a schematic for the architecture of an OFDM system is shown. The binary

data stream, with $f_b$ bit rate, is divided in block composed by $M$ bits. These blocks are mapped to data symbols with a symbol rate of $1/T_S$, employing a phase and amplitude modulation scheme that associates each sequence to a point of a constellation composed by $L_n = 2_n^M$ elements. The serial symbols are applied to a serial-to-parallel convertor and are demultiplexed in a block of $N$ parallel symbols $B_0, \ldots, B_{N-1}$. The symbol rate becomes $1/NT_S$. The $N$ parallel symbols are then applied to an IFFT component that converts the symbols in a sequence of complex coefficients in the time domain: the $b_0, \ldots, b_{N-1}$ coefficients represent the OFDM signal.

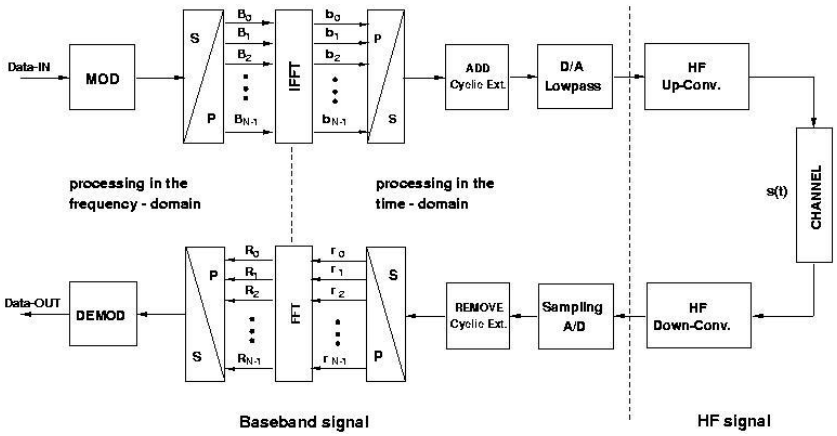


Figure 3.8: Schematic of an OFDM system.

The serial to parallel conversion can be seen as applying every $Nth$ symbol to a modulator, producing the effect of interleaving the symbols into each modulator. As a consequence, the symbol duration is longer (Fig.3.9) and the intersymbol interference (ISI) can affect only one adjacent symbol, increasing the robustness of the system. The signalling interval of the subbands in the parallel system is $N$-times longer than that of the serial system giving $T = N\Delta t$, which corresponds to an $N$-times lower signalling rate. During a N-symbol duration period of a conventional serial system, each of the N sub-channels carry only one symbol, each of which has a $N$-times longer duration, so an identical-duration channel fade would only affect a fraction of the duration of each of the extended symbol transmitted in parallel [96].

Since the system could be affected by ISI and ICI, as said in Section 3.2.2, a guard

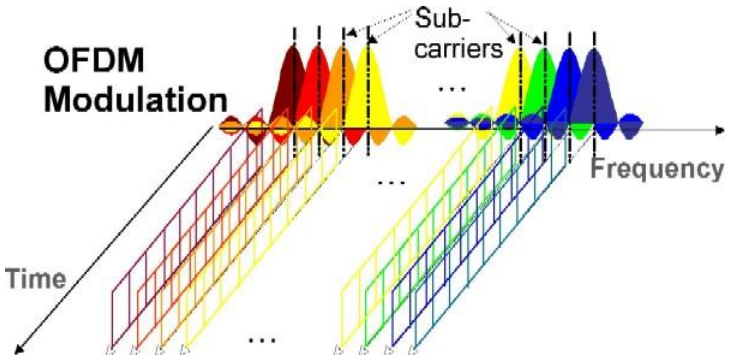


Figure 3.9: Frequency and time occupation of OFDM symbols.

interval is introduced to reduce the effect of the interference. During the guard interval, the cyclic prefix is transmitted.

Afterwards, the real and imaginary part of the signals are sent to a digital to analog converter (D/A) to modulate the quadrature carriers $\cos \omega_n t$ and $\sin \omega_n t$. Then the signal is modulated on a RF carrier and sent into the channel.

At the receiving side, each block performs the inverse function of the corresponding block in the transmitter: a spectral decomposition of the received time domain samples $r_n$ is computed by a N-tap FFT and the recovered $R_n$ data symbols are restored in serial order and demodulated.

Thanks to the use of FFT algorithm it is possible to obtain a real time processing, with a computational complexity equal to $O_{FFT} = N \log_2 N$.

### 3.2.2 Cyclic Prefix and equalization

Telecommunication systems are affected by intersymbol and interchannel interferences (ISI, ICI), that can be solved by adding a guard interval between the channels, thus the OFDM symbol duration becomes the sum of the effective symbol part and the guard interval duration [93].

An OFDM signal is composed of different wavelengths, as shown in Fig.3.10, and fibre dispersion introduces a different delay to each sub-band, consequently the received signal is altered by these delays and a portion of the signal can be shifted out of the receiver FFT

window.

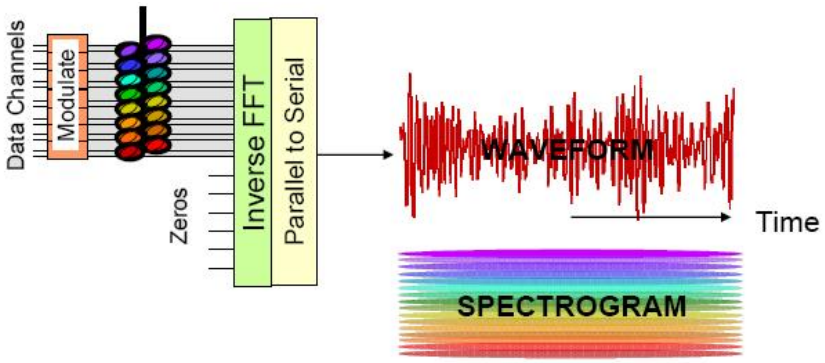


Figure 3.10: OFDM signal waveform and spectrogram, [94].

As an example, in Fig.3.11 the reddest sub-carriers are shifted out from the FFT window and could overlap on adjacent symbols and loose information. Therefore, to cope with this effect, a cyclic prefix is added to the signal before transmission. A cyclic prefix consists of a copy of part of the symbol before and after the symbol itself, as illustrated in Fig.3.12

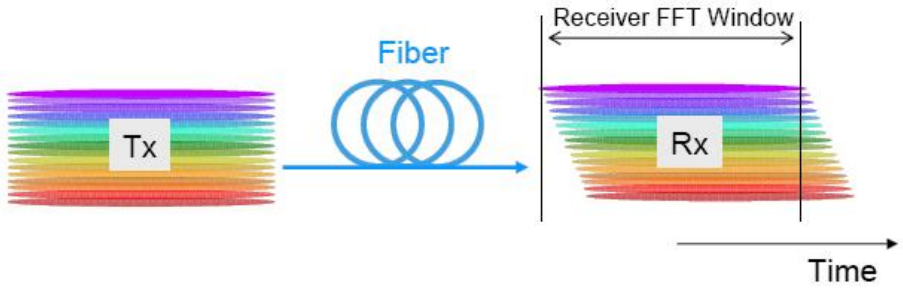


Figure 3.11: Effect of fiber dispersion on OFDM signal spectrum, [94].

The effect of cyclic prefix insertion is shown in Fig.3.13: The portion of sub-carriers shifted out by the FFT window due to the different delays is recovered by the portion of symbol inserted as a cyclic prefix, so no information is lost. However, this solution does not come without some costs, because inserting a cyclic prefix the maximum bit rate of the transmission decreases and the bandwidth increases, entailing spectral efficiency penalty. For this reason, the cyclic prefix is usually chosen equal to 20%-30% of the actual symbol.

Furthermore, in the OFDM technique, data bits are modulated on symbols, by QAM

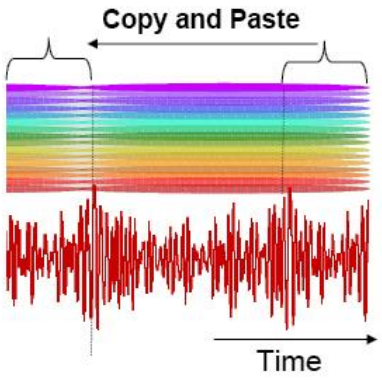


Figure 3.12: Cyclix prefix adding, [94].

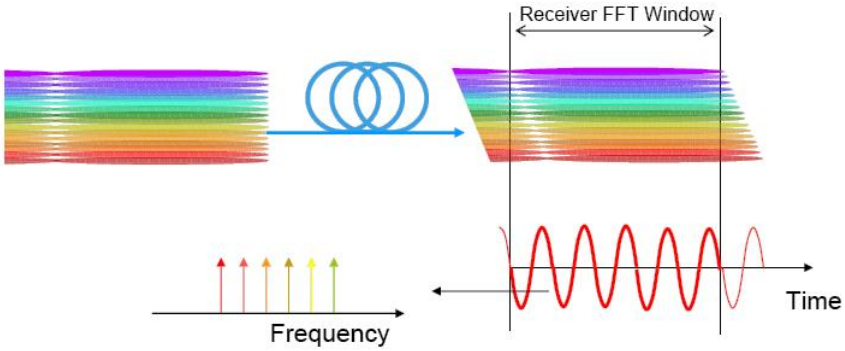


Figure 3.13: Effect of cyclic prefix adding and FFT time window on transmitted signal, [94].

modulation for instance, so data are encoded onto the phase. Dispersion shifts the phases of the sub-carriers depending on their frequency: A phase shift larger than 45 degree causes an error. Therefore, to be received without error a symbol should fall into the correct quadrant in the phase space.

For this reason, an equalization process is introduced in OFDM transmission. It solves the problem of phase distortion, placing the received symbols in the correct quadrants. Equalization is based on training symbols, whose position in the constellation is known or on pilot tones within a symbol. Also in this case, the attempt to fix the dispersion effects causes an overhead, reducing data rate. Coherent systems require frequent equalization because of the evolving relative phases of the transmitter oscillator and local oscillator

[94].

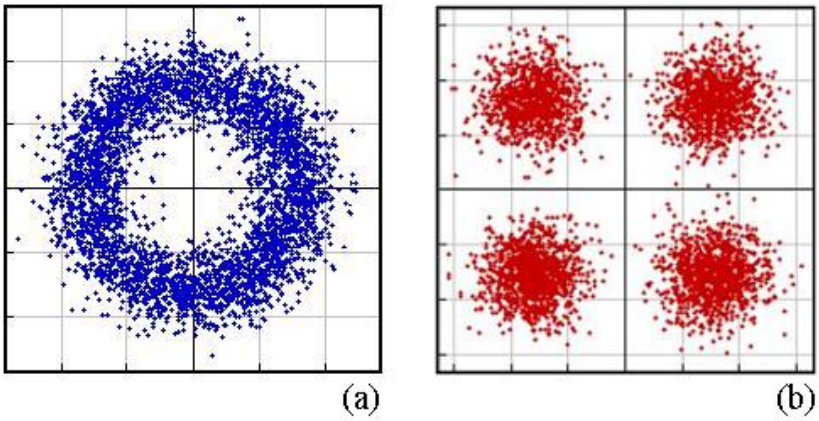


Figure 3.14: (a) Non equalized constellation; (b) equalized constellation, [94].

In Fig.3.14 an example of an unequalized constellation and its relative equalized constellation are shown: The unequalized constellation in Fig.3.14(a) shows that the phases of the received electrical sub-carriers are spread over a circle due to the fiber's dispersion inducing a frequency-dependent phase shift, whilst he equalized constellation in Fig.3.14(b) shows the QAM symbols are tightly grouped. The slight spread in amplitudes and phases is due to the higher-order intermodulation products and can be reduced by increasing the carrier power [90]. The OFDM equalizer successfully compensates for the phase errors caused by fiber dispersion.

### 3.2.3 DHT-based OFDM

The Discrete Hartley Transform (DHT) is a real-valued trigonometric transform that can be defined as follows:

$$h(k) = \frac{1}{\sqrt{N}} \sum_{n=0}^{N-1} x(n) cas(2\pi kn/N) \quad k = 0, \ldots, N-1 \tag{3.12}$$

where $x(n)$ is a real sequence and

$$cas(2\pi kn/N) = \cos(2\pi kn/N) + \sin(2\pi kn/N) = \sqrt{2}\cos(2\pi kn/N - \pi/4)$$

is the kernel of the transform.

The DHT and IDHT are formally identical, so that they can be implemented by the same program module and by the same devices.

For a comparison, the expression for the discrete Fourier transform is reported below:

$$y(k) = \frac{1}{\sqrt{N}} \sum_{n=0}^{N-1} x(n) \exp(-2\pi kn/N) \quad k = 0, \ldots, N-1 \tag{3.13}$$

In this case, the kernel of the transform is represented by complex exponentials. Although in the first case the basis function is the *cas* function, while in the latter is a complex exponential, the kernels for both of them can be decomposed into a combination of a sine and cosine [97]. Therefore, Hartley and Fourier transforms present similarities and many theorems of the Fourier transform can be applied to the Hartley transform, in some cases after slight modifications [99]. Furthermore, the real $R(k)$ and imaginary $X(k)$ parts of the Discrete Fourier Transform (DFT) coincide with the even and the negative odd parts of the Discrete Hartley Transform (DHT), respectively [98]. The difference relies in the fact that standard Fourier transform performs a complex processing on the signal and the phase always carries fundamental information, while the Hartley transform of a real signal is real, and this is more suitable for real signal processing. For a N-point real sequence, the computational complexity of DHT is lower than DFT [99].

As for the FFT, also the DHT can be implemented by a fast algorithm, [100]. The computational complexity of FHT is lower than FFT, because only real multiplications have to be calculated and no complex algebra has to be applied, resulting in a faster and simpler algorithm to implement [101].

Thanks to these characteristics, the fast Hartley transform is suitable for processing real signals and can advantageously replace the FFT in the OFDM modulation/demodulation, as demonstrated for high-speed wireless communications [102, 103].

In order to study the DHT-based OFDM modulation, the frequency response of the DFT and the DHT of a unitary symbol sequence over $N = 32$ points have been analyzed. The spectra are shown in Fig.3.15(a) and 3.15(b) for different OFDM sub-carriers, by varying the value of the parameter $k$. Due to the DHT kernel, two mirror-symmetric sub-bands carry each symbol of the data sequence, as it is possible to appreciate from Fig.3.15(b), especially for the sub-carriers corresponding to $k = 10$ and $k = 20$ [107]. Frequency sub-

channels separation and orthogonality are preserved, and since the DHT spectra are split into mirror-symmetric sub-bands, the frequency diversity is enhanced.

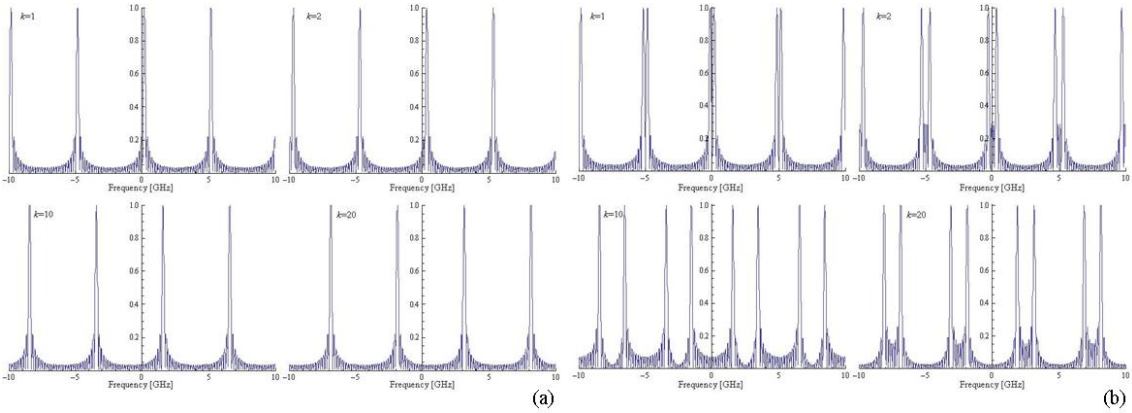


Figure 3.15: (a) DFT and (b) DHT frequency responses for different values of k; the spectra amplitude has been normalized.

Exploiting the properties of the real trigonometric transform, for optical networks, it is possible to propose an alternative OFDM scheme based on the FHT, depicted in Fig.3.16, with the aim of streamlining the conventional OFDM scheme, based on FFT.

If the input data sequence is mapped into a real constellation, e.g. BPSK and MPAM [103], the inverse FHT (IFHT) gives real values, so that only the in-phase component, and no imaginary contribution, has to be processed, reducing the number of required electronic devices and achieving a low cost system. In standard OFDM modulation/demodulation based on FFT, two digital-to-analog (DAC) and two analog-to-digital converters (ADC) converters are required: one for the real and one for the imaginary part. Whilst, by the use of FHT, the number of needed DACs and ADCs is halved, as shown in Fig.3.16. Moreover, the direct and inverse Hartley transforms are identical, so that the same device can be used at the transmitter and at the receiver. The real processing implemented by DHT also simplifies the conversion of the OFDM signal into an optical signal to be transmitted over intensity modulated direct detection systems.

A FHT-based OFDM system has been numerically simulated by *VPITransmissionMaker* software. The realized setup is shown in Fig.3.17. A PRBS signal with a Bit Rate of 10Gb/s

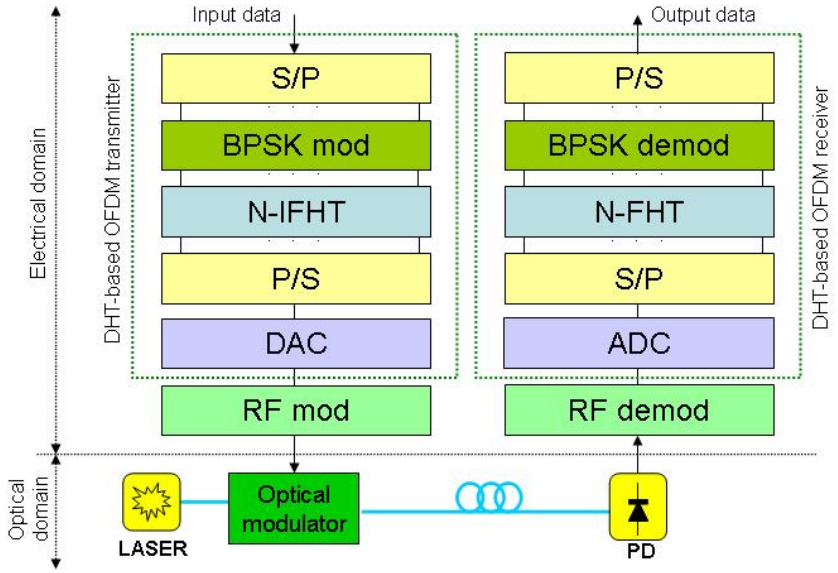


Figure 3.16: DHT-based OFDM system.

is sent to a module called "OFDM coder", which performs the BPSK modulation, mapping the signal on a real constellation, and then processes the signal by the IFHT. The OFDM coder contains a cosimulation interface which makes possible to process the signal with *Matlab*. The IFHT produces a real-valued signal which is then converted in a time domain waveform by the DAC. This waveform is modulated onto a RF-carrier of 7.5GHz, which displaces the subcarriers from DC. This creates a gap in the spectrum between the optical carrier and the OFDM subbands, which has two purposes: it displaces the signal band from the region where second-order intermodulation products due to photodetection fall and makes possible the use of realizable filters [90].

Subsequently, the electrical waveform is modulated onto an optical carrier at 193.1THz. The optical signal is sent into a standard single mode fibre, after being filtered to obtain a single side band signal, Fig.3.18. The average transmitted power is 5mW.

After propagating through the fibre link, the photodiode produces an electrical waveform, which is RF-demodulated and analog-to-digital converted for being sent into the "OFDM decoder". Similarly to the transmitter, this module performs the FHT by means of *Matlab*. In this system neither cyclic prefix nor equalization have been used. Only one

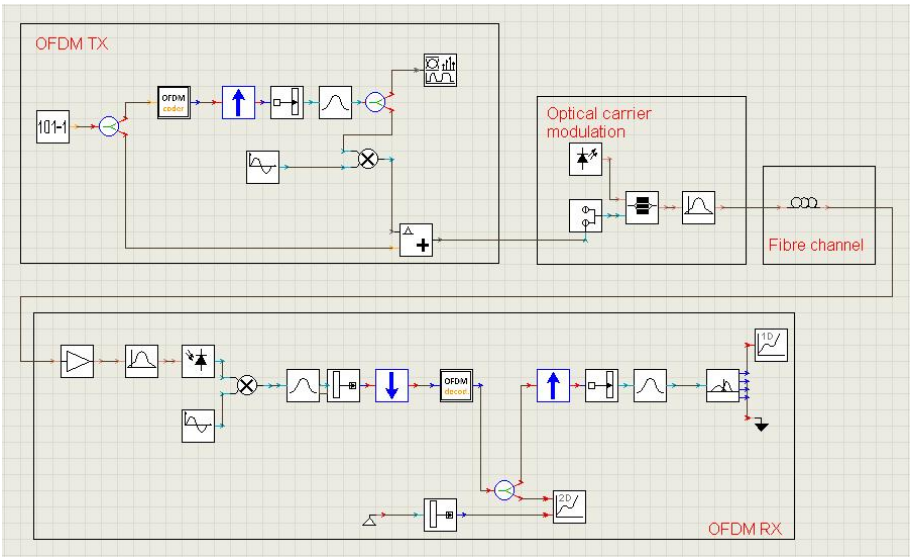


Figure 3.17: Numerical simulation setup of FHT-based OFDM system.

DAC and ADC are necessary in each side of the transmission link, thanks to the real-valued signal processed by the Hartley transform, so reducing the number of necessary devices for each transmitter and each receiver.

In Fig.3.19 the BPSK constellations for different fibre lengths are shown. It is possible to notice that with FHT-based OFDM it is still possible to reach distances suitable for access networks without the overhead introduced by the cyclic prefix and the training symbols used for equalization.

Finally, in order to test the performance of the proposed system, BER measurements have been done and are shown in Fig.3.20: where a BER of $10^{-12}$ have been achieved.

### 3.2.4 Optical OFDM for PON applications

The ever increasing bandwidth demand in access networks has brought the research focus for optical access networks to next generation PON systems, such as TDM-based 10G-PON and WDM-PON. TDM-PON is a point-to-multipoint architecture and data are broadcasted to each ONU by the shared transmission link [7]. TDM-based PON requires expensive components, complex scheduling algorithms and framing technology, synchronization between packets coming from different ONUs and it is highly sensitive to packet

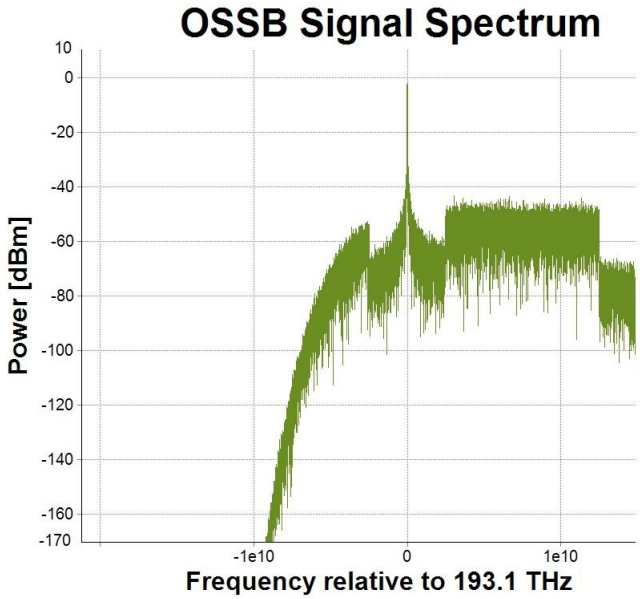


Figure 3.18: Optical single side band spectrum of the DHT-OFDM signal, after the filter.

latency. Moreover, it can be easily affected by interference due to other data traffic flowing through the same link and the time-sharing transmission in the uplink limits the bandwidth of the individual users. On the other hand, in WDM-PON, each ONU uses a different wavelength to send its packets to the OLT. A wavelength mux/demux device at the splitting point can route the wavelength channels from the OLT to the proper ONU and backward. These wavelength channels constitute independent communication channels and thus may carry different signal formats. No time synchronization between the channel is needed and the same wavelength may be used for upstream and for downstream, because reflections in the link are negligible [7]. Despite of all these characteristics and other advantages over TDM-PON, such as high bandwidth and protocol transparency, there are some issues that prevent WDM-PON from large-scale application: it lacks the flexibility to dynamically allocate the bandwidth among multiple services and raises system cost due to requirements for multiple transceivers.

OFDM is an attractive format for communications over various types of optical channels, thanks to the progress in the field of digital signal processing (DSP).

In particular, for the access segment of a network, a more and more widespread proposal

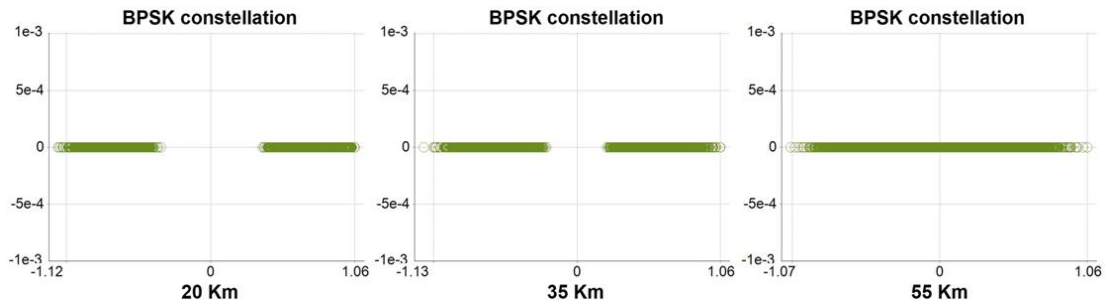


Figure 3.19: BPSK constellation received after 20km, 35km and 55km fibre links.

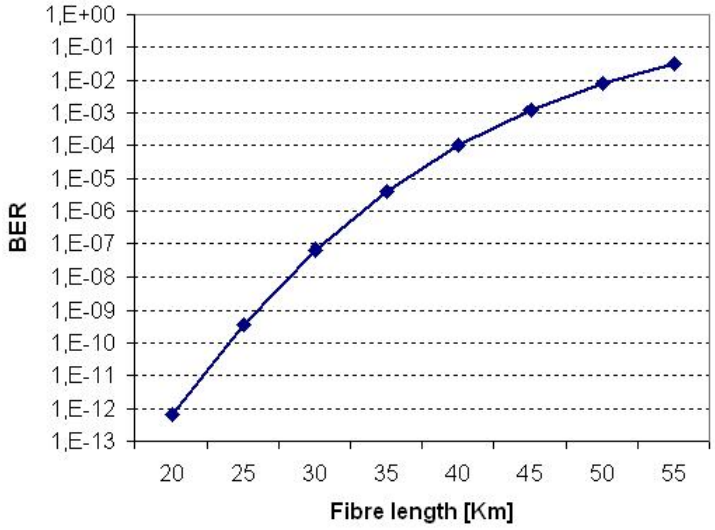


Figure 3.20: BER versus fibre channel length in a FHT-based OFDM system.

is the OFDMA-PON, which is a hybrid technique coming from the combination between OFDM and TDM. In Fig.3.21 a schematic for the architecture of an OFDM-based PON is illustrated. It can be an interesting solution to transparently support various applications and enable dynamic bandwidth allocation among them, because OFDM sub-carriers can be dynamically assigned to different services in different time slots. Moreover, OFDM-based PON solutions may use different modulation and constellation expansion for each sub-carrier and this can help in cost-effectively upgrading the data rate of the existing networks from 1Gb/s to 10Gb/s, increasing the spectral efficiency [104]. Due to the frequency domain equalization, OFDM-PON is robust against frequency domain distortions and ripple caused

by the fibre and low cost components.

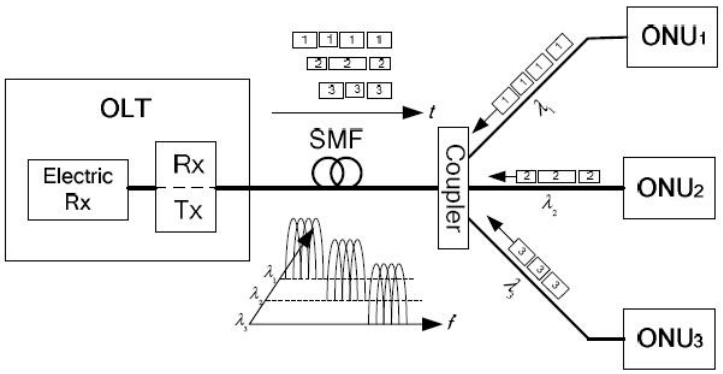


Figure 3.21: OFDM-based PON architecture, [7].

The bandwidth is divided into orthogonal parallel sub-carriers by OFDM system and one or more OFDM sub-carriers can compose a sub-channel, which becomes a transparent pipe for arbitrary analog or digital signals delivery for both circuit and packet switched systems. Dedicated sub-carriers can be reserved as orthogonal transparent pipes for different services, such as legacy TDM services and RF mobile base station signals, e.g. Moreover, it has been demonstrated that it is an architecture capable of transmitting standard WiMAX signal along with two PON channels with no throughput loss and without altering the BER performance of the two PON channels [105].

Each ONU is allocated with one sub-channel and can implement different modulation and security schemes. For the upstream traffic, each ONU maps the data and/or the signal to the given sub-carriers and sets all the other subcarriers to zero and completes the modulation. Each subcarrier symbol can be modulated with QAM. These subcarrier symbols are converted to a real-valued waveform with IFFT, called OFDM symbol, and the DAC converts the digital word stream into an analog signal to generate an ODFM frame. The OFDM frame is then converted into optical OFDM symbols at slightly different wavelengths to avoid beat noise. The OFDM symbols from different ONUs will be combined at the optical coupler, forming a single OFDM frame and detected by a single photodetector at the OLT receiver. At the OLT receiver, the OFDM signal is detected and the synchronizer extracts the carrier phase and aligns the OFDM symbol boundaries. The data

from different ONUs are demodulated.

Thanks to the orthogonal nature of the channels, there is no interference among signals from different ONUs, but in the case of presence of non linear components, for the upstream traffic a small guard band between two ONUs' signals is necessary to minimize the inter-carrier interference (ICI).

For downstream traffic, the OLT encapsulates the data into the given sub-carriers and time slots, according to the frequency/time domain scheduling results, and then converts it to OFDM frame. The DAC similarly converts the digital signal to the analog one. A directly modulated laser is driven by the signal current and the signal is converted into optical OFDM symbols at same wavelengths. When the traffic reaches the ONUs, each of them demodulates the OFDM frame and picks out its own data from the proper sub-carriers and time slots. For downstream traffic no guard bands are necessary [106]. Schematics for OLT and ONUs in the case of OFDM-based PON are shown in Fig.3.22.

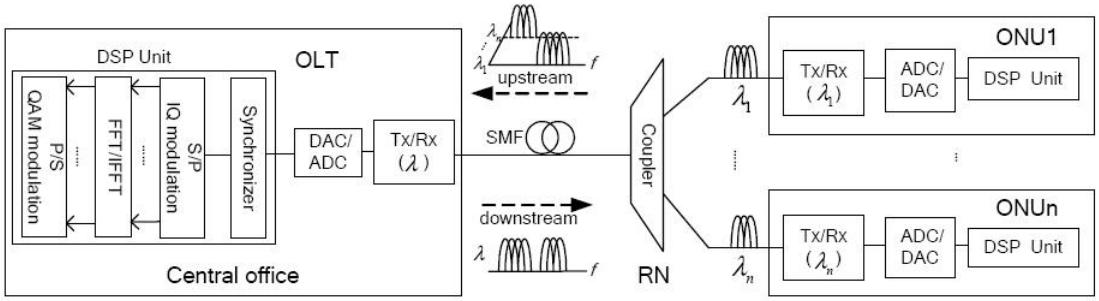


Figure 3.22: Schematic diagram of OLT and ONU for OFDM PON, [7].

Compared with TDM-PON, OFDM based PON utilizes multiple wavelengths to transmit, so it can have larger capacity and longer transmission distance. Compared with WDM-PON, the use of OFDM reduces multiple receivers to a receiver and eliminates the need for WDM demultiplexing in the upstream direction. Moreover, the system can dynamically allocate bandwidth among ONUs with different wavelengths and support various ONUs with different bandwidths. In addition, ONUs can be easily added or reduced without reconfiguring any hardware [7].

Chapter 4

# Optical Wireless Networks

## 4.1 Free Space Optics systems

The use of LASER for free space communications is generally known as Free Space Optics (FSO) or Optical Wireless technology, which is able to provide line of sight wireless high-bandwidth digital communication links between remote sites, which was developed for military purposes in the 80's. It is the ideal solution for the last hundred meters of broadband requirements (the *last mile*) and can be an alternative to wired and wireless technology. The last mile is typically seen as a key challenge for telecommunication companies mainly because of its high installation costs.

FSO communications refer to the transmission of modulated infrared (IR) beams through the atmosphere to set an optical communication link. Like optical fibres, Free Space Optics uses lasers to transmit data, but instead of enclosing the data stream in a glass fibre, it transmits through the air. The idea upon which Free Space Optics is based is the transmission of collimated light beams from one telescope to another, using low power infrared lasers in the THz spectrum. The used laser wavelength is invisible and eye safe. The light from a Free Space Optical channel is intercepted by a lens (or a system of lenses) capable of focusing photons on a highly sensitive detector receivers.

On Fig.4.1 the main blocks of a FSO based communication system are shown. The upper blocks constitute the transmission part while on the bottom are shown the blocks on the

receiver side. The light source commonly used is the Vertical Cavity Surface Emitting Laser (VCSEL), as it generates a circular beam waist. The transmission lens collimates the beam over a long distance. On the receiver side, a lens focuses the beam on the active region of a photo detector. The choice of the photodiode is a very critical point in the design of an Optical Wireless system. Detectors are generally either PIN diodes or avalanche photodiodes (APD).

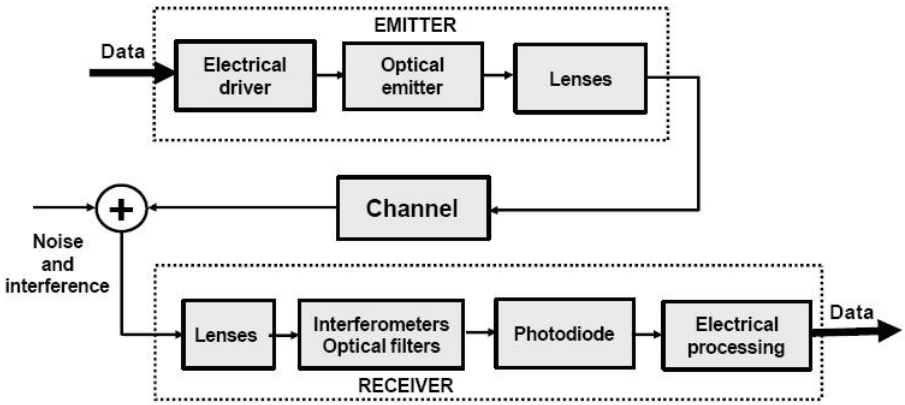


Figure 4.1: Block schematic of a FSO system.

Optical Wireless systems can cover distances of several kilometers. As long as there is a clear line of sight between source and destination and enough received power, the communication is guaranteed. Communications are demonstrated to be possible up to 5km; however the shorter the link range, the higher the quality of the transmission service which can be reached. Data rates comparable to optical fibre transmission can be carried out with very low error rates, and thanks to the extremely narrow laser beam widths, FSO ensures that there is almost no practical limit to the number of separate Free Space Optics links that can be installed in a given location and the communication link is intrinsically secure as intrusion is quite improbable.

A new concept of Optical Wireless is a fully transparent FSO system, where the optical beam is transmitted into the air directly from Single-Mode Fibres (SMF) and it is received directly in a SMF, so the fibers are used as light-launchers and light-collectors, Fig.4.2. Since this technique bypasses the conversion into the electrical domain, an all-optical treatment

of the information can be realized and, as a consequence, the high performances achieved in the optical fibre systems can be exploited. This technology makes possible high data rate transmission [8]. The first transparent fibre communication system appeared in the early 1990's as a consequence of the invention of Erbium-doped fibre amplifiers. The signal could be directly re-generated while propagating in an all-optical medium. No conversion in the electrical domain was required. That was the first step towards Terabit global optical networks. FSO opaque systems have been available on the market since the last decade and still represent an optimal solution for optical networks. Instead, transparent systems yet are a research project, but are expected in the next years to have a great impact on the market.

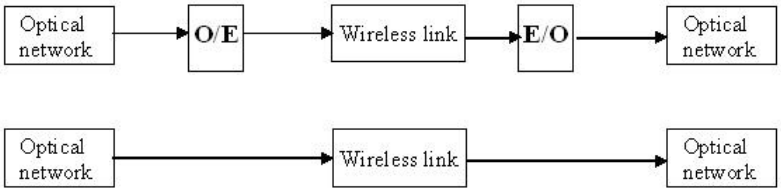


Figure 4.2: (top) Opaque transmission system; (bottom) transparent transmission system.

The only essential requirement for FSO or optical wireless transmission is line of sight between the two ends of the link. It can thus be fully considered as a wireless way of transmitting information like radio-frequency wireless systems [108]. The apparatuses can include the implementation of a system with variable tracking, generally for the apparatuses inside the buildings, in order to compensate the thermal movements, or the the line of sight can be maintained also by means of an adequate ray divergence. FSO is generally referred to for outdoor communications, but indoor systems are also available.

Moreover, transparent FSO makes possible the use in FSO systems of Dense Wavelength Division Multiplexing (DWDM) transmission [109], which is well-known for the possibility of increasing the transmission bandwidth. This allows to enhance the capacity of optical wireless links, exploiting the full capacity of optical fibres and bringing DWDM into the access network. However, coupling loss and atmospheric attenuation limit transparent systems to short range links [110].

A free space optical system can be described by the link equation of the light transmission in atmosphere: the amount of received power is proportional to the amount of power transmitted and the area of the collection aperture, it is inversely proportional to the square of the beam divergence and the square of link range. It is also inversely proportional to the exponential of the product of the atmospheric attenuation coefficient (in units of $1/distance$) times the link range [119].

$$P_{rec} = P_{transm} \frac{A_{rec}}{(Div \times Range)^2} e^{-\gamma(\lambda) Range} \tag{4.1}$$

where:

- $P_{rec}$ is the signal power at distance $L$ from the transmitter;
- $P_{transm}$ is the emitted power;
- $\gamma(\lambda)$ is the attenuation or the total extinction coefficient per unit of length;
- $A_{rec}$ is the area of the receiver telescope lens;
- $Div$ is the divergence of the beam;
- $Range$ is the distance between the transmitter and the receiver.

The variables that can be varied are: transmit power, receive aperture size, beam divergence, and link range. The atmospheric attenuation coefficient is uncontrollable in an outdoor environment and is roughly independent of wavelength in heavy attenuation conditions. The system designer should choose a link range short enough to ensure that atmospheric attenuation is not the dominant term in the link equation. The attenuation coefficient is composed of absorption and scattering terms. Generally is the sum of the following terms:

$$\gamma(\lambda) = \alpha_m(\lambda) + \alpha_a(\lambda) + \beta_m(\lambda) + \beta_a(\lambda) \tag{4.2}$$

where $\alpha_{m,a}$ are molecular and aerosol absorption coefficient respectively and $\beta_{m,a}$ are molecular and aerosol scattering coefficient respectively.

### 4.1.1 Limiting factors

FSO systems allow high data-rates, virtually the same optical transmission band as fibre, and it has advantages over other transmission systems, namely low cost, compact transmission equipment, simple and rapid installation. Moreover this technology is compatible with any kind of communication protocol, it is not affected by any interference other than line-of-sight obstacles and it is safe because of high beam directivity.

The advantages of free space optical wireless do not come without some costs: there are some factors that can limit the use of such systems, like variable attenuation due to atmospheric conditions, need of line of sight, and limited transmission distance, e.g., approx. 5km [111]. The air transmission in fact doesn't ensure the integrity of the data characteristic of the fibre transmission. The elements that limit the use of this technique are caused by the propagation in the air of the electromagnetic field produced by the emitter (LASER or LED). The weather factors and the optical signal loss have a certain dependence degree on the working wavelength. The typically used wavelength is about 800-1550nm. These choices come out the fact that the FSO apparatus realization was possible only after the LASER perfecting in the optical fibre systems, so that the wavelengths used in the FSO are the ones already used in the fibre transmission system: 800nm, 1300nm, 1550nm. But $\lambda = 1300$nm is not used because at this wavelength the weather loss even in cloudless sky conditions is excessive.

Intensity and extent of the atmospheric effects influence the distance and the availability of the links. In general, weather and installation characteristics, that impair or reduce visibility ,also affect the FSO performance. Atmosphere and weather conditions affect light propagation because of absorption and scattering by molecular or aerosols, scintillation due to the air index variation under the temperature effect, attenuation by hydrometeor (rain, snow). However fog appears as the more penalizing element in the free space optical link operation. FSO links are impaired by absorption and scattering of light by earth's atmosphere. The atmosphere interacts with light due to the atmosphere composition which, under normal conditions, consists of a variety of different molecular species and small suspended particles called aerosols. This interaction produces a wide variety of

optical phenomena: in particular molecular and aerosol absorption, molecular and aerosol scattering, rain and snow attenuation, scintillations effects.

A selective absorption of radiation that propagates at specific optical wavelength in the atmosphere results from the interaction between photons and atoms or molecules ($N_2$, $O_2$, $H_2$, $H_2O$, $CO_2$, $O_3$, $Ar$, etc.) which leads to an elevation of the temperature due to the adsorption of the incident photon. The absorption coefficient depends on the type of gas molecules and on their concentration.

Attenuation is a function of frequency but also of the visibility related to the particle size distribution. This phenomenon constitutes the most restrictive factor to the deployment of Free Space Optical systems for long distances. The visibility is a concept defined for the needs of the meteorology. It characterizes the transparency of the atmosphere estimated by a human observer: visibility is the distance at which it is just possible to distinguish a dark object against the horizon. Under the influence of thermal turbulence inside the propagation medium, random distributed cells are formed. They have variable size (10cm–1km) and different temperature. These various cells have different refractive indexes thus causing scattering, multipath, variation of the arrival angles: the received signal fluctuates quickly at frequencies ranging between 0.01 and 200Hz. The wave front varies similarly causing focusing and defocusing of the beam. Such fluctuations of the signal are called scintillations.

**Molecular and aerosol absorption**

Molecular absorption is a selective phenomenon which results in a spectral transmission of the atmosphere presenting transparent zones, called atmospheric transmission window, and opaque zones, called atmospheric blocking windows. Aerosols, such as fog, dust and maritime spindrift particles, are extremely fine solids or liquids particles suspended in the atmosphere with very low fall speed by gravity (ice, dust, smoke, etc). Their size generally lies between $10^{-2}$ and $100\mu$m. Aerosols influence the atmospheric attenuation due to their chemical nature, their size and their concentration.

In the spectrum region used by FSO, attenuation coefficient is only approximated by

the coefficient of scattering by the particles present in the atmosphere. The absorption coefficient depends on the type of gas molecules and on their concentration and the bands centered at 850nm and at 1550nm are characterized by a low attenuation coefficient: these bands correspond to two of the three fibre transmission windows. Therefore, devices and techniques used in fibre networks are compatible [120].

**Scattering**

The attenuation coefficient $\gamma(\lambda)$ depends on the absorption and scattering of laser photons by different aerosols and gaseous molecule in the atmosphere. Since laser communication wavelengths (typically 785nm, 850nm, and 1550nm) are chosen within the transmission windows of the atmospheric absorption spectra, the contributions of absorption to the total attenuation coefficient are very small. The effects of scattering, therefore, dominate the total attenuation coefficient. Atmospheric scattering results from the interaction of a part of the light with the atoms and/or the molecules in the propagation medium. It causes an angular redistribution of this part of the radiation with or without modification of the wavelength. Aerosols scattering occurs when the particle size are of the same order of magnitude as the wavelength of the transmitted wave. In optics it is mainly due to mist and fog.

The type of scattering is determined by the size of the atmospheric particle, with respect to the transmission laser wavelength. This is described by a dimensionless number called the size parameter $\alpha = \frac{2\pi r}{\lambda}$, where $r$ is the radius of scattering particle and $\lambda$ is the laser wavelength [120].

Depending on the relationship between the particle size and wavelength, there are three types of scattering: Rayleigh, Mie, and non-selective or geometric scattering. Rayleigh scattering occurs when the atmospheric particles are much smaller than the wavelength. As the particle size approaches the laser wavelength, the scattering of radiation off the larger particles becomes more dominant in the forward direction as opposed to the backward direction. This type of scattering, where the size parameter varies between 0.1 and 50, is called *Mie* scattering. The laser communication wavelengths are *Mie* scattered by haze and

smaller fog particles. The third generalized scattering regime occurs when the atmospheric particles are much larger than the laser wavelength. For size parameters greater than 50, the scattering is called geometric or non-selective scattering.

### Weather conditions

The most limiting factor for optical beams propagating in a free space channel [121] is the weather. In fine conditions, the propagation can almost be as good as in a glass fibre. Typical loss factor for clear sky is less than 0.6 dB/Km. In such an ideal situation, the link range could brought to tens of kilometers. In order to keep the link on in most situations, the range cannot ever be more than 5km, and hundreds of meters in the many common cases. Very bad condition (heavy fog) can lead to attenuation coefficient up to 300dB/Km. The attenuation coefficient, approximated by the *Kruse* relation [122], depends on atmospheric visibility. The technical definition of visibility or visual range is the distance that light decreases to 2% of the original power, or qualitatively, visibility is the distance at which it is just possible to distinguish a dark object against the horizon.

The fog is the most limiting element because the physical dimensions of the drops are comparable in size with the working wavelength and therefore the interaction degree is very high. Fog attenuation for light is due to the *Mie* Scattering. Normally, the fog is divided is dense and thick. Dense fog corresponds at a visibility of 5 m and the attenuation is up to 300 dB/km. In case of thick fog (visibility at 200 m) the fog attenuation is 85 dB/km. Therefore the fog is the main weather condition dangerous for optical wireless system. The fog effect on these systems is similar to the rain effect on the RF systems. Observing right statistics about the presence and the duration of the fog, a FSO link can be dimensioned to work in the right way even if with thick fog. Besides we have to be sure to respect the actual regulation to keep the power density under the level of eye safety.

Interaction of photons with rain particles belongs to non-selective or geometrical scattering as the size parameter is higher than 100. In this case, the attenuation is very weakly dependent on the wavelength. Thus 850nm and 1550nm are equally affected by the rain [123]. The momentum of water particles is smaller than the wave vector module for some

orders of magnitude. For this reason, due to the momentum conservation, the resultant vector doesn't differ too much from the incident wave. This is why rain effect is not particularly harmful. Typically the rain is classified depending on the rain rate, $R$, measured in $mm/h$. Cloudburst (visibility 1km) corresponds at $R = 100$mm/h and in this case the rain attenuation is approximately estimated at 20dB/km. In case of $R = 25$mm/h the rain is defined intensive (visibility $1,9$km) and corresponds at a attenuation of 7dB/km. Medium rain ($R = 12$mm/h and visibility $2,8$km) the attenuation is $4,6$dB/km and finally low rain ($R = 2,5$mm/h and visibility $5,9$km) are considered at a attenuation of $1,8$dB/km. Thus rain doesn't represent a great concern for a FSO system design.

For snow size, the scattering is geometric or non-selective scattering. The scattering particles are large enough that the angular distribution of scattered radiation can be described by geometric optics. There is no dependence of the attenuation coefficient on laser wavelength. Falling snow simply absorbs the light by the irregular shapes of particles in the size of about 2 up to 25mm, leading to a varying attenuation depending on the relation of particle and receiver optics area. The attenuation due to snow fall has been modeled based on dry or wet snows. the attenuation value due to the snow is bigger than the rain. The attenuation increases up to 100dB/km in case of heavy snow.

In Fig.4.3, the effects of weather conditions on FSO link are resumed.

**Turbulence**

Occasional burst errors of the order of 1 ms or less occur during laser communication transmission primarily due to small-scale dynamic variations in the index of refraction of the atmosphere. Atmospheric turbulence produces temporary pockets of air with slightly different temperatures, different densities, and thus different indices of refraction. These air pockets are continuously being created and then destroyed as they are mixed. Light transmission in media follows the principle of Fermat, which states that light going from one point to another follows the shortest optical path length, which depends on geometrical distance and optical properties of the medium, given by the refraction index $n$. Consequently, the refraction index has an impact on light propagation for free air, in particular,

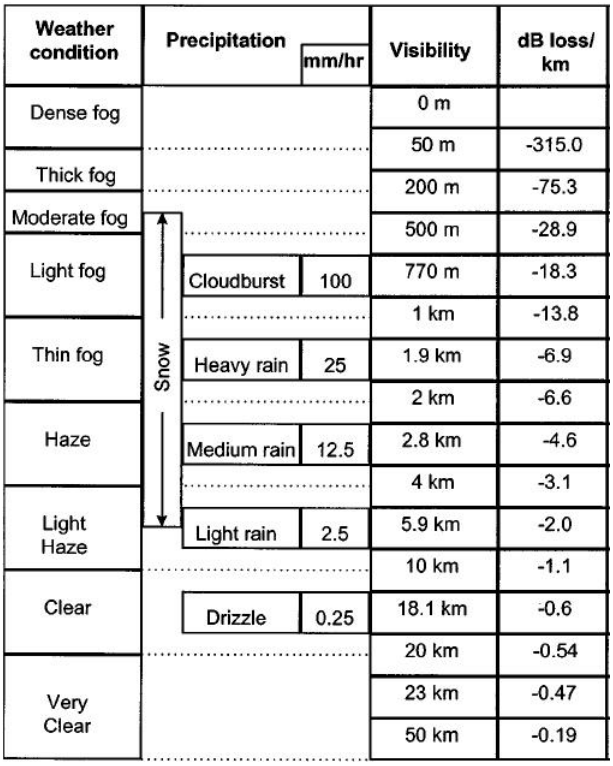


Figure 4.3: Effects of different weather conditions on a FSO transmission link.

different refractive indexes cause scattering, multipath and variation of the arrival angle, so the received signal fluctuates quickly. At sea level $n$ is in the order of 1.0003, but it depends on many factors, at least on: Wavelength, Temperature, Pressure, Humidity. The constant mixing of the atmosphere produces unpredictable turbulent cells of all sizes, resulting in received signal strength fluctuations that are a combination of beam wander and scintillation. So, due to these effects, data can be lost as the laser beam becomes deformed propagating through these index of refraction inhomogeneities.

These random distributed cells, generated by the effects of atmospherical turbulence caused by solar heating and by the consequent thermal gradient inside the propagation medium, have variable size, from 10cm to 1km, and different temperature. The influence of each effect depends on the size of these turbulence cells with respect to the laser beam diameter [124]. When the received signal fluctuates, also the wave-front varies similarly (changing the angle of received light and causing a spot of light dancing around the focal

point), causing focusing and defocusing of the beam and a varying input power at the receiver. Such fluctuations of the signal are called scintillations (see Fig.4.4(a)). The amplitude and frequency of scintillations depend on the size of the cells compared to the beam diameter; if the size of the turbulence cells is smaller than the laser beam diameter, ray bending and diffraction cause distortions in the laser beam. The intensity and the speed of the fluctuations (scintillations frequency) increase with wave frequency. A redistribution of the power within the aperture occurs: small variations in the arrival time of various components of the beam wave front produce constructive and destructive interference, and result in temporal fluctuations in the laser beam intensity at the receiver. These fluctuations in the received power are similar to the twinkling of a distant star. Without turbulence the power is supposed to have a Gaussian profile, instead in turbulence condition the random interference pattern generates speckles. The speckle can be "dark" (corresponding to destructive interference) or "light" (corresponding to constructive interference). The radius of the speckle scales like $(\lambda R)^{1/2}$, which translates into smaller size for both shorter distance and wavelength. Scintillation can be reduced through the use of large transmit and receive apertures, and multiple transmit beams [124]. An automatic gain control with sufficient bandwidth can prevent variations in received power from distorting the received data, maintaining an adequate SNR, by keeping the power level constant.

When the light crosses different sheets of air, the beam is deviated (reflection of light) because of a temperature or pressure gradient. This effect leads to results similar to misalignment or building sway, causing a reduction of received power which can get critical for very small divergence. In this case, the size of the turbulence cells is larger than the beam diameter and the laser beam as a whole randomly bends, causing possible signal loss if the beam wanders off the receiver aperture (see Fig.4.4(b)).

#### Solar interference

Sunlight can affect FSO performance when the sun is collinear with the free space optical link. In clear sky condition an intensity of $1000W/m^2$ reaches the ground of the earth. The light of the sun represents noise for a wireless optical system [125], especially for opaque

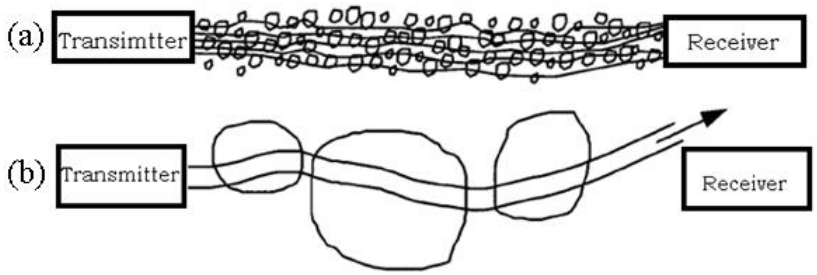


Figure 4.4: (a) Scintillation; (b) beam wandering.

systems, in fact photons can enter the receiving optic and can be focused on the active area of the PIN or APD photo-detector. This gives rise to a further unwanted photo-generated current which adds to the signal current. The effect of solar noise is amplified sunrise and sunset. In such circumstances the sun is very low over the horizon and solar beams might set in-axis with the receiver lens. As a consequence bursts of errors can occur. The so-called windows of transmittance of the atmosphere include the two most important wavelength regions, leading to specific intensities of about 0.5 to 0.9 Watts per square meter and per nanometer ($W/m^2nm$) in the 850nm spectral region and about $0.17W/m^2nm$ in the 1550nm region for direct sunlight on ground. Values for specific attenuation between 0.2dB/km under very clear atmospheric conditions up to about 10dB/km due to dust in urban regions are reasonable. Ambient light effect can be limited using spatial filters or cylindrical shields, as in the typical structure of the telescopes, or alternatively optical filters that let pass through only the desired wavelength or, where possible, by orientating the system in such a way as the receiver to be not exposed to ambient light.

### Objects interference

A problem existing only for the FSO is that of the interference due to objects that cross the beam, particularly the passage of birds. Anyway the use of large receiving optics and transmission redundancy reduce the impact of this phenomenon. In standard conditions the interposition of an object that leaves uncovered even one transmitter at only 2% of the receiving optic will not cause the link drop.

### Line of sight

Another important aspect of optical wireless systems, related also with objects interference illustrated in the previous paragraph, is the necessity of the line of sight between transmitters and receivers. The two devices need to be in reciprocal visibility in order to guarantee that the transmission would be received. Sometimes it is possible to create a "virtual line of sight" by means of properly placed mirrors, if permitted by the installation field, as it will be shown in the experimental tests of Section 4.2.

### Mechanical stability

The last, but not the least, factor in FSO systems performance, is the mechanical stability of the assembled transmitting/receiving devices that could give some problems. In fact a small angular variation (generally one or two milli-radians) is enough to determine the misalignment of the system, especially in path longer than 1km. A more widespread beam can be used to solve the problem, in order to let the receiver always illuminated also in presence of angular variations. Nowadays are available devices with automatic alignment.

### Pointing

An essential aspect of the installation of an optical wireless link is pointing [112]. Pointing is important both at the transmitter and the receiver sides. The transmitter has to be pointed accurately to ensure efficient delivery of energy to the receiver. The receiver has to be pointed properly to ensure that the signal entering the receiver aperture reaches the detector. To ensure good reception, the divergence of the transmitted beam and the receiver field-of-view has to be greater than the beam (or pointing) jitter. Let's assume that a transmitter with a full-width-at-half-maximum (FWHM) beam divergence $\theta$ is used. A 3dB mispointing allowance implies that the transmitted beam should never be pointed more than $\pm\theta/2$ from the nominal direction. Furthermore, assume that the long-term statistics of mispointing takes a Gaussian distribution having a standard deviation $\sigma$. If we want the pointing loss to be less than 3dB for 99.999% of the time, then the FWHM must be greater than $8\sigma$. Clearly, the optimum beam divergence is dictated by the pointing jitter

and greatly depends on the location and mounting of the transceiver. Even in the absence of the atmosphere, keeping two transceivers pointed accurately at each other at all time, to better than one milli-radian is a challenge. A great deal depends on how and where the transceivers are located. When a transceiver is mounted on a roof of a high building, building sway contributes significantly to the pointing error. A high-rise building can sway more than a meter (equivalent to one milli-radian for a one-kilometer link). The roof itself often houses air-conditioning and ventilation units, as well as lift and other mechanisms that cause vibration in the low tens of Hertz. Moreover, some roofs are not very solid and can deform when someone walks on them. Temperature changes (diurnal and seasonal) and uneven heating by the sun can deform the mount enough to throw the pointing off. Some FSO customers have indicated that they need to realign the transceiver units few times a year for this reason. Optical wireless transceivers and their mounts have enough wind resistance that they are tilted in heavy winds.

### 4.1.2 Advantages

Besides all the limiting factors that affect an FSO system, there are a lot of reasons why the optical wireless technology seems to be a valid solution for the "Last mile problem".

**No license:** No licenses are necessary required to install optical wireless system based on laser emission. Therefore the installation of the links can be realized with reduced costs respect to radio wireless technology.

**Costs saving:** Optical wireless systems reduce the installation and license costs. As there are no considerable costs to wire the cables, cost of installation are minimized and much more compared with traditional cabling technology.

**Investment protection:** Free space optics solution protects the client investment. The equipments are designed to be easily updated, increasing bandwidth and distance, without raising costs.

**Interference:** Since the systems links transmit infrared light, performance are not sensible to electromagnetic noises and is not subject to interference with other wireless

devices.

**Bandwidth:** The data communication of free space optics technology allows the same bandwidth of fibre optics.

**Flexibility:** Optical wireless system is different depending on the distance required by the client. Links can be realized roof-to-roof, window-to-window and roof-to-window. Therefore the user can make the best choice of equipments depending of the installations. Moreover, the FSO transceivers have small dimensions, generate an extremely narrow beam and can transmit across the windows, can therefore be installed inside building in case of overcrowded roofs, without any necessity of wiring as far the roof. The only necessity of these systems is the existence of a visibility wave between the two apparatuses extremities LOS.

### 4.1.3 Security

Network operators and administrators have a great interest in the security, because optical wireless systems send and receive data through the air between remote networking locations. Network security is one of the major concerns for any business or organization transporting sensitive and confidential information over the network. Such topics involve the lowest network layer, typically referred to as the physical layer (layer one), as well as higher software layers of the networking protocols. Most of the interception activity by outside intruders occurs within higher protocol software layers. Password protection or data encryption are examples of counter measures to protect the network from outside and unwanted tampering. Intrusion of the physical layer itself can be another concern for network operators, although it is a far less likely target for unauthorized access to networking data. This can be a threat if information is transported over a copper based infrastructure that can be easily intercepted, but optical wireless transmissions are among the most secure connectivity solutions, regarding network interception of the actual physical layer [113]. Security and interference problems are very common in radio frequency (RF) or microwave-based communication systems. The wide spreading of the beam in microwave systems, combined with the fact that microwave antennas launch very high power level

signals is the main reason for security concerns. An outside intruder can easily intercept the beam or power reflected from the target location and pick up sensitive network information by using a "spectral scanner" tuned to the specific RF or microwave transmission frequency. Unlike in microwave systems, it is extremely difficult to intercept the optical wireless light beam carrying networking data, because the information is not spread out in space but rather kept in a very narrow cone of light. Moreover, optical wireless systems operate in the infrared wavelength range above the visible spectrum, therefore the human eye cannot see the transmission beam. As a consequence, FSO systems are intrinsically secure thanks to their nature of narrow and invisible beam. The small diameter of the beam at the target location is one of the reasons why it is extremely difficult to intercept the communication path of an FSO-based optical wireless system. As shown in Fig.4.5, on the contrary to microwave systems, optical beams are featured by very low beam divergence, especially when an active system is used. Beam size is important to secure the connection: the larger the beam, the easier it would be for someone to find the beam and to place a mirror or receiver the beam and without breaking the connection.

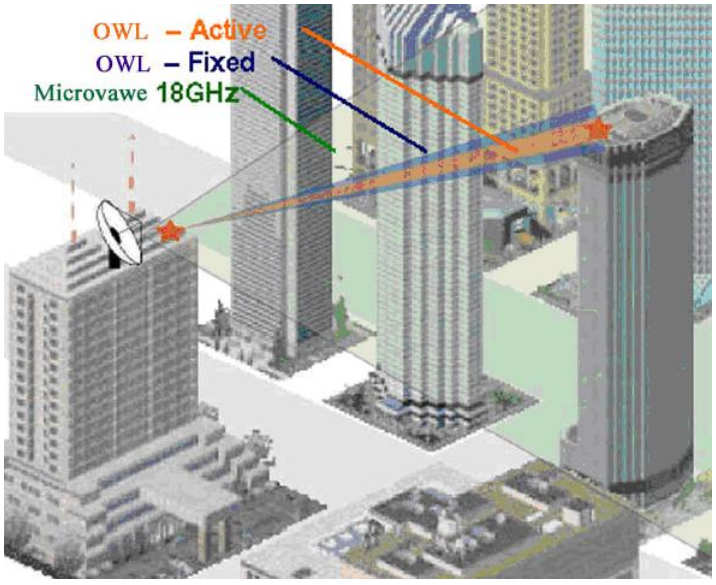


Figure 4.5: A narrow beam is less interceptable and this makes an FSO system more secure.

Many obstacles made very unlikely to intercept an optical wireless communication:

- The intruder must know the exact origination or target location, in fact the beam is narrow and invisible making harder to find and even harder to intercept and crack. Moreover it cannot be sensed with a spectrum analyzer or with an RF meters.

- The intruder must have free and undisturbed access to the installation location of the optical wireless transceiver; usually the location is part of the costumer premise as the roof or an office, when optical wireless equipment is installed behind the windows. The two remote networking locations the beam typically passes through the air at an elevation well above ground level, so the direct interception of an optical wireless beam is very difficult.

- The intruder must to be able to install electronic equipment without being observed and he needs a matching FSO transceivers carefully aligned, which is a difficult operation.

- Even if the intruder would succeed in overcoming all other obstacles, he would obscure the LOS, therefore it would be immediately noticed that something is happening. The chance of being discovered is real, because by blocking one of the beams, the company when investigating the problem could discover the intrusion attempt. Due to the fact that the transmission beam is invisible and that any attempts to block the beam would occur near the optical wireless equipment terminus points, the transmission process imposes another obstacle. Since the beam needs to be line of sight, surveillance cameras could easily be used to monitor the installation and beam path to detect any suspicious activity.

- Picking up the signal from a location that is not directly located within the light path, by using light photons scattered from aerosol, fog, or rain particles that might be present in the atmosphere is virtually impossible because of the extremely low infrared power levels used during the optical wireless transmission process.

Moreover, thanks to the huge bandwidth available higher protocol layers can be used in conjunction with layer one optical wireless physical transport technology to encrypt sensitive network information and provide additional network security.

For all these reasons, optical wireless communication systems are among the most secure networking transmission technologies, to the point that in the early days of FSO development, the ability to transmit information at high data rates was actually a less important factor than the fact that FSO technologies offered one of the easiest and most secure ways to exchange information between remote locations. In fact, military organizations or government entities that rely heavily on extremely secure transmission technologies were among the earliest users of optical wireless communication systems as a way to avoid signal interception. Therefore, it is understandable why the study of FSO technology in military labs and security agencies dates back several decades.

### 4.1.4 Comparison with other technologies

Nowadays the "last mile" is still a dilemma for the world's telecommunications carriers, despite the many attempts to fix the problem with different technologies:

- DSL and cable modems can, to some extent, take advantage of existing wired networks; however, they cannot provide true broadband services in a deterministic way. DSL technology is plagued by the actual topology of the copper to which it is attached, and is limited in distance (from the central office) and capacity (several Mbps). Cable modems enjoy higher capacity, yet the channel is shared and the amount of bandwidth at any given time is not guaranteed.

- Unlicensed wireless RF technologies are also limited in capacity, and carriers are reluctant to install systems that might have interference issues. Licensed wireless RF technologies can provide very high capacity, but the non recurring initial capital expenditures for spectrum licenses usually makes the business model very difficult to implement. Additionally, in any given city the licenses permit only two carriers to participate.

- FSO technologies offer optical capacity but are typically deployed at lengths under a kilometer for reasonable availability. FSO has a major time-to-market advantage over fibre. Fibre builds often take 6 to 9 months, whereas an FSO link can be operational

in a few days.

- Millimetre wave technology at $60GHz$ is unlicensed due to oxygen absorption and is capable of higher capacity than frequencies at longer wavelengths. However, it is susceptible to outage in heavy rain regions and is thus limited in range (about $400m$ or so).

- W-band technologies are just starting to come out of the lab and are being licensed on a link-by-link basis. However, they are likely to be licensed in the future due to their relatively good propagation characteristics.

Regarding the access network, nowadays many technologies exist and it is important to state beforehand that each technology has an own area of usage, where it is the best solution, but does not exist a unique technology that would be a solution for every problem.

Optical wireless communication links up to 6km (exactly the distance required for last mile applications) with a bandwidth up to 2.5Gbps, larger respect the radio wireless and microwave technology [114].

Traditional cabling offer performances much more high (distance and bandwidth) but even time and cost of installation are very high compared with free space optic communication [115].

Fibre-based passive optical networks (PONs) represent a highly attractive approach, due to the relatively low cost per subscriber. However, the inherent high capacity of fibres is shared among a number of users, thereby reducing the capacity per user, and the deployment times can still be quite long, depending on the location of any particular subscriber. The comparison with fibre optics emphasizes the versatility of free space optics technology due to low costs and fast and easy installation.

Radio frequency (RF) fixed wireless systems are a credible access option, but they are limited in data rate, require FCC licensing, are subject to rain fading, and are costly relative to other access schemes. The logical consequence of this situation is that one must select an approach that best meets the needs of a specific deployment.

In Fig.4.6 the different available technologies in the world telecommunications carriers are shown. For each of them are defined the characteristic referred at distance, bandwidth,

security and other important qualities.

| | FSO | Microwave | Radio Wireless | Traditional Cabling (fibre) |
|---|---|---|---|---|
| Distance Range | Up to 6000 m | Typically under 10km (longer distances are possible) | 100m indoors (regulations limit the outdoors use to a few km) | 100km |
| Supported Bandwidth (max.) | 2.5 Gbps (higher bandwidth enabled by the technology) | Practically 155 Mbps (300 Mbps possible) | 11 Mbps (Wi-Fi) 54 Mbps (802.11a) | Unlimited |
| IP Compatible | Yes | Yes | Yes | Yes |
| SNMP Compatible | Yes | Yes | Yes | Yes |
| Investment Protection (can it be upgraded) | Yes | Yes | No | No |
| Security | High due to positioning and beam size | High | No encryption: Low Encryption: Medium | High |
| Deployment | Quick (within a day) | Moderate (several days) Long (several months) Incl. Frequency licensing | V. quick (hours)- indoors Moderate (days)- outdoors | Very long (up to a year) |
| Installation Complexity | Easy | Complex | Moderate | Moderate to complex |
| Safety | No | Electromagnetic radiation in public areas | No | No |
| Licence Required | No | Yes | No | Yes (in public areas) |
| Interference Issues | No | Yes | Yes | No |
| Line of Sight required | Yes | Yes | No- indoors Yes- outdoors | No |
| Transparent Operation | Yes | No | No | Yes |
| Special Features | Very high power budget, best cost per bit. High reliability. | | | High reliability |
| Price Brand | Low | Moderate High (with frequency licence) | Low | Very high |

Figure 4.6: Different access technologies comparison.

### 4.1.5 Applications

FSO applications span over a wide range from satellite links to robotics and generates interest for several distinct markets, namely: the last mile high bandwidth internet connectivity, the temporary high bandwidth data links, the mobile telephony backhaul ($3G$), satellite links as well as the various applications where the optical fibres cannot be used. Optical wireless represents an approach with wide and broadly based applications appeal because of its many features.

**Last mile:** Optical wireless systems represent one of the most promising approaches for

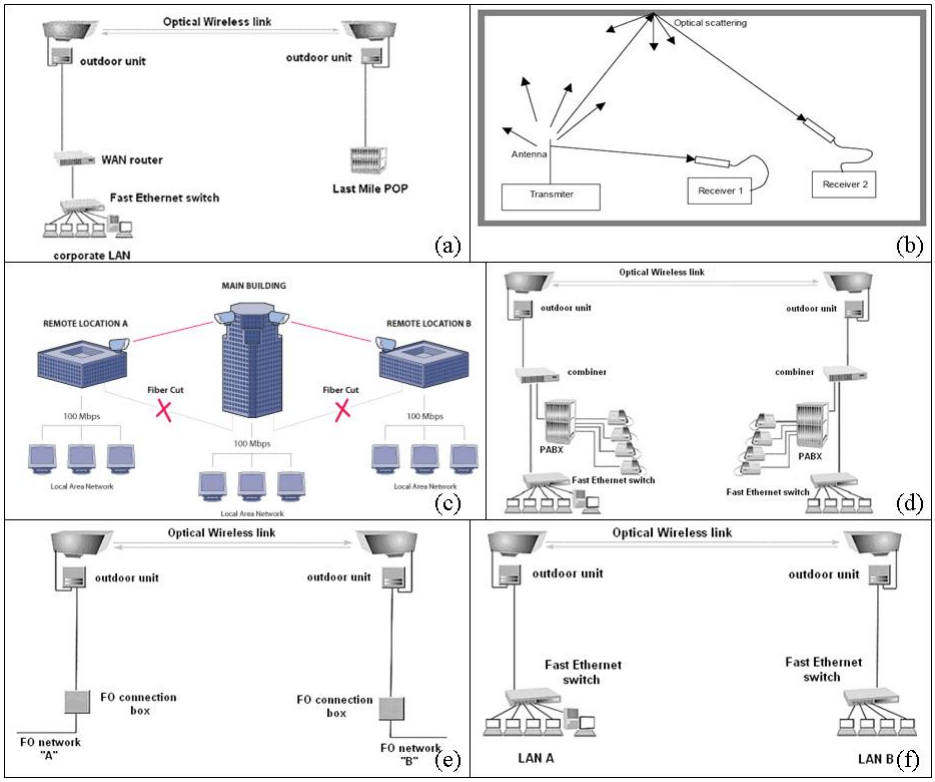


Figure 4.7: FSO technology application examples: (a) last mile; (b) indoor; (c) back-up/disaster recovery; (d) telephony; (e) fibre extension; (f) local area networks.

addressing the emerging broadband access market and its "last mile" bottleneck. These robust systems, which establish communication links by transmitting laser beams directly through the atmosphere, have matured to the point that mass-produced models are now available. Optical wireless systems offer many features, the most important are low start-up and operational costs, rapid deployment, and high fibre-like bandwidths [116]. Available systems offer capacities in the range of 100Mbps to 2.5Gbps, and demonstration systems report data rates as high as 160Gbps.

The ideal attributes of a generic broadband access approach are low installation cost as well as cost per bit/second associated with each subscriber and low first-in cost (i.e. the cost of launching access service for the first few subscribers). Moreover, an ideal broadband access approach should also offer rapid deployment, so carriers can begin

generating revenue as quickly as possible. Another important feature is the capability to provide a high capacity to each subscriber, thereby enabling multiple services to be utilized. This capacity should be easily scalable, not only in overall bandwidth, but also in the total number of subscribers that can use the access equipment. The ideal access approach should be available for a high percentage of the time (up to 99.999% availability), and able to propagate data over relatively long distances. Each broadband-access approach offers a "zone of advantage", that is, each approach offers a more optimal performance for certain specific applications and deployment strategies.

Optical wireless can be seen as an appealing solution for the last mile bottleneck, as shown in Fig.4.7(a).

**Indoor systems:** Optical wireless is an optimal solution for indoor, such as LAN applications. It enables very high transmission speed and multi-channel operation. This properties adapted to the wireless type of communication can be a very promising alternative to traditional radio wireless techniques (802.11$x$). Contrary to outdoor applications, an undirectional transmitter is required, since receivers are free to be placed wherever into a cell. Thus tens of degrees divergences have to be considered for systems design. In this case multiple reflections from walls and ceilings can be exploited. The idea is shown in Fig.4.7(b).

Different approaches can be used as antenna to distribute a signal over a room, such as LEDs transmitter that diffuses signals with wide angles (similarly to IrDA systems and remote control), focusing controlling of a lens or a system of lenses, taper fabricated on a fibre end.

The first two solutions are extremely simple and have been already used in thousands of circumstances. The last is nowadays the most prospective. Tip fabrication is made controlling fibre's etching in a hydrogen fluoride acid (HF) solution. The fibre is first immersed in the solution and then pulled out slowly. The pull out speed controls the shape of the tip and thus the angular pattern radiated from the fibre end [117].

**Back-up and disaster recovery:** Thanks to the use of a completely different transmission method and to the fact that FSO can be virtually integrated into any infrastructure due to their unparalleled bandwidth range and industry standard interface selection, FSO technology is usually named a "nomadic solution" [110]. Consequently, FSO offers a perfect backup solution regardless the type of the main link, by providing consistent connection should the primarily link fail (Fig.4.7(c)). The tragic event of September $11th$, 2001 was an example of FSO for disaster recovery.

The attacks severely damaged segments of the court's communications system. To reconnect the Manhattan buildings to each other and to facilities located throughout the state, telecommunications specialists at the court system turned to Free Space Optics. Each FSO system, which reconnected the main buildings at Ground Zero and recovered the main infrastructure, provided an OC-12 line with 622Mbps.

**Telephony:** For corporate users the 2Mbps $E1$ line is a frequently used solution to interconnect telephone exchanges. The interconnection however is often via leased lines, which means recurring costs. Through FSO there are no rental costs or frequency allocation fees thus making the interoffice calls completely free. Offering both balanced and unbalanced connection on the industry standard G.703 2Mbps copper interface assures compatibility with any standard $E1$ port without the need for additional hardware (Fig.4.7(d)).

**Fibre extension:** The principle of operation of FSO corresponds to the fibre optics transmission one and there are many similarities between these two transmission methods [118]. One of the most important is that in theory the same transmission capacity can be achieved with both technologies, so that FSO is often referred to as "wireless fibre". FSO links can easily be used either to extend the coverage of fibre optic network, as shown in Fig.4.7(e), or to interconnect two fibre segments where laying down fibre optic cable is not viable.

**Local Area Network (LAN):** Delivering true wire speed full duplex connection FSO links can extend the boundaries of LAN's even at Gigabit speed without creating

bottlenecks. The physical layer connectivity is transparent to all protocols and does not require any configuration. Offering industry standard copper and fibre interfaces the integration into the local infrastructure is easy and straightforward. The FSO technology is a one-time investment as neither frequency allocation nor leasing fees are involved. Basically FSO is an ultimate connectivity solution for LAN users (Fig.4.7(f)) exhibiting the best price-performance and reliability available on the market today.

## 4.2 Experimental transparent system

A transparent system launches and collects power directly through single mode optical fibers, so, eliminating the bottleneck due to electrical-optical-electrical (EOE) conversion, transparent FSO systems allow to exploit all the optical bandwidth offered by the use of fibers [8] and to realize a direct connection with access networks [126, 109]. Moreover, they allow the use of WDM technology, increasing the total capacity of the system [109]. On the other hand, the coupling losses and the atmospheric attenuation limit transparent systems to short-range links, such as hundreds of meters [111].

In this section, an experimental transparent system realized in collaboration with the Istituto Superiore delle Comunicazioni (ISCOM) at The Italian Economical Development Ministry (former Italian Communication Ministry) is presented.

A field trial test-bed with a real 100-meter long transparent FSO link has been realized, that can provide high bit rate connectivity and supports DWDM transmission.

As a first step, two micrometer devices to allow all the degrees of freedom for the fibres and lens have been assembled, (Fig.4.8). These devices can move in all directions to guarantee an accurate alignment of fibre and lens in both transmitter and receiver sides, because, as said in Section 4.1.1, pointing is an important aspect for wireless optical systems.

The devices that realize the fibre-air-fibre coupling are placed inside two side-by-side rooms, not in reciprocal visibility, at the first floor of the Ministry. The line of sight is obtained by using a mirror placed 3.5m below the laboratories, outside in the courtyard,

Figure 4.8: Devices for transparent FSO field trial.

as shown in Fig.4.9.

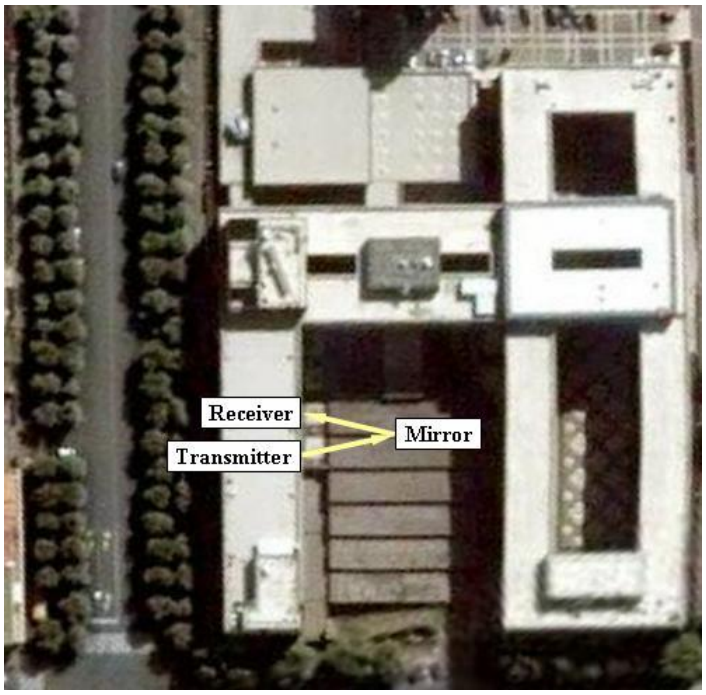


Figure 4.9: Top view of the site of the experiment.

The complete setup is distributed across two floors: the lab with the transmitter (ITU DFB multi-source) and the receiver (BER Tester) is on the ground floor, the devices for optical wireless connection are at the upper floor. The signal generated by the transmitter is sent into a single mode fiber and reaches the upper floor, there, it is amplified and transmitted through the air by a telescopic lens capable of collimating beams over long

distances. Then, it passes through the FSO transparent system via the outside mirror, is collected by a GRIN lens, to efficiently couple the power back into a single mode fibre core, and comes back to the lab at the ground floor.

The transmitter consists of three DFB laser sources at the 1549.3nm, 1550.1nm and 1550.9nm ITU-T wavelengths ($L1$, $L2$, $L3$ in Fig. 4.10), and, for the sake of experiment, they carry data modulated at 2.5, 10 or 40Gb/s with a PRBS pattern length of $2^{31} - 1$. The DFB laser sources are coupled together and modulated. In order to simulate distinct communication channels, different channels have been decorrelated using a Mux-DeMux cascade with different delays. The multiplexer used has a $-3$dB channel width equal to 420pm.

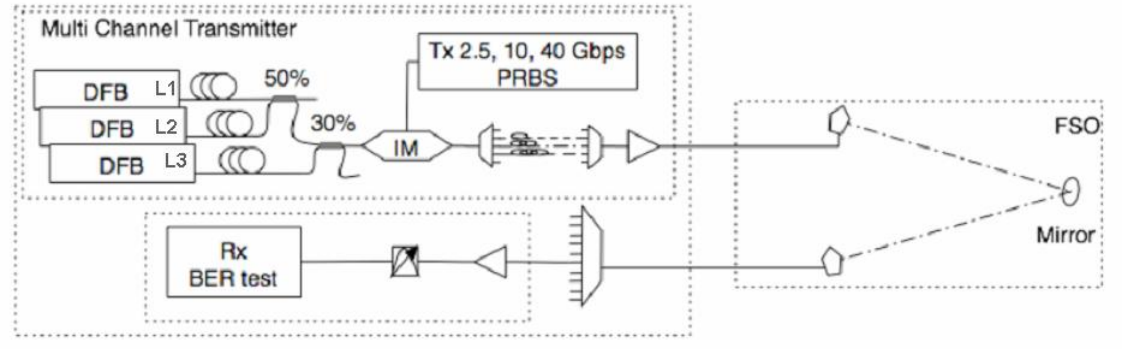


Figure 4.10: Schematic of the experimental set up.

The total attenuation faced by the signal and due to coupling losses, free space transmission, and misalignment is about 21dB. The optical signal passed through two glass windows responsible for an increased attenuation equal to 1.5dB. The power launched through the air, at the output of the lens, necessary to obtain error free reception is equal to $-5$dBm.

The Bit Error Rate (BER) value has been measured for every channel in the WDM transmission. These measurements have been made using an *Anritsu* BER tester with a digital *NEL* receiver. A variable attenuator (VAT) along the optical path has been used to measure the BER versus different channel power received.

A critical point was to assemble the receiving and transmitting devices, because they have to be be completely adjustable in the three dimensions in order to make possible

the alignment of the whole system. This leads to mechanical instability (typical limitation in this kind of system, as illustrated in Section 4.1.1), that can be easily solved by using suitable commercial devices. Another critical point was the mechanical instability introduced by the mirror, that can be solved according to the peculiar site configuration. The impact of these instabilities is derived from the comparison of back-to-back and in-field measurements with different weather conditions.

For the first experiment, BER versus received power measurement of a 2.5Gb/s transmission have been done. In order to test the performance of the transparent system, three different situations have been considered: a BTB connection, an in field experiment with good environmental conditions and the same in field system in presence of high wind condition (Fig.4.11). These early results underline the impact of the mechanical instability on the link performance. Nevertheless, in the worst case situation the realized link can ensure complete reliability with a power emission far below the regulations threshold (IEC 60825).

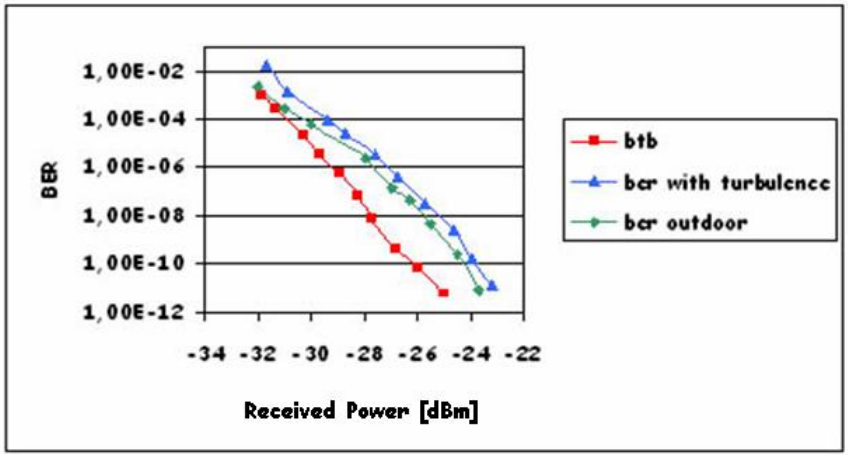


Figure 4.11: BER versus received power: (squares) BTB; (triangles) field trial test with turbulence; (diamonds) field trial test without turbulence.

Then, two transmissions at 10Gb/s and 40Gb/s respectively have also been sent and the performance of both in the field systems were evaluated for DWDM data transmission, considering 3 channels, with a channel separation equal to 100GHz. In Fig.4.12(b) BER measurement for the 10Gb/s transmission are shown: triangles are related to a single

channel BER measurement without interfering channels, while dots and squares are related to BER measurements with interfering channels, simulating WDM data transmission, taken in the late afternoon, around 6 : 00 pm, of two different days with different atmospherical conditions. In particular, dots are related to a measurement taken in a day when station readings were $T = 12°C$ with 60% humidity and no wind, whereas squares are related to measurement with a temperature of $T = 14°C$ with 70% humidity and no wind. Error free transmission has been achieved in both cases. As it can be noticed by the eye diagram on the left side of the Fig.4.12, there were small fluctuations on the ones, probably due to stabilization problems. The optical head of the oscilloscope has a bandwidth equal to 60GHz. Furthermore, from the analysis of the BER curves at different temperature values (dots and squares in Fig.4.12), it is possible to notice that a temperature increase affects the system performance, as expected.

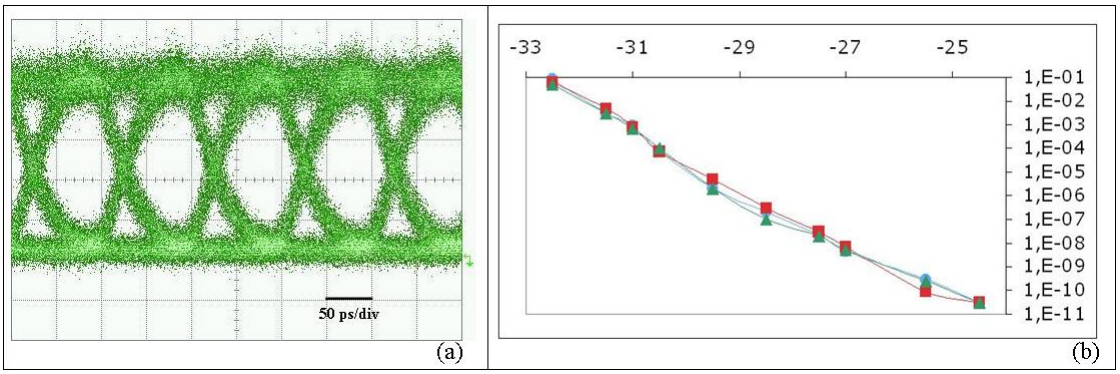


Figure 4.12: 10Gb/s transmission. (a) Eye diagram, (b) BER measurements at different conditions: (triangles) no inerfering channel, (dots) two interfering channels, $T = 12°C$ with 60% humidity and no wind, (squares) two interfering channels, $T = 14°C$ with 70% humidity and no wind.

In addition, several tests have been performed to evaluate the performance of the 40Gb/s system. The signal is obtained via electrical multiplexing of four 10Gb/s sequences. The eye diagram and the measure of the Q-Factor of the 40Gb/s signal versus the received power are reported. In this case, the measurements have been made under good atmospheric conditions. For the Q-factor a value of 7.8 has been achieved, which corresponds to a BER

of about $10^{-12}$, granting a virtually error free transmission.

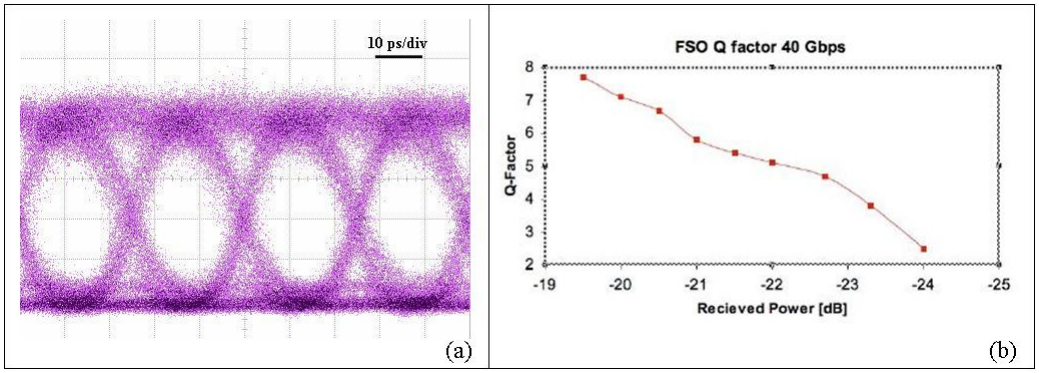


Figure 4.13: 40Gb/s transmission: (a) Eye diagram, (b) Q-factor.

For both data bit rates, no inter-channel interference was observed. The tests highlight the importance of the mechanical stability in this kind of system, underlined in particular by the BER measurements of the first trial (Fig.4.11) with 2.5Gb/s transmission, but also the possibility of integrating these systems with the current access networks, decreasing the installations costs and maintaining high transmission quality.

Chapter 5

# Conclusions

In the following section, the main results of this Thesis work will be summarized and some concluding remarks will be given.

The aim of this thesis has been to investigate the use of optical techniques in the next generation access networks, which is growing ever and ever, considering three different aspects: the level of security related to the use of optical code division multiple access techniques in the last segment of the network, the enhancement of network performance thanks to the use of advanced modulation formats and the free space optic technology proposal that is an alternative optical connection that could be a versatile and cost-saving solution, maintaining the bandwidth of fibres.

In Chapter 2, OCDMA techniques and characteristics of optical codes have been described and the analysis have been focused on the level of security assured by this technique, because, due the increasingly application of optical technologies in access networks, physical layer security is gaining a lot of interest to avoid information theft along the optical link.

OCDMA has been indicated as a potential secure technique, thanks to the fact that the transmitted signal is encoded by a specific code word and the intended receiver needs the same code word to correctly rebuild the transmission. However, several theoretical and experimental studies have demonstrated that ODCMA technique presents some vulnerabilities and cannot be considered secure without some precautions. Therefore, two solutions

have been proposed in order to increase the confidentiality level in OCDMA networks.

The former is related to optical "cryptographic" techniques, by means of a multiport encoder/decoder device, able to generate and process $N$ PSK codes at the same time. The multiport E/D is an AWG based device with $N$ input/output ports, which exploits the characteristics of an AWG to generate PSK codes as a copy of the input laser pulse on a single wavelength and using a time-spreading technique. It can process both unidimensional and $n$-dimensional codes, generated by sending $n$ laser pulses to the encoder input simultaneously.

Different configurations of this device can perform bit- and block-ciphering schemes, realizing signal encryption at physical layer.

The bit-ciphering consists of a direct correspondence between bits and optical codes; $n$-dimensional codes and spectral-phase codes have been considered. The first family of code is generated by sending $n$ laser pulses to the input port at the same time, obtaining codes that are the sum of $n$ PSK codes and that are composed of $n$ frequency channels. In order to increase network confidentiality, a further degree of freedom have been introduced with a set of phase shifter at the encoder input ports, obtaining a spectral-phase code by changing the phases of the input coherent laser pulses. For the bit-coding scheme, network security have been calculated in term of the number of years required to find the matched code with an exhaustive search attack, or brute force code searching. It is possible to observe that spectral-phase encoding is more robust than $n$-dimensional encoding, thanks to the fact that it allows the generation of $2^N$ codes, where the secret key is the sequence of $N$ phases of the codes that can be varied. Instead, $n$-dimensional encoding allows the generation of $\begin{pmatrix} N \\ n \end{pmatrix}$ code words. In both cases the eavesdropper is considered able to test $10^7$ codes per second, even if, with the present level of optical technology, it is quite unlikely to test million optical codes per second, therefore the obtained results can be considered an upper bound for optical network security.

In the block-ciphering technique, a sequence of $m$ bits is encoded onto one of $M = 2^m$ code words, therefore in this case, the secret key is based on the logic of assigning a different code to each bit sequence. The number of possible secret keys coincides with

all possible permutations of $n$ bits, $2^n!$, therefore block-ciphers are more secure than bit-ciphers. Unidimensional and $n$-dimensional encoding have been considered, measuring the security level assured first in term of the years required to break the code, considering, as in the previous case, the test of $10^7$ codes per second and demonstrating that this technique is robust against brute force code searching attack. Then the robustness against chosen plaintext attack has been investigated, considering the number of plaintext bits that a potential eavesdropper needs to know. This parameter is the lower bound security parameter of modern cryptanalysis. The $n$-dimensional block-ciphering scheme results the more robust against this kind of attack, while in bit-ciphering scheme just a single bit is enough to intercept data.

Therefore, it is possible to conclude that bit-coding technique can be considered computationally secure against brute force code searching attacks, but it is vulnerable against the other kind of attacks, whilst block-coding technique, with $n$-dimensional configuration, results enough robust also against the chosen plaintext attack, increasing the confidentiality of an OCDMA network.

In collaboration with the Telecommunication Institute of Aveiro University, Portugal, a different proposal to increase physical layer confidentiality in OCDMA transmission have been studied. It makes possible the use of simple, cost-saving and off-the shelf devices to "encrypt" the signal before the transmission. The system is based on the introduction of scrambling in the optical domain, in order to allow a transparent and all-optical processing of the signal, with the aim of increasing the confidentiality, preserving the total bandwidth of the fibre. Optical scrambling is realized by the means of a cascade of OCDMA encoders in each transmitter, that makes the bit overlapping, producing a signal fully distorted. The measurement of such signal shows an eye-diagram with many level, so that the transmission cannot be revealed by power or differential detection. Data signal is convolved with two, or more, codes and the impulse response of the encoder chain is the convolution between the codes: the more the codes are uncorrelated, the more the signal is degraded. Therefore, the introduction of scrambling increases the degrees of freedom of the system, forcing a potential eavesdropper to test all the possible combination between the codewords

assigned to each user. The encoding devices are realized with SSFBGs, making simple the implementation of the system, but also increasing the decryption difficulty of a potential eavesdropper due to the tunability time of the gratings.

The exhaustive code search attack is considered, while the robustness against the other two kinds of security attack could be the subject of further studies.

First, a P2P transmission has been considered, both in back-to-back and in channel transmission configuration, considering a 20-km fibre link, which is the typical distance for a PON network. In both cases the system shows good performance in term of BER, showing that only the user, who possesses the matching code, is able to reveal correctly the transmission. The codes used are coherent time-spreading codes, the *Kasami* codes, due to the large number of code words available with this family of codes and to their good correlation property.

Then, two multiuser configurations have been considered to investigate the applicability of the system in real networks. In this case, the critical point is the orthogonality between the codes, because in a multiuser application to preserve the orthogonality of the channels for OCDMA transmission, not only the code words must be orthogonal, but also the convolutions between the pair of codes used in each channel. One and two interfering channels have been considered to study the interference between them. Both configurations present good performance in terms of BER, showing that the security level is preserved, as in the case P2P transmission, and that the MAI noise helps in hiding the message and, at the same time, the presence of the interfering channel do not affect too much the transmission of the intended receiver.

In Chapter 3, the use of different advanced modulation formats have been studied in order to increase the performance of an optical system in terms of spectral efficiency and robustness against fibre dispersion.

OOK, DUOBINARY, DPSK and DQPSK, have been analyzed in an OCDMA transmission, considering both incoherent and coherent encoding, by the use of OOCs and *Gold* codes, respectively. The introduction of advanced modulation formats improves the spectral efficiency of the transmission, increasing the number of users that can simultaneously

access the network. In both incoherent and coherent cases, DPSK and DQPSK improve the performance of the system in terms of BER and, regarding the spectral efficiency, the DQPSK modulation seems to be the best choice because halves the bandwidth occupation of the signal.

Then, the introduction of OFDM in optical networks have been investigated in order to improve their performance. Optical OFDM seems to be a valid solution in optical technologies because meets the twofold requirement of mitigating the transmission impairments of the fibre channel and of increasing the allowed data rate. Thanks to the low bandwidth occupied by each subchannel, the OFDM is characterized by a high spectral efficiency and high tolerance to chromatic and polarization mode dispersions. These characteristics allow to reach large distances, to hundreds of kilometers, with high bit rates, before significant distortions in the transmission, without any dispersion compensation.

Recently, optical OFDM has been also considered as a suitable application for passive optical networks, because, along with the cited advantages, it allows to assign different subchannel to different ONUs, that can modulated independently each subchannel, increasing the supported bit-rate and consequently the spectral efficiency. Furthermore, different service can be associated to different subchannels in a transparent way and the bandwidth can be allocated dynamically between them.

A different scheme to realize optical OFDM have been investigated, in collaboration with the Technologic Telecommunication Center of Catalunya (CTTC). Exploiting the properties of trigonometric transforms, such as Hartley transform, an optical OFDM system can be simplified, preserving the advantage of traditional OFDM system. Thanks to the kernel of the DHT, frequency division and orthogonality are preserved, but at the same time the number of devices necessary to process the signal is halved, realizing a simpler and cost-saving system. Each symbol of the information sequence is modulated on two symmetrical subbands, increasing the frequency diversity, moreover the IDHT and the DHT are identical, therefore it is possible to use the same device to perform the processing in both directions. Since the DHT transform of a real signal is still a real signal, this simplifies the conversion of the electrical OFDM signal in optical domain, by the use of

intensity modulation and direct detection.

Preliminary numerical simulations have demonstrated the feasibility of the DHT-based system, reaching distances useful for access networks, without equalization.

In Chapter 4, optical wireless is proposed as a valid alternative to wired optical connection for the last mile, in order to offer a transparent and cost-saving solution for the access segment of the networks, exploiting the same bandwidth of the fibre links.

In collaboration with the Istituto Superiore delle Comunicazioni in Rome, a transparent free space optical system have been experimentally studied to eliminate the electrical-to-optical-to electrical conversions typical of commercial opaque wireless optical systems, exploiting the potentiality of optical connectivity, allowing the use of DWDM system to increase the bit-rate and realizing a direct and fast connection for the access networks. In transparent systems, the optical beam is transmitted directly into the air by a trunked fibre, by means of a system of lens able to collimate the beam over long distances. The beam propagates in the free space and then, at the receiving side, it is directly focused into the core of a standard single mode fibre, by the use of a GRIN lens, that allows a more effective coupling. In the proposed system, the transmitting and receiving devices have been realized over mountings that allow micrometers movements, necessary for a correct alignment of the system; furthermore, the LOS is obtained with the use of a mirror in the optical path, making the system more versatile. The system have been characterized in terms of BER and Q factor. The effects of atmospherical conditions have been investigated, which are in agreement with what expected from literature. Furthermore a DWDM transmission have been tested, in presence of one and two interfering channels, showing that the performance are not affected by inter-channel interference. The experimental measurements have underlined the importance of mechanical stability of the system and the critical state of pointing, that is an important aspect in free space optical technologies.

# List of Figures

# Bibliography

[1] H. Yin, D.J. Richardson, *Optical Code Division Multiple Access Communications Networks, Theory and Application*, Tsingua University Press - Springer, 2007.

[2] R. Ramaswami, K. N. Sivarajan, *Optical networks, A practical perspective*, Morgan Kaufmann Publishers, 1998.

[3] http://www.telcordia.com/services/testing/integrated-access/pon/

[4] M. de Bortoli, R. Mercinelli, P. Solina, A. Tofanelli, "Tecnologie ottiche per l'accesso: le soluzioni Passive Optical Network", Notiziario Tecnico Telecom Italia, Year 13, No.1, pp.104-119, June 2004.

[5] A. Banerjee, Y. Park, F. Clarke and H. Song, S. Yang, G. Kramer, K. Kim, B. Mukherjee, "Wavelength division multiplexed passive optical network (WDM-PON) technologies for broadband access: a review", (Invited) IEEE J. Lightw. Technol., Vol.4, No.11, pp.737-758, Nov. 2005.

[6] K. Kitayama, X. Wang, N.Wada, "OCDMA Over WDM PON – Solution Path to Gigabit Symmetric FTTH", IEEE J. Lightw. Technol., Vol.24, No.4, pp.1654-1662, Apr. 2006.

[7] Z. Zheng, Z. Qian, G. Shou, Y. Hu, "Next-Generation Passive Optical Network Based on OFDM Transmission", Proc. WASE International Conference on Information Engineering, Taiyuan, Shanxi, pp.329-332, July 2009.

[8] M. Marciniak, "Towards broadband global optical and wireless networking", Proc. International Conference on Transparent Optical Networks (ICTON 2004), Wroclaw, Poland, Vol.2, pp.13-16, July 2004.

[9] P.R. Prucnal, M.A. Santoro, T.R. Fan, "Spread Spectrum Fiber-optic Local Area Network Using Optical Processing", IEEE J. Lightw. Technol., Vol.4, No.5, pp. 547-554, May 1989.

[10] P.R. Prucnal, M.A. Santoro, S.K. Sehgal, "Ultrafast All-Optical Synchronous Multiple Access Fiber Networks", IEEE J. on Selec. Areas in Comm., Vol.4, No.9, pp. 1484-1494, 1986.

[11] A. M. Weiner, J. P. Heritage and J.A. Salehi, "Encoding and decoding of femtosecond pulses", Optics Letters, Vol.13, No.4, pp. 300-302, Apr. 1988

[12] A. M. Weiner, J. P. Heritage and E.M. Kirschner, "High resolution femtosecond pulse shaping", IEEE J. Opt. Soc. Am. B, Vol.5, No.8, pp. 1563-1571, Aug. 1988

[13] J.A. Salehi, "Code Division Multiple-Access Techniques in Optical Fiber Networks-Part I: Fundamental Principles", IEEE Trans. on Comm., Vol.37, N.8, pp. 824-833, Aug. 1989.

[14] J.A. Salehi and C.A. Brackett, "Code Division Multiple-Access Techniques in Optical Fiber Networks-Part II: System Performance Analysis", IEEE Trans. on Comm., Vol.37, N.8, pp. 834-842, Aug. 1989.

[15] F.R.K. Chung, J.A. Salehi, V.K. Wei, "Optical Orthogonal Codes: Design, analysis and applications", IEEE Trans. on Information Theory, Vol.35, N.3, pp. 595-605, May 1989.

[16] A.S. Holmes and R.R. Syms, "All-optical CDMA using "quasi-prime" codes", IEEE J. Lightw. Technol., vol.10, n.2, pp. 279-286, Feb. 1992.

[17] G.C. Yang and W.C. Kwong, "Performance analysis of optical CDMA with prime codes", IEE Elec. Letters, vol.31, n.7, pp. 569-570, Mar. 1995.

[18] E. Park, A.J. Mendez, and E.M. Garmire, "Temporal/spatial optical CDMA networks-design, demonstration, and comparison with temporal networks", IEEE Phot. Tech. Letters, Vol.4, N.10, pp. 1160-1162, Oct. 1992.

[19] L. Tancevski, I. Andonovic, "Wavelength hopping/time spreading code division multiple access systems", IEE Elec. Letters, vol.30, n.17, pp. 1388-1390, Aug. 1994.

[20] L. Tancevski, I. Andonovic, "Hybrid wavelength-hopping/time-spreading schemes for use in massive optical networks with increased security", IEEE J. Lightw. Technol., Vol.14, N.12, pp. 2636-2646, Dec. 1996.

[21] N. Wada, K.I. Kitayama, "A 10 Gb/s Optical Code Division Multiplexing Using 8-Chip Optical Bipolar Code and Coherent Detection", IEEE J. Lightw. Technol., Vol.17, No.10, pp. 1758-1765, (1999).

[22] C.H. Lee, S. Zhong, X. Lin, J.F. Young and, Y.J. Chen "Planar lightwave circuit design for programmable complementary spectral keying encoder and decoder", IEE Elec. Letters, Vol.35, No.21, pp. 1813-1815, (1999).

[23] P.C. Teh, P. Petropoulos, M. Ibsen, and D. J. Richardson, "Phase Encoding and Decoding of Short Pulses at 10 Gb/s Using Superstructured Fiber Bragg Gratings", IEEE Phot. Techn. Letters, Vol.13, No.2, pp.154-156, (2001).

[24] P. Teh, P. Petropoulos, M. Ibsen, and D.J. Richardson, "A Comparative Study of the Performance of Seven and 63-Chip Optical Code-Division Multiple-Access Encoders and Decoders Based on Superstructured Fiber Bragg Gratings", IEEE J. Lightw. Technol., Vol.19, No.9, pp.1352-1365, Sept. 2001.

[25] X. Wang, K. Matsushima, A. Nishiki, N. Wada, K.K. Kitayama, "High refelectivity superstructured FBG for coherent optical code generation and recognition", Optics Express, Vol.12, No.22, pp.5457-5468, Nov. 2004.

[26] Z. Zhang, C. Tian, P. Petropoulos, D.J. Richardson and M. Ibsen "Distributed Phase OCDMA Encoder Decoders Based on Fiber Bragg Gratings", IEEE Phot. Techn. Letters, Vol.19, No.8, pp.574-576, Apr. 2007.

[27] Z. Wei, H. Ghafouri-Shiraz, and H. M. H. Shalaby, "A New Code Families for Fiber-Bragg-Grating-Based Spectral-Amplitude-Coding Optical CDMA Systems", IEEE Phot. Tech. Letters, Vol.13, No.8, pp. 890-892, (2001).

[28] A. Grunnet-Jepsen, A.E. Johnson, E.S. Maniloff, T.W. Mossberg, M.J. Munroe and J.N. Sweetser, "Fibre Bragg grating based spectral encoder/decoder for lightwave CDMA", IEE Elec. Letters, Vol.35, No.13, pp. 1096-1097, 1999.

[29] A. Grunnet-Jepsen, A.E. Johnson, E.S. Maniloff, T.W. Mossberg, M.J. Munroe, and J.N. Sweetser, "Demonstration of All-Fiber Sparse Lightwave CDMA Based on Temporal Phase Encoding", IEEE Phot. Tech. Letters, Vol.11, No.10, pp. 1283-1285, (1999).

[30] N. Wada, H. Sotobayashi and K. Kitayama, "2.5Gbit/s time-spread/wavelength-hop optical code division multiplexing using fibre Bragg grating with supercontinuum light source", IEE Elec. Letters, Vol.36, No.9, pp. 815-817, (2000).

[31] X. Wang, N. Wada, T. Miyazaki, G. Cincotti and K.I. Kitayama, "Field Trial of 3-WDM x 10-OCDMA x 10.71Gbps, truly-asynchronous, WDM/DPSK-OCDMA using hybrid E/D without FEC and optical threshold", Proc. Optical Fiber Communications Conference (OFC 2006), Anaheim, CA, Mar. 2006, PDP44.

[32] X. Wang, N. Wada, N. Kataoka, T. Miyazaki, G. Cincotti and K.I. Kitayama, "100km field trial of 1.34 Tbit/s, 0.45 bit/s/Hz asynchronous WDM/DPSK-OCDMA with 50 x 50 ports E/D and FEC", Proc. Optical Fiber Communication Conference (OFC2007), Anaheim, CA, Mar. 2007.

[33] X. Wang and K.I. Kitayama, "Analysis of Beat Noise in Coherent and Incoherent Time-Spreading OCDMA", IEEE J. Lightw. Technol., Vol.22, No.10, pp.2226-2235, Oct. 2004.

[34] T. Pfeiffer, J. Kissing, J.-P. Elbers, B. Deppisch, M. Witte, H. Schmuck, and E. Voges, "Coarse WDM/CDM/TDM Concept for Optical Packet Transmission in Metropolitan and Access Networks Supporting 400 Channels at 2.5 Gb/s Peak Rate", IEEE J. Lightw. Technol., Vol.18, No.12, pp.1928-1938, (2000).

[35] M. Razavi and J.A. Salehi, "Statistical Analysis of Fiber-Optic CDMA Communication Systems-Part I: Device Modeling", IEEE J. Lightw. Technol., Vol.20, No.8, pp.1304-1316, Aug. 2002.

[36] J.A. Salehi, A.M. Weiner and J.P. Heritage, "Coherent Ultrashort Light Pulse Code-Division Multiple Access Communication Systems", IEEE J. Lightw. Technol., Vol.8, No.3, pp.478-491, Mar. 1990.

[37] M. E. Marhic, "Coherent optical CDMA networks", IEEE J. Lightw. Technol., Vol.11, No.5/6, pp.854-864, (1993).

[38] K. Kitayama, "Code division multiplexing lightwave networks based upon optical code conversion", IEEE J. Selec. Areas Commun., Vol.16, pp.1209-1319, (1998).

[39] K. Kitayama and N. Wada, "Photonic IP routing", IEEE Phot. Tech. Lett., Vol.11, pp.1689-1691, (1999).

[40] C. C. Chang, H. P. Sardesai, and A. M. Weiner, "Code-division multiple-access encoding and decoding of femtosecond optical pulses over a 2.5 Km fiber link", IEEE, Phot. Tech. Lett., Vol.10, pp.171-173, (1998).

[41] H. Fathallah, L. A. Rusch, and S. LaRochelle, "Passive optical fast frequency-hop CDMA communications system", J. Lightw. Technol., Vol.17, pp.397-405 (1999).

[42] P. C. Teh, P. Petropoulos, M. Ibsen and D. J. Richardson, "A comparative study of the performance of sevenand 63-chip optical code-division multiple-access encoders and decoders based on superstructured fiber Bragg gratings", J. Lightw. Technol., Vol.9, pp.1352-1365 (2001).

[43] S. Yegnanarayanan, A.S. Bhshan, and B. Jalali, "Fast wavelength-hopping time-spreading encoding/decoding for optical CDMA", IEEE Phot. Tech. Lett., Vol.12, No.5, pp.573-575, May 2000.

[44] T. W. Mossberg, "Planar holographic optical processing devices", Optics Lett., Vol.26, pp.414-416, (2001).

[45] P. Ebrahimi, M. Kargar, M. Hamer, A. E. Willner, K. Yu and O. Solgaard, "A 10-ms-tuning MEMS-actuated Gires-Tournois filter for use as a tunable wavelength demultiplexer and a tunable OCDMA encoder/decoder", Proc. Optical Fiber Communication Conference (OFC 2004), Washington, D.C., Mar. 2004, ThQ2.

[46] T. Dennis, and J. F. Young, "Optical implementation of bipolar codes", IEEE J. Quantum Electronics, Vol.35, No.3, pp.287-291, (1999).

[47] G.C. Yang, "Optical Orthogonal Codes with Unequal Auto- and Cross-correlation constraints", IEEE Trans. on Inf. Theory, Vol.41, No.1, pp.96-106, (1995).

[48] K. Sato, T. Ohtsuki, H. Uehara and I. Sasase, "Performance of Optical Direct Detection CDMA Systems Using Prime Sequence Codes", IEEE Trans. Commun., Vol.14, No.4, pp.1312-1316, Apr. 1995.

[49] W.C. Kwong, G.C. Yang and J.G. Zhang, "2N Prime Sequence Codes and Coding Architecture for Optical Code Division Multiple Access", IEEE Trans. Commun., Vol.44, No.9, pp.1152-1162, Sept. 1996.

[50] J.-G. Zhang, W. C. Kwong and S. Mann, "Construction of 2N extended prime codes with cross-correlation constraint of one", IEE Proc. Commun., Vol.145, No.5, pp. 297-303, Oct. 1998.

[51] T. Shake, "Security performance of optical CDMA against eavesdropping", J. Lightw. Technol., Vol.23, No.2 pp.655-670, Feb. 2005.

[52] T. Shake, "Confidentiality performance of spectral-phase-encoded optical CDMA", J. Lightw. Technol., Vol.23, No.4, pp.1652-1663, Apr. 2005.

[53] A. Stok, E.H. Sargent, "The role of optical CDMA in access network", IEEE Comm. Mag., Vol.40, pp.83-87, Sept. 2002.

[54] Z. Jiang, D.S. Seo, S.D. Yang, D.E. Leaird, R.V. Roussev, C. Langrock, M.M. Fejer, A.M. Weiner, "Four user, 2.5 Gb/s, spectrally coded OCDMA system demonstration

using low-power nonlinear processing", J. Lightw. Technol., Vol.23, No.1, pp.143-158, Jan. 2005.

[55] D.E. Leaird, Z. Jiang, A.M. Weiner, "Experimental investigation of security issues in OCDMA: a code-switching scheme", Electronic Letters., Vol.41, No.14, Jul. 2005.

[56] Z. Jiang, D. E. Leaird, and A. M. Weiner, "Experimental investigation of security issues in O-CDMA", J. Lightw. Technol., Vol.24, No.11, pp.4228-4334, Nov. 2006.

[57] V. O'Byrne, "Verizon's Fiber to the Premises: Lessons Learned", Proc. Optical Fiber Communication Conference (OFC 2005), Anaheim, CA, Mar. 2005, OWP6.

[58] N. Nadarajah, W. Wong, and A. Nirmalathas, "Implementation of multiple secure virtual private networks over passive optical networks using electronic OCDMA", IEEE Photon. Technol. Lett., Vol.18, No.3, pp.484-186, (2006).

[59] X. Wang, N. Wada, T. Miyazaki, G. Cincotti and K. Kitayama, "Asynchronous coherent OCDMA system with code-shift-keying and balanced detection", IEEE J. Select. Topics Quantum Elect. Vol.13, No.5, Sept./Oct. 2007.

[60] L. Tancevski, and I. Andonovic, "Hybrid wavelength hopping/time spreading schemes for use in massive optical networks with increased security", IEEE J. Lightw. Technol., Vol.14, No.12, pp.2636-2647, Dec. 1996.

[61] F. Xue, Y. Du, S. J. B. Yoo, Z. Ding, "Security issues on spectral-phase-encoded optical CDMA with phase-masking Scheme", Proc. Optical Fiber Communication Conference (OFC 2006), Anaheim, CA, USA, Mar. 2006, OThT3.

[62] G. Cincotti, N. Wada, K.K. Kitayama, "Characterization of a full encoder/decoder in the AWG configuration for code-based photonic routers-Part I: modeling and design", IEEE J. Lightw. Technol., Vol.24, No.1, pp.103-112, Jan. 2006.

[63] N.Wada, G. Cincotti, S. Yoshima, N. Kataoka, K. Kitayama, "Characterization of a full encoder/decoder in the AWG configuration for code-based photonic Routers-part II:

experiments and applications", IEEE J. Lightw. Technol., Vol.24, No.1, pp.113-121, Jan. 2006

[64] G. Manzacca, M. Svaluto Moreolo, G. Cincotti, "Performance analysis of multi-dimensional codes generated/processed by a single planar device", IEEE J. Lightw. Technol., Vol.25, No.6, pp.1629-1637, June 2007.

[65] R. Oppliger *Contemporary chryptography*, Artech House, London, 2005.

[66] X. Wang, N. Wada, G. Manzacca, G. Cincotti, T. Miyazaki and K. Kitayama, "Demonstration of 8 × 10.7 Gbps asynchronous code-shift-keying OCDMA with multi-port en/decoder for multi-dimensional optical code processing", European Conference on Optical Communication (ECOC2006), Cannes, France, Sept. 2006.

[67] G. Manzacca, X. Wang, N. Wada, G. Cincotti, and K. Kitayama, "Comparative study of multiencoding scheme for OCDM using a single multi-port optical encoder/decoder", Photon. Technol. Lett. Vol.19, No.8, pp.559-561, Apr. 2007.

[68] T. Li, S. Zhou, Z. Zeng, Q. Ou, "A new scrambling method based on semi-frequency domain and chaotic system", Proc. IEEE International Conference on Neural Networks and Brain (ICNN&B 2005), Vol.2, pp.607-610, Oct. 2005.

[69] I.J. Fair, W.D. Grover, W.A. Krzymien, R.I. MacDonald, "Guided scrambling: a new line coding technique for high bit rate fiber optic transmission system", IEEE Trans. on Comm., Vol.39, No.2, pp.289-297, Feb. 1991.

[70] G. Di Crescenzo, R. Mendez, and S. Estemad, "OCDM-based photonic encryption with provable security", Proc. Optical Fiber Communication Conference (OFC 2008), San Diego, CA, Feb. 2008.

[71] S. Li, N.A. Daniel, D.V. Kuksenkov, and R. Hemenway, "Passive scrambling and unscrambling for secure fiber optic communications", Proc. Optical Fiber Communication Conference (OFC 2008), San Diego, CA, Feb. 2008.

[72] A.M.D. Turkmani and U.S. Goni, "Performance Evaluation of Maximal-length, Gold and Kasami Codes as Spreading Sequences in CDMA Systems", International Conference on Universal Personal Communications, Vol.2, pp.970-974, Oct. 1993.

[73] G. Cincotti, G. Manzacca, V. Sacchieri, N. Wada, X. Wang, K. Kitayama, "Security performance of optical multicoding transmission using a single multiport encoder/decoder", invited paper OptoElectronics and Communications Conference/International Conference on Integrated Optics and Optical Fiber Communications (OECC/IOOC 2007), Yokohama, Japan, July 2007.

[74] G. Cincotti, V. Sacchieri, G. Manzacca, N. Kataoka, N. Wada, N. Nagakawa, K. Kitayama, "Physical layer security: all-optical cryptography in access networks", invited paper International Conference on Transparent Optical Networks (ICTON 2008), Athens, Greece, June 2008.

[75] G. Cincotti, G. Manzacca, V. Sacchieri, X. Wang, N. Wada, K. Kitayama, "Secure OCDM transmission using a planar multiport encoder/decoder", IEEE Journal of Lightw. Technol., Vol. 26, No. 13, pp. 1798-1806, July 2008.

[76] http://www.vpiphotonics.com/

[77] P. Teixeira, B. Neto, A. Teixeira, R. Nogueira, P. André, "Automatic Apodization Profiling of Super Structured Fiber Bragg Gratings for OCDMA Coding Applications", Proc. Optical Fiber Communication Conference (OFC 2008), San Diego, CA, Feb. 2008, JThA29.

[78] V. Sacchieri, P. Teixeira, A. Teixeira, G. Cincotti, "A novel scrambling technique using OCDMA encoders", Proc. VI Symposium on Enabling Optical Networks (SEON 2008), Porto, Portugal, June 2008.

[79] V. Sacchieri, P. Teixeira, A. Teixeira, G. Cincotti, "Secure OCDMA transmission using data pattern scrambling", Proc. International Conference on Transparent Optical Networks (ICTON 2008), Athens, Greece, June 2008.

[80] V. Sacchieri, P. Teixeira, A. Teixeira, G. Cincotti, "Enhanced OCDMA security by code scrambling", BONE Summer School, Mons, Belgium, Oct. 2008.

[81] V. Sacchieri, P. Teixeira, A. Teixeira, G. Cincotti, "Tecniche di scrambling per incrementare la sicurezza nelle reti di accesso ottiche", Proc. Convegno Nazionale sulle Tecniche Fotoniche nelle Telecomunicazioni (FOTONICA 2009), Pisa, Italy, May 2009.

[82] V. Sacchieri, S. Di Lucente, P. Teixeira, A. Teixeira, G. Cincotti, "Multi-user application of code scrambling for enhanced optical layer confidentiality", Proc. International Conference on Transparent Optical Networks (ICTON 2009), Ponta Delgada, Azores, July 2009.

[83] V. Sacchieri, P. Teixeira, A. Teixeira, G. Cincotti, "A scrambling technique to enhance OCDMA network confidentiality", IEEE Photonics Society (formerly LEOS) Summer Topicals 2009, Newport Beach, California, July 2009.

[84] X. Wang, N. Wada, N. Kataoka, T. Miyazaki, G. Cincotti, and K. Kitayama, "100 km Field Trial of 1.24 Tbit/s, Spectral Efficient Asynchronous 5 WDM x 25 DPSK-OCDMA using one set of 50x50 Ports Large Scale En/Decoder", Proc. Optical Fiber Communication Conference (OFC 2007), Anaheim, CA, Mar. 2007, paper PDP14.

[85] P. Toliver, A. Agarwal, T. Banwell, R. Menendez, J. Jackel and S. Etemad, "Demonstration of High Spectral Efficiency Coherent OCDM using DQPSK, FEC, and Integrated Ring Resonator-based Spectral Phase Encoder/Decoders", Proc. Optical Fiber Communication Conference (OFC 2007), San Diego, CA, Mar. 2007, paper PDP7.

[86] G. Manzacca, F. Benedetto, V. Sacchieri, G. Giunta, G. Cincotti, "Advanced modulation formats in optical code division multiple access networks", Proc. International Conference on Transparent Optical Networks (ICTON 2007), Rome, Italy, July 2007.

[87] E. Ip and J. M. Kahn, "Power Spectra of Return-to-Zero Optical Signals", IEEE J. of Lightw. Technol., Vol.24, pp.1610-1618, Mar. 2006.

[88] X. Wang, K. Kitayama, "Analysis of beat noise in coherent and incoherent time-spreading OCDMA", IEEE J. of Lightw. Technol., Vol 22, pp.2226-2235, Oct. 2004.

[89] W. Rosenkranz, J. Leibrich, M. SA. Ali, "Orthogonal Frequency Division Multiplexing (OFDM) and other Advanced Options to achieve 100Gb/s Ethernet Transmission", Proc. International Conference on Transparent Optical Networks (ICTON 2007), Rome, Italy, July 2007, paper Mo.B1.2.

[90] A.J. Lowery, J. Armstrong, "Orthogonal-frequency-division multiplexing for dispersion compensation of long-haul optical systems", Optics Exp., Vol.14, No.6, pp.2079-2084, Mar. 2006.

[91] S.L. Jansen, I. Morita, T.C.W. Schenk, N. Takeda, and H. Tanaka, "Coherent optical 25.8-Gb/s OFDM transmission over 4160-km SSMF", IEEE J. Lightw. Technol., Vol.26, No.1, pp.6-15, Jan. 2008.

[92] W. Shieh, I. Djordjevic, *OFDM for Optical Communications*, Academic Press, Elsevier, 2010.

[93] I.B. Djordjevic and B. Vasic, "Orthogonal frequency division multiplexing for high-speed optical transmission", Optics Exp., Vol.14, No. 9, pp.3767-3775, May 2006.

[94] A. Lowery and J. Armstrong, "Adaptation of Orthogonal Frequency Division Multiplexing (OFDM) to Compensate Impairments in Optical Transmission Systems", Tutorial European Conference and Exhibition on Optical Communication (ECOC 2007), Berlin, Ge, Sept. 2007.

[95] J. Armstrong, "OFDM: From Copper and Wireless to Optical", Tutorial Optical Fiber Communication Conference (OFC 2008), San Diego, CA, Feb. 2008.

[96] L. Hanzo, T. Kellet, *OFDM and MC-CDMA, A Primer*, Wiley&sons, 2006.

[97] J.D. Villasenor, "Optical Hartley transforms", Proc. IEEE, Vol.82, No.3, Mar. 1994.

[98] M. Svaluto Moreolo, G. Cincotti, "Fiber Optic Transforms", Proc. International Conference on Transparent Optical Networks (ICTON 2009), Athens, Greece, July 2008.

[99] R.N. Bracewell, "Discrete Hartley transform", J. Opt. Soc. Amer., Vol.73, pp.1832-1835, Dec. 1983.

[100] R.N. Bracewell, "The Fast Hartley transform", Proc. IEEE, Vol.72, No.8, Aug.1984.

[101] H.S. Hou, "The fast Hartley transform algorithm", IEEE Trans. Computers, Vol.C-36, pp.147-156, (1987).

[102] C. Wang, C.H. Chang, J.L. Fan. and J.M. Cioffi, "Discrete Hartley transform based multicarrier modulation", Proc. IEEE International Conference on Acoustics, Speech, and Signal Processing, Vol.5, pp.2513-2516, 2000.

[103] D. Wang, D. Liu, F. Liu, and G. Yue, "A novel DHT-based ultra-wideband system", Proc. IEEE International Symposium on Communications and Information Technology (ISCIT 2005), Oct. 2005.

[104] D. Qian, N. Cvijetic, J. Hu, T. Wang, "Optical OFDM Transmission in Metro/Access Networks", Proc. Optical Fiber Communication Conference (OFC 2009), San Diego, CA, Mar. 2009, paper OMV1.

[105] D. Qian, J. Hu, P. Nan Ji, T. Wang, "10-Gb/s OFDMA-PON for Delivery of Heterogeneous Services", Proc. Optical Fiber Communication Conference (OFC 2008), San Diego, CA, Feb. 2008, paper OWH4.

[106] D. Qian, J. Hu, J. Yu, P. Ji, L. Xu, T. Wang, M. Cvijetic, T. Kusano, "Experimental Demonstration of a Novel OFDM-A Based 10Gb/s PON Architecture", Proc. European Conference and Exhibition on Optical Communication (ECOC 2007), Berlin, Ge, Sept. 2007, paper Mo.5.4.1.

[107] M. Svaluto Moreolo, V. Sacchieri, G. Cincotti, "Signal processing based on trigonometric transforms for high-speed optical networks", invited paper Proc. International Conference on Transparent Optical Networks (ICTON 2009), Ponta Delgada, Azores, July 2009.

[108] A. Boucouvalas, "Editorial: Optical wireless communications", IEE Proc. Optoelectron., Vol.150, No.5, Oct. 2003.

[109] Y. Aburakawa, T. Otsu, "Dense wavelength division multiplexed optical wireless link toward terabit transmission", Proc. at Microwave Photonics, Budapest, Hungary, pp.135-138, Sept. 2003.

[110] S.S. Muhammad, C. Chlestil, E. Leitgeb, M. Gebhart, "Reliable Terrestrial FSO systems for higher bit rates", Proc. International Conference on Telecommunications (ConTEL 2005), Zagreb, Croatia, June 2005.

[111] I.I. Kim et al., "Wireless optical transmission of fast Ethernet, FFDI, ATM, and ESCON protocol data using the TerraLink laser communication system", Opt. Eng., Vol.37, No.12, pp.3143-3155,(1998).

[112] S. Lee, J.W. Alexander, M. Jeganathan, "Pointing and tracking subsystem design for optical communications link between the International Space Station and ground", Proc. International Society for Optical Engineering (SPIE), Vol.3932, pp.150-157, May 2000.

[113] White Paper Free-Space Optics: Laser Safety, 2002, LightPointe, http://www.lightpointe.com/home.cfm

[114] P. F. Szajowski, G. Nykolak, J. J. Auborn, "2.4 km free-space optical communication 1550 nm transmission link operating at 2.5 Gb/s - experimental results", Optical Wireless Communications, Proc. SPIE, 3532, pp. 29-40, (1998).

[115] S. Sheikh Muhammad, P. Köhldorfer, E. Leitgeb, "Channel Modeling for terrestrial Free Space Optical Links", Proc. Proc. International Conference on Transparent Optical Networks (ICTON 2005), Barcelona, Spain, Vol.1, pp.407-410, July 2005.

[116] C. Davis, I.I. Smolyaninov, S.D. Milner, "Flexible Optical Wireless Links and Networks", IEEE Communications Magazine,Vol.41, No.3, pp.51-57, Mar. 2003.

[117] P.R. Kaczmarek, M. Ciemniak, K.M. Abramski, "Fiber Antennas for Fiber Free-Space Communication", Proc. International Conference on Transparent Optical Networks (ICTON 2005), Barcelona, Spain, Vol.2, pp.363-366, July 2005.

[118] G.P. Agrawal, N.Nutta, *Semiconductor laser*, Van Nostrand Reinhold, 1993.

[119] M. Al Naboulosi, H. Sizun , F. de Fornel, "Propagation of optical and infrared waves in the atmosphere", www.ursi.org/Proceedings/ProcGA05/pdf/F01P.7(01729).

[120] E. Korevaar, I.I. Kim, B. McArthur, "Comparison of laser beam propagation at 785 nm and 1550 nm in fog and haze for optical wireless communications", Proc. International Society for Optical Engineering (SPIE), Vol.4124, pp.26-37, Feb 2001.

[121] M. Gebbart, E. Leitgeb, J. Bregenzer, "Atmospheric effects on Optical Wireless links", Proc. International Conference on Telecommunications (ConTEL 2003), Vol.2, pp.395-401, Zagreb, Croatia, June 2003.

[122] B.R. Strickland, M.J. Lavan, "Effects of fog on the bit error rate of a free-space laser communication system", Applied Optics, Vol.38, pp. 424-431, (1999).

[123] M. Achour, "Simulating atmospheric free space optical propagation; Part II, Haze, fog and low clouds attenuations", Proc. International Society for Optical Engineering (SPIE), Vol.4873, pp.1-12, Dec. 2002.

[124] I.I. Kim, M. Mitchell, and E. Korevaar, "Measurement of scintillation for free-space laser communication at 785 nm and 1550 nm", Optical Wireless Communications II, Proc. International Society for Optical Engineering (SPIE), Vol.3850, pp.49-62, Sept. 1999.

[125] A.J.C. Moreira, R.T. Valadas, A.M. de Oliveira Duarte, "Characterization and modelling of artificial light interference in optical wireless communication systems", Proc. IEEE International Symposium on Personal, Indoor and Mobile Radio Communications (PIMRC'95), Vol.1, pp.326 - 331, Sept. 1995.

[126] G. Nykolak, G Raybou, B. Mikkelsen, B. Brown, P. F. Szajowski, J. J. Auborn, H. M. Presby, "A 160 Gb/s free space transmission link", Proc. Conference on Lasers and Electro-Optics (CLEO 2000), San Francisco, California, pp.682-683, May 2000.

[127] V. De Sanctis, V. Sacchieri, G. Cincotti, F. Curti, M. Guglielmucci, G. Tosi Beleffi, D. Forin, "Sistemi FSO opachi e trasparenti per applicazioni WDM in- e out-door", Convegno Nazionale sulle Tecniche Fotoniche nelle Telecomunicazioni (FOTONICA 2007), Mantova, Italy, May 2007.

[128] D. M. Forin, G. M. Tosi Beleffi, F. Curti, N. Corsi, V. De Sanctis, V. Sacchieri, G. Cincotti, "WDM Free Space Optics transmission at high bit rates", Proc. International Conference on Telecommunications (ConTEL 2007), Zagreb, Croatia, June 2007.

[129] V. De Sanctis, V. Sacchieri, M. Svaluto Moreolo, G. Cincotti, F. Curti, M. Guglielmucci, G. Tosi Beleffi, D. Forin, A. Teixeira, "DWDM Transparent FSO System for ultrahigh bit rate applications", Proc. Conference on Lasers and Electro-Optics (CLEO EUROPE 2007), Munich, Germany, June 2007.

[130] V. Sacchieri, V. De Sanctis, N. Corsi, F. Curti, M. Guglielmucci, G.M. Tosi Beleffi, D. Forin, G. Cincotti, "DWDM Transparent FSO System for In/Outdoor Applications at high Bit Rates", Proc. International Conference on Transparent Optical Networks (ICTON 2007), Rome, Italy, July 2007.

[131] D.M.Forin, G.M.Tosi Beleffi, F. Curti, N. Corsi, V. De Sanctis, V. Sacchieri, G. Cincotti, "Very high bit rates WDM transmission on a Transparent FSO System", Proc. European Conference on Optical Communication (ECOC 2007), Berlin, Germany, Sept. 2007.